

**Alzheimer disease: Identification and characterization of the
putative binding partners of amyloid precursor protein (APP)
and
cell adhesion molecules as biochemical markers**

Dissertation

zur Erlangung des Doktorgrades des Fachbereiches Biologie
der Universität Hamburg

vorgelegt von Elena Strekalova

Hamburg, 2003

Name: Elena Strekalova

Titel der Dissertation: Alzheimer disease: Identification and characterization of putative binding partners of amyloid precursor protein (APP) and cell adhesion molecules as biochemical markers

Gutachter: Frau Prof. Dr. M. Schachner
Herr Prof. Dr. L. Renwrantz

Genehmigt vom
Fachbereich Biologie der
Universität Hamburg
auf Antrag von Frau Professor. Dr. M. SCHACHNER
Weitere Gutachter der Dissertation:
Herr Professor Dr. L. RENWRANTZ

Tag der Disputation: 04. Juli 2003

Hamburg, den 20. Juni 2003



A handwritten signature in black ink, appearing to read "Frühwald".

Professor Dr. A. Frühwald
Dekan

I. INTRODUCTION.....	1
1. ALZHEIMER DISEASE.....	1
1.1 <i>Amyloid precursor protein</i>	2
1.2 <i>Proteolytic processing of APP</i>	5
1.2.1 α -Secretase	5
1.2.2 β -Secretase.....	6
1.2.3 γ -Secretase	7
2. CELL ADHESION MOLECULES OF IMMUNOGLOBULIN SUPERFAMILY	9
2.1 <i>The cell adhesion molecule L1</i>	10
2.2 <i>The neural cell adhesion molecule (NCAM)</i>	13
2.3 <i>Implication of CAMs in neurological disorders</i>	18
3. INTRODUCTION TO THE THEORY OF COMPLEMENTARY HYDROPATHY	19
II. AIMS OF THE STUDY	20
III. MATERIALS	22
1. CHEMICALS	22
2. SOLUTIONS AND BUFFERS	22
3. BACTERIAL MEDIA.....	27
4. BACTERIAL STRAINS AND CELL LINES	28
5. CELL CULTURE MEDIA	28
6. MOLECULAR WEIGHT STANDARDS.....	28
7. PLASMIDS	29
8. ANTIBODIES.....	30
8.1 <i>Primary antibodies</i>	30
8.2 <i>Secondary antibodies</i>	32
9. PEPTIDES	32
9.1 <i>Antisense peptides</i>	32
9.2 <i>Biotinylated peptides</i>	33
IV. METHODS	34
1. PROTEIN-BIOCHEMICAL METHODS	34
1.1 <i>SDS-polyacrylamide gel electrophoresis</i>	34
1.2 <i>Western Blot-analysis</i>	34
1.2.1 Electrophoretic transfer	34
1.2.2 Immunological detection of proteins on Nitrocellulose membranes.....	35
1.2.3 Immunological detection using enhanced chemiluminescence.....	35
1.3 <i>Coomassie staining of polyacrylamide gels</i>	35
1.4 <i>Silver staining of polyacrylamide gels</i>	35
1.5 <i>Determination of protein concentration (BCA)</i>	36
1.6 <i>Enzyme-linked immunosorbent assay (ELISA), binding assay</i>	36
1.7 <i>Capture ELISA</i>	36
1.8 <i>Preparation of membrane subfractions</i>	37
1.9 <i>Solubilisation of membrane fractions</i>	38
1.10 <i>Isolation of IgG fractions</i>	38
1.11 <i>Affinity chromatography</i>	39
1.12 <i>Sample preparation for protein sequencing</i>	39
1.13 <i>Purification of rabbit IgG using protein A</i>	40
1.14 <i>Immunoprecipitation</i>	40
2. MOLECULAR BIOLOGY	40
2.1 <i>Bacterial strains</i>	40

2.1.1 Maintenance of bacterial strains	40
2.1.2 Production of competent bacteria	41
2.1.3 Transformation of bacteria	41
2.2 <i>Plasmid isolation of E. coli</i>	41
2.2.1 Plasmid isolation from 3 ml cultures (Minipreps)	41
2.2.2 Plasmid isolation from 15 ml-cultures	41
2.2.3 Plasmid isolation from 500 ml-cultures (Maxipreps)	42
2.3 <i>Enzymatic modification of DNA</i>	42
2.3.1 Digestion of DNA	42
2.3.2 Dephosphorylation of Plasmid-DNA	43
2.3.3 Ligation of DNA-fragments	43
2.4 <i>DNA Gel-electrophoresis</i>	43
2.5 <i>Extraction of DNA fragments from agarose gels</i>	43
2.6 <i>Purification of DNA fragments</i>	44
2.7 <i>Determination of DNA concentrations</i>	44
2.8 <i>DNA-Sequencing</i>	44
3. CELL CULTURE	45
3.1 <i>CHO cell culture</i>	45
3.2 <i>Stable transfection of CHO-cells</i>	45
3.3 <i>Cell culture of stable transfected CHO cells</i>	46
3.4 <i>Preparation of dissociated hippocampal cultures</i>	46
4. IMMUNOCYTOCHEMISTRY	47
4.1 <i>Fixation of hippocampal neurons</i>	47
4.2 <i>Immunocytochemistry of fixed hippocampal neurons</i>	47
4.3 <i>Co-capping on hippocampal neurons</i>	47
4.4 <i>Confocal laser-scanning microscopy</i>	48
5. CLINICAL METHODS	48
5.1 <i>Patients and collection of cerebrospinal fluid</i>	48
6. COMPUTER ANALYSIS	49
6.1 <i>Sequence analysis</i>	49
6.2 <i>Statistical analysis</i>	49
V. RESULTS	50
STUDY 1: IDENTIFICATION AND CHARACTERIZATION OF PUTATIVE BINDING PARTNERS OF AMYLOID PRECURSOR PROTEIN (APP)	50
1. IDENTIFYING PROTEINS INVOLVED IN APP PROTEOLYSIS	50
2. CHARACTERIZATION OF THE ANTIBODIES	51
3. ORGAN SPECIFICITY OF IDENTIFIED PROTEINS	52
4. FRACTION CO-LOCALIZATION OF IDENTIFIED PROTEINS AND APP	53
5. SOLUBILIZATION OF SYNAPTOSOMAL MEMBRANES WITH TRITON X-100	54
6. OPTIMISATION OF SOLUBILIZATION PROCESS	54
7. AFFINITY CHROMATOGRAPHY	55
8. PROTEIN SEQUENCING	56
9. CONFIRMATION OF THE PRESENCE OF IDENTIFIED PROTEINS IN FRACTIONS PURIFIED BY AFFINITY CHROMATOGRAPHY	57
10. DISTRIBUTION OF CALRETICULIN, VERSICAN AND CREATINE KINASE B IN BRAIN SUBFRACTIONS	58
11. BINDING STUDY OF IDENTIFIED PROTEINS AND APP USING AN ELISA APPROACH	59
12. VERIFICATION OF THE INTERACTION OF IDENTIFIED PROTEINS AND APP BY CO- IMMUNOPRECIPITATION	61

13. CO-LOCALIZATION AND CO-CAPPING OF IDENTIFIED PROTEINS AND APP IN PRIMARY HIPPOCAMPAL CULTURES	62
STUDY 2: CELL ADHESION MOLECULES AS BIOCHEMICAL MARKERS FOR ALZHEIMER DISEASE	67
1. INTRODUCTION IN "CAPTURE" ELISA	67
2. ESTABLISHMENT OF A CAPTURE ELISA FOR QUANTIFICATION OF L1 LEVEL IN THE CSF	68
2.1 <i>Checking of the specificity and working titre of the detection polyclonal anti-human L1 antibodies</i>	68
2.2 <i>Establishment of the optimal coating concentration of the capture monoclonal anti-human L1 antibody (Neuro 4.1.1.3.3)</i>	68
2.3 <i>Standard antigen-binding curve</i>	70
2.4 <i>Determination of the optimal test sample (CSF) dilution</i>	70
2.5 <i>Optimizing the ELISA</i>	71
2.6 <i>Sensitivity of the L1-Fc ELISA test</i>	72
3. ESTABLISHMENT OF A CAPTURE ELISA FOR QUANTIFICATION OF NCAM AND PSA-NCAM LEVELS IN THE CSF	72
3.1 <i>Checking of the specificity and working titre of the detection polyclonal anti-human NCAM antibodies (3731)</i>	72
3.2 <i>Establishment of the optimal coating concentrations of the capture monoclonal anti-human NCAM antibody (14.2) and monoclonal anti-PSA antibody (735)</i>	74
3.3 <i>Standard antigen binding curves</i>	75
3.4 <i>Determination of the optimal test sample (CSF) dilutions</i>	76
3.5 <i>Optimizing the ELISA</i>	78
3.6 <i>Sensitivity of the NCAM-Fc and PSA-NCAM-Fc ELISA tests</i>	78
4. LEVELS OF L1, NCAM AND PSA-NCAM IN THE CEREBROSPINAL FLUIDS OF DIFFERENT PATIENT GROUPS	78
5. L1, NCAM AND PSA-NCAM LEVELS IN CEREBROSPINAL FLUID OF DEMENTIA AND NON-DEMENTIA GROUPS	82
6. LEVELS OF L1, NCAM AND PSA-NCAM IN THE CSF OF PATIENTS WITH NEURODEGENERATIVE DISORDERS AND NON-DEGENERATIVE DISEASES	84
7. STEPWISE MULTIPLE REGRESSION ANALYSIS WITH L1, NCAM OR PSA-NCAM AS DEPENDENT AND AGE, GENDER, PRESENCE OF DEMENTIA AND NEURODEGENERATIVE ETIOLOGY AS INDEPENDENT VARIABLES	86
VI. DISCUSSION	88
STUDY 1	88
1. CHARACTERIZATION OF THE APP - CALRETICULIN INTERACTION	88
2. CHARACTERIZATION OF THE APP - VERSICAN INTERACTION	91
3. CHARACTERIZATION OF THE APP - CREATINE KINASE B INTERACTION	93
STUDY 2	95
VII. SUMMARY	98
(STUDY 1)	98
(STUDY 2)	99
VII. ZUSAMMENFASSUNG	101
(ERSTER TEIL)	101
(ZWEITER TEIL)	102
VIII. APPENDIX	104
1. ABBREVIATIONS	104
2. ACCESSIONNUMBERS	106

3. PLASMIDS	107
3.1 <i>NCAM-Fc in pcDNA3</i>	107
IX. BIBLIOGRAPHY	108
POSTER PRESENTATIONS.....	133
CURRICULUM VITAE.....	134
ACKNOWLEDGMENTS	135

I. Introduction

1. Alzheimer disease

Alzheimer disease (AD) is a neurodegenerative disorder characterized by a progressive memory loss, cognitive decline, and, eventually, by death. AD is the most common cause of dementia among older people. The main clinical features of this disease are cognitive decline and mental deterioration, which are the consequence of a massive, progressive loss of neurons. The disease process selectively damages regions and neural circuits critical for cognition and memory, including neurons in the neocortex, hippocampus, amygdala, basal forebrain cholinergic system, and brainstem monoaminergic nuclei. At autopsy two characteristic lesions, plaques and tangles are seen in the brains of affected patients (Figure 1). Neurofibrillary tangles consist of paired helical filaments, which mainly composed of the hyperphosphorylated form of the microtubule-associated protein tau. The major protein component of the core of senile plaques is amyloid β -protein ($A\beta$), a 39-43 amino acid-long peptide derived from the amyloid β -protein precursor (APP). Besides $A\beta$, several proteoglycans with the ability to modulate amyloid fibril formation accumulate in senile plaques, e.g. agrin, perlecan, glypican, syndecan and versican. Plaques can be subdivided into classical and diffuse types. In the classical plaques, a dense central core of $A\beta$ is surrounded by diseased neurons that project neurites towards and around the core. In the diffuse plaques the amyloid deposit is more amorphous and is not associated with significant cell loss. Although these histopathological features were described over 90 years ago by the German psychiatrist Alois Alzheimer (Alzheimer, 1907), they are still of central importance for the post-mortem diagnosis of AD. It is presently unclear what the relationship is between the plaques and tangles or to which degree the amount of plaque and tangle pathology is associated with disease state.

AD is a multifactor disorder, with both genetic and environmental factors implicated in its pathogenesis. Mutations in three genes – the presenilin 1 gene on chromosome 14, the presenilin 2 gene on chromosome 1, and the APP gene on chromosome 21 – all of them are able to transmit AD via autosomal-dominant inheritance. This form of AD is referred as familial Alzheimer disease (FAD) and is characterized by earlier onset of disorder. The other genes that are considered to be risk factors of AD include apolipoprotein E (Apo E, e4 allele) (Poirier et al., 1995), α 2 macroglobulin (Blacker et al., 1998), the K-variant of butyryl-cholinesterase (Lehmann et al., 1997), and several mitochondrial genes (Law et

al., 2001). Epidemiological studies have demonstrated risk factors for AD that include age, gender, previous head injury and cardiovascular disease (Law et al., 2001).

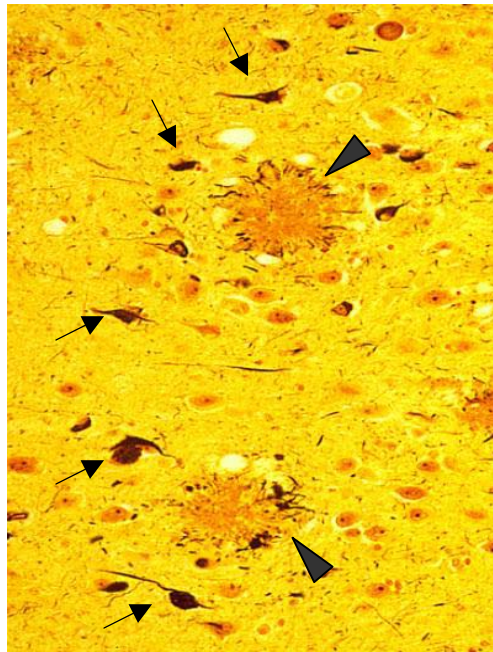


Figure 1: High-power photomicrograph of a section of the amygdala from a patient with Alzheimer disease demonstrating the classical neuropathological lesions of this disorder

Silver stain reveals two senile (neuritic) plaques (indicated with arrowheads) consisting of compacted, spherical deposits of extracellular amyloid surrounded by dystrophic neurites, which can include both axonal terminals and dendrites. Some of the pyramidal neurons in this field contain neurofibrillary tangles, darkly staining masses of abnormal filaments occupying much of the perinuclear cytoplasm (indicated with arrows).

Two major hypotheses on the cause of AD have been proposed: the “neuronal cytoskeletal degeneration hypothesis” (Braak and Braak, 1991), which states that cytoskeletal changes are the triggering events, and the “amyloid cascade hypothesis”, which proposes that the neurodegenerative process is a series of events triggered by the abnormal processing of the APP (Hardy and Higgins, 1992).

1.1 Amyloid precursor protein

β -Amyloid precursor protein (APP) is a receptor-like transmembrane protein of approximately 110 kDa consisting of an extracellular domain, a transmembrane domain, and a short cytoplasmic domain (Selkoe, 1999) (Figure 2, top panel). It is widely

expressed on the cell surface. APP belongs to the conserved APP family (APPs), which includes amyloid precursor-like protein 1 and 2 (APLP1 and APLP2) in mammals, APP747 in *Xenopus*, eAPP in electric ray, APL-1 in *Caenorhabditis elegans*, and APP-like (APPL) in *Drosophila* (Coulson et al., 2000). The cytoplasmic domains of APPs are more highly conserved than the other domains among a wide variety of species and are important for intracellular metabolism (Perez et al., 1999; Tomita et al., 1998) and physiological functions (Allinquant et al., 1995; Ando et al., 1999; Perez et al., 1997; Xu et al., 1999). APP is expressed as several isoforms by alternative splicing. The three major isoforms contain 695 (APP695), 751 (APP751), or 770 (APP770) amino acids (Selkoe, 1994b).

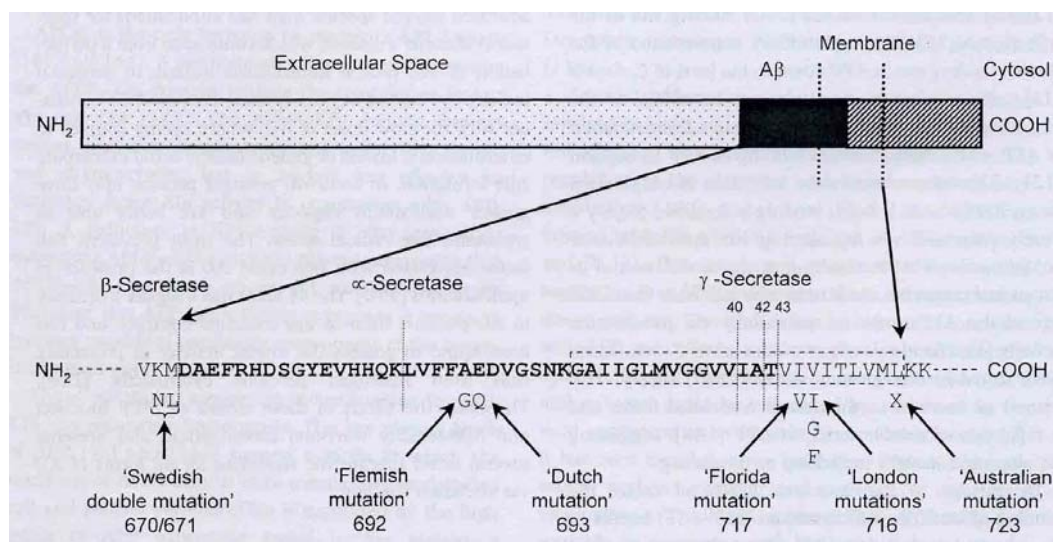


Figure 2: APP structure

Top panel: Cartoon of APP, showing location of Aβ, partially overlapping the transmembrane domain. Bottom panel: Amino acid sequence of Aβ. The transmembrane domain is indicated by dashed box. Secretase cleavage sites are indicated by vertical dotted lines. The sites and residue changes of pathogenetic mutations are shown below the amino acid sequence.

Several proteins have been reported to interact with the cytoplasmic domain of APP, including Fe65, X11 and Disabled (Borg et al., 1996; Guenette et al., 1996; Trommsdorff et al., 1998), all of which share characteristics of adapter proteins that could potentially link APP to intracellular signalling pathways. The search for ligands or receptors that interact with the large ectodomain of APP has not been very successful, but several functional subdomains have been identified – for example, the RERMS sequence that appears to have growth-promoting properties (Ninomiya et al., 1993), and the two

heparin-binding domains that are responsible for binding to the glycan moieties of proteoglycans, such as glypican (Williamson et al., 1996). The large, promiscuous lipoprotein receptor-related protein (LRP) is the only known receptor that binds to APPs containing the Kunitz-type proteinase inhibitor sequence (Knauer et al., 1996; Kounnas et al., 1995). Proteins that bind to other parts of the APP tail have also been identified. It has been demonstrated that the GTP-binding protein G_0 binds to the His657-Lys676 sequence in the APP tail (Nishimoto et al., 1993). It has been also shown that PAT1 (protein interacting with the APP tail 1) provides a potential link between APP and microtubules (Zheng et al., 1998), and the binding of this novel protein requires Tyr653 in the APP tail. APPs are expected to be functionally important because mice lacking all genes of the APP family die in the early postnatal period (Heber et al., 2000). Its functional properties are not clearly defined, but range from repair of vascular injury to mediation of growth and adhesion of neural and nonneural cells (Selkoe, 1994a). APP has also been implied in pro- and anti-apoptotic functions (Wolozin et al., 1996; Xu et al., 1999; Yamatsuji et al., 1996). A recent report proposed that APP normally behaves in the brain as a cell surface signalling molecule, and that an alteration of this function is one of the possible causes of the neurodegeneration and consequently AD (Neve et al., 2000). It has been also suggested that APP has a function in the regulation of nuclear transcription (Cao and Sudhof, 2001).

As mentioned before, specific mutations in APP gene can lead to rare autosomal dominant forms of familial Alzheimer disease (FAD) (Tanzi et al., 1992). The mutations cluster at the three secretase sites (Figure 2, bottom section). The ‘London mutations’ at position 717 were described first (Goate et al., 1991). They lead to an increase in the ratio of $A\beta_{1-42}/A\beta_{1-40}$ (Suzuki et al., 1994), and an increase in total serum $A\beta_{1-42}$ in asymptomatic carriers (Kosaka et al., 1997). The recently described ‘Florida mutation’ at position 716 produces the same effect and it appears that the ‘Australian mutation’ at position 723 does as well (Eckman et al., 1997). The ‘Swedish double mutation’ at positions 670/671 (Mullan et al., 1992) increases the total production of $A\beta$ without affecting the ratio of $A\beta_{1-42}/A\beta_{1-40}$ (Cai et al., 1993). The ‘Dutch mutation’ at position 693 near the α -secretase site results in hereditary cerebral haemorrhage with amyloidosis-Dutch type secondary to vascular amyloid deposition (Levy et al., 1990). Another mutation near the α -secretase site at position 692, known as ‘Flemish mutation’, produces a phenotype, which combines features of Alzheimer disease with those of hereditary cerebral haemorrhage with amyloidosis (Hendriks et al., 1992).

1.2 Proteolytic processing of APP

APP is cleaved by three types of proteases, which are designated α -, β - and γ -secretases (Figure 3).

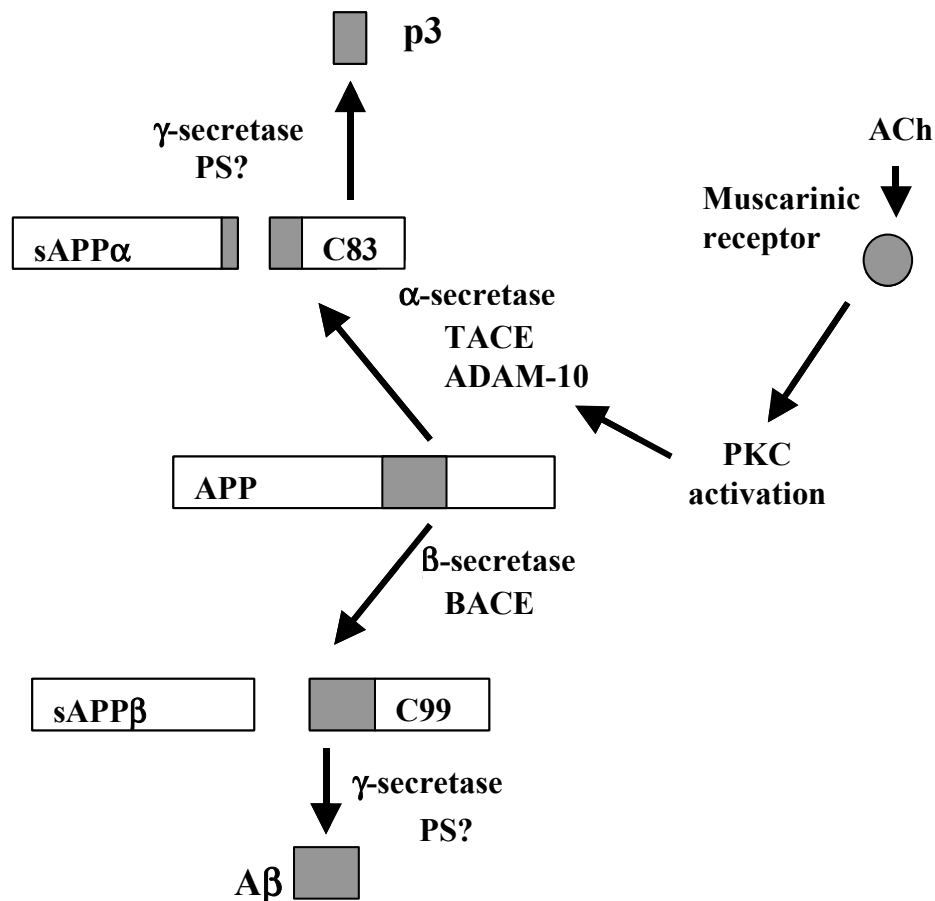


Figure 3: Proteolytic processing pathways of APP by α -, β - and γ -secretases

Cleavage by α -secretase (TACE or ADAM-10) produces sAPP α and C-terminal fragment C83. Both TACE and ADAM-10 can be activated by protein kinase C (PKC), which is regulated by muscarinic acetylcholine (ACh) receptor. C83 is cleaved by γ -secretase to produce p3. Cleavage of APP by β -secretase (BACE) produces sAPP β and C99. γ -Secretase cleaves C99 to release A β .

1.2.1 α -Secretase

A major route of APP processing (90% of protein) is via α -secretase pathway, which cleaves between Lys 16 and Leu 17 (residues 612 and 613 of APP), generating an 83-residue C-terminal fragment (C83) (Esch et al., 1990). Subsequent cleavage by γ -secretase

releases a short peptide (p3) containing the C-terminal region of the A β peptide. As cleavage of APP by α -secretase destroys the A β sequence, it is generally thought that the α -secretase pathway mitigates amyloid formation. In addition, the C-terminally truncated form of APP released by α -secretase may have trophic actions (Small, 1998), which could antagonize the neurotoxic effects of aggregated A β (Mok et al., 2000). The exact subcellular localisation of the α -secretase is unclear, although the trans-Golgi has been proposed as one of the sites of α -cleavage (Kuentzel et al., 1993). More recently, a membrane-bound endoprotease at the cell surface has been found to have α -secretase-like activity (Lammich et al., 1999). Furthermore, α -secretase has both constitutive and regulated components. Regulated α -secretase cleavage appears to be under the control of protein kinase C (PKC), which is regulated by the muscarinic acetylcholine (ACh) receptor (Sinha and Lieberburg, 1999). Phorbol esters also increase α -secretion of APP above basal level, while PKC inhibitors leave a residual cleavage action (Hung et al., 1993).

Two members of the ADAM (a disintegrin and metalloprotease) family, tumour necrosis factor- α (TNF α)-converting enzyme (TACE or ADAM-17) and ADAM-10, are candidate α -secretases. It has been shown that knockout of TACE decreases the release of the α -cleaved product sAPP α , however, cells deficient in TACE still have a residual α -secretase activity that cannot be increased by phorbol esters (Buxbaum et al., 1998). ADAM-10 exists only in a proenzyme (inactive) form in the Golgi, but becomes activated in the plasma membrane. Overexpression of ADAM-10 increased α -secretase cleavage of APP in a phorbol ester-inducible manner (Lammich et al., 1999). Recently the prohormone convertase PC7 has been shown to be involved in the constitutive α -secretase activity. Overexpression of PC7 in HEK293 cells has been found to increase sAPP α secretion, while overexpression of α_1 -antitrypsin Portland (an inhibitor of precursor convertases) was found to inhibit endogenous sAPP α production (Lopez-Perez et al., 1999).

1.2.2 β -Secretase

A β -site APP cleaving enzyme (BACE or Asp2) has been identified by several groups both by genetic screening and by direct enzyme purification and sequencing (Hussain et al., 1999; Lin et al., 2000; Sinha et al., 1999; Vassar et al., 1999; Yan et al., 1999). BACE is a type I integral membrane protein. It is a member of the pepsin family of aspartyl proteases, which has an N-terminal catalytic domain, containing two important aspartate

residues, linked to a 17-residue transmembrane domain and a short C-terminal cytoplasmic tail. BACE contains four potential N-linked glycosylation sites and a propeptide sequence at the N-terminus. Within the cell, BACE is expressed initially as a proprotein, which is then efficiently processed to its mature form in the Golgi (Haniu et al., 2000). BACE cleaves full-length APP at Asp1, releasing the N terminus of the A β peptide, and also at Glu11, releasing a shorter form of the A β (Vassar et al., 1999). The Swedish NL mutation, which is known to enhance β -secretase cleavage, also promotes cleavage of APP at Asp1 by BACE (Forman et al., 1997; Vassar et al., 1999). BACE is expressed coordinately with APP in many regions of the brain, particularly in neurones, and has a subcellular distribution similar to that of β -secretase (Vassar et al., 1999). A related transmembrane aspartyl protease (BACE2 or Asp1) shows similar substrate specificity (Farzan et al., 2000) but is not highly expressed in the brain (Bennett et al., 2000). In addition, BACE 2 also cleaves APP near the α -secretase site, in the middle of the A β domain between phenylalanines 19 and 20, resulting in reduced production of A β species (Fluhrer et al., 2002).

1.2.3 γ -Secretase

Since cleavage of the APP C99 fragment by γ -secretase is the final step in the production of A β , the exact position of cleavage by γ -secretase is critical for the development of AD. Production of the more amyloidogenic long A β species by γ -secretase adjacent to residues 42 or 43 is closely associated with disease pathogenesis (Scheuner et al., 1996; Small and McLean, 1999). Although the γ -secretase has not been identified, presenilin (PS) 1 and 2 are two candidates, which were initially identified through genetic linkage analysis of families with autosomal dominant forms of Alzheimer disease. PSs are integral membrane proteins with eight putative transmembrane domains, encoded by genes on chromosomes 14 and 1 (Nishimura et al., 1999). In the brain, both *in situ* hybridization and immunohistochemistry studies indicate that PS-1 and PS-2 are predominantly expressed in neurons (Cook et al., 1996; Kovacs et al., 1996); however, expression in glia has also been observed (Lah et al., 1997). Northern blot results indicate that PS-1 and PS-2 mRNAs are present in a wide variety of peripheral tissues. The constitutive proteolytic cleavage site occurs within the large cytoplasmic loop between the sixth and seventh transmembrane domain of PS1 (Li and Greenwald, 1998; Podlisny et al., 1997). It has been shown that presenilins undergo proteolytic processing in this region to form stable heterodimeric complexes (Capell et al., 1998) (Figure 4).

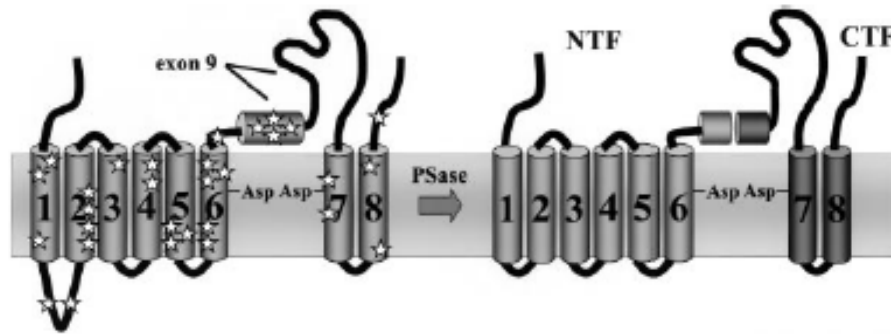


Figure 4: Topology and proteolytic processing of presenilins

Presenilins are cleaved within the hydrophobic region of the large cytosolic loop between TM6 and TM7, resulting in the formation of a heterodimeric complex composed of the N-terminal fragment (NTF) and the C-terminal fragment (CTF). Stars represent sites of mutation that cause FAD. The two conserved aspartates required for presenilin endoproteolysis, and γ -secretase processing of APP is predicted to be within TM6 and TM7.

The observation that knockout of both PS1 and PS2 completely inhibits all γ -secretase activity demonstrates that PSs are required for γ -secretase activity (Herreman et al., 2000). Furthermore, PSs are localised to subcellular compartments (i.e. ER-Golgi) known to be the site of γ -secretase processing. However, intracellular generation of A β seemed unique to neurons, since the nonneuronal cells were shown to produce significant amounts of A β only at the cell surface (Hartmann et al., 1997). In addition, γ -secretase inhibitors can affinity-label PS subunits (Esler et al., 2000) and both PSs bind to APP (Weidemann et al., 1997; Xia et al., 1997). Inhibitor studies show that γ -secretase is likely to be an aspartyl protease (Wolfe et al., 1999a). At the same time it has been found that mutation of two aspartate residues (Asp257 and Asp385) in the transmembrane domain of PS1 inhibited γ -secretase activity (Wolfe et al., 1999b).

Subcellular and biochemical fractionation experiments have shown that PS and γ -secretase copurify as a high molecular weight complex around 400 kDa (Li et al., 2000). Recently, an integral membrane protein nicastrin has been identified as a major binding partner for the presenilins (Yu et al., 2000). It has been proposed that nicastrin may play a role in

cellular trafficking of PS to the cell surface, or may be involved in the regulation of the stability of the γ -secretase complex. Furthermore, it has been demonstrated that PEN-2 (presenilin enhancer 2) is an integral component of the γ -secretase complex required for coordinated expression of presenilin and nicastrin (Steiner et al., 2002). It has been also shown that the mammalian APH-1 protein physically associates with nicastrin and the presenilin heterodimers *in vivo*, and is required for the processing of APP (Lee et al., 2002). PSs have been shown to interact with a wide array of different proteins, and have been implicated in IP₃-mediated release of ER calcium (Leissring et al., 2001), capacitative calcium entry (Leissring et al., 2000; Yoo et al., 2000), β -catenin signalling (Kang et al., 1999; Yu et al., 1998; Zhang et al., 1998b) and protein trafficking (Naruse et al., 1998). However, the identity of γ -secretase has not yet been established and PS may simply be a regulatory subunit of γ -secretase or a protein that is involved in a step necessary for transport or maturation of the γ -secretase.

2. Cell adhesion molecules of immunoglobulin superfamily

An increasing number of data indicates that abnormalities in expression or functions of cell adhesion molecules (CAMs) have been associated with a wide range of neurological disorders, including hydrocephalus, schizophrenia and AD, providing new insights into both clinical and basic research. CAMs comprise a large group of cell surface macromolecules that provide recognition and adhesion between cells. CAMs are critical for migration and recognition of appropriate cells to form functional assemblies of neurons and for innervation of appropriate targets. They are involved in most of the major developmental processes, including cell migration, neurite outgrowth, axon pathfinding, axon fasciculation, synaptogenesis, synapse stabilization, and myelination (Cotman et al., 1998). They perform these functions not only by regulating cell adhesion, but also by activating signalling cascades that in turn control cytoskeletal dynamics, cell morphology, and neurite outgrowth. The immunoglobulin superfamily is a group of calcium-independent CAMs. These molecules share a similar extracellular structure, consisting of several immunoglobulin (Ig) domains and often fibronectin (Fn) type III repeats (Figure 5). Various isoforms are known, and many are regulated by phosphorylation and glycosylation.

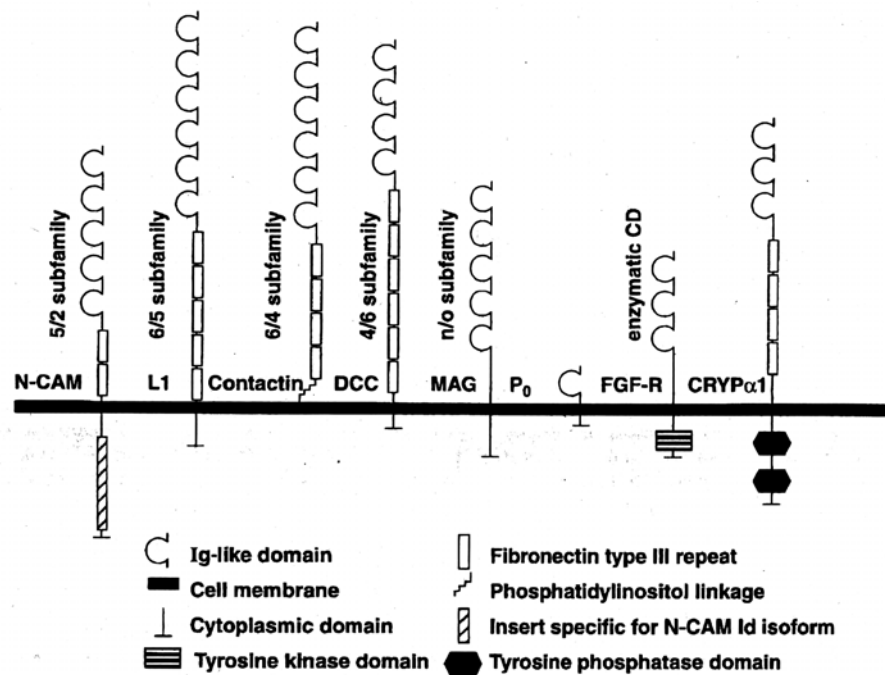


Figure 5: Neural cell adhesion molecule subfamilies of the immunoglobulin superfamily

The majority of molecules of the immunoglobulin superfamily fall into classes depending on the number of Ig-like domains and fibronectin repeats, which are denoted representative molecule. For example, the 5/2 family is exemplified by NCAM and contains five Ig domains and two fibronectin type III-like repeats. The enzymatic cytoplasmic domain (CD) category exhibits protein tyrosine kinase or phosphatase activities in their cytoplasmic domain.

2.1 The cell adhesion molecule L1

The L1 cell adhesion molecule is a 200-220 kDa transmembrane glycoprotein which belongs to the immunoglobulin superfamily (Kadmon and Altevogt, 1997; Rathjen and Schachner, 1984). The molecule consists of six Ig-like domains and five fibronectin-type III repeats followed by a transmembrane region and a highly conserved cytoplasmic tail of approximately 114 amino acids.

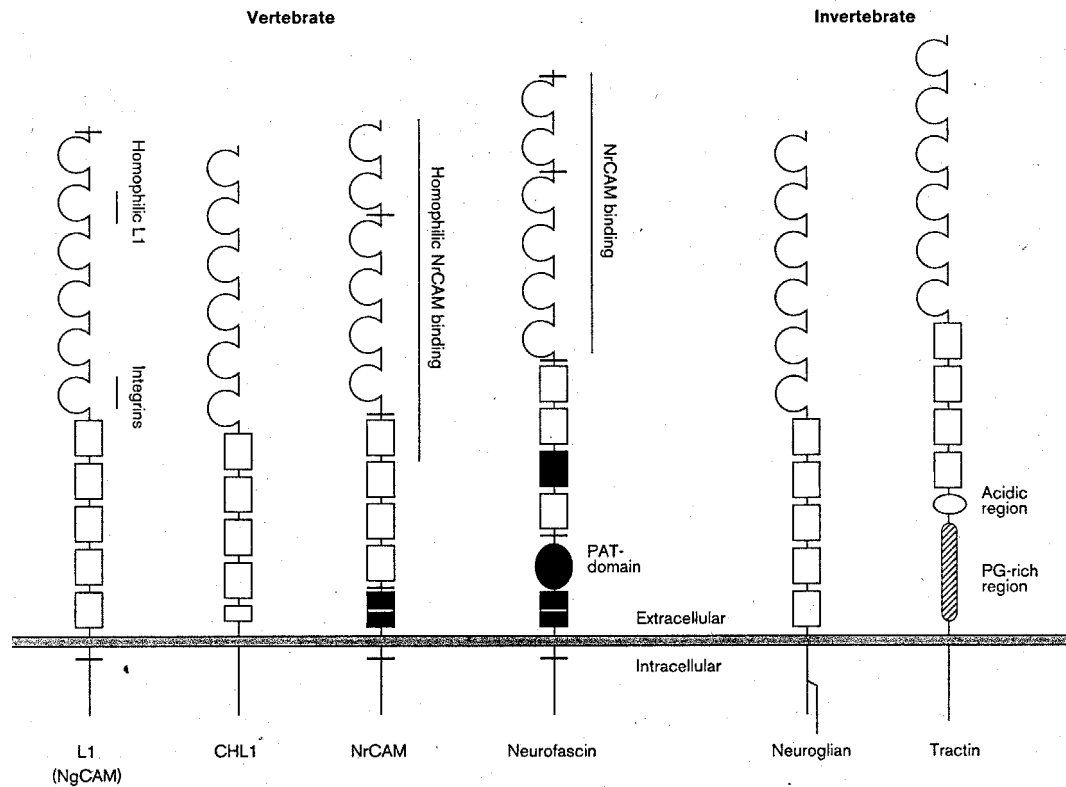


Figure 6: Schematic representation of L1 and other members of the L1 subfamily

Ig-like domains are indicated by horse-shoe shapes and Fn III-like repeats by boxes. Horizontal bars and dark grey areas indicate alternatively spliced small segments and domains, respectively. Thin vertical bars indicate regions identified to be important for binding in extracellular regions. PAT, proline/alanine/threonine-rich; PG, proline/glycine-rich.

In mammals, L1 is expressed throughout the nervous system on subsets of developing and differentiated neurones as well as on Schwann cells of the peripheral nervous system. On differentiated neurones L1 is found at regions of contact between neighbouring axons and on the growth cones, the structures at the leading tip of axons that are responsible for sensing extracellular growth and guidance cues. Although primarily expressed in the nervous system, L1 is also found at other specialized sites including a subclass of leukocytes, intestinal crypt cells and kidney tubule epithelia (Debiec et al., 1998; Kowitz et al., 1992; Thor et al., 1987). Homologous molecules exist in several species including mouse (L1) (Faissner et al., 1985), rat (NILE) (McGuire et al., 1978), chick (NgCAM) (Burgoon et al., 1991), *Drosophila* (neuroglian) (Bieber et al., 1989) and human (L1) (Kobayashi et al., 1995; Wolff et al., 1988) (Figure 6). L1 sequences from a number of

vertebrates share sequence identities of 50-85% with that of human L1 (Hlavin and Lemmon, 1991; Reid and Hemperly, 1992).

L1 has been originally recognized as a neural adhesion molecule shown to be involved in granule neuron migration in the developing mouse cerebellar cortex (Lindner et al., 1983), the fasciculation of neurites (Fischer et al., 1986) and neurite outgrowth on other neurites and Schwann cells (Chang et al., 1990; Seilheimer and Schachner, 1987). Recent studies on L1-knockout mice have confirmed that L1 is an important molecule for the development of the nervous system (Cohen et al., 1998; Dahme et al., 1997). L1 is also involved in synaptogenesis, myelination, neuronal cell survival (Chen et al., 1999) and long-term potentiation (Fields and Itoh, 1996).

Studies in the nervous system have shown that L1 can mediate cell adhesion by several mechanisms, such as homophilic binding involving L1-L1 interactions (Kadmon et al., 1990a) and assisted homophilic binding between L1 and L1/NCAM complexes at the surface of adjacent cells (Kadmon et al., 1990b). Furthermore, L1 mediated heterotypic binding with the axon-associated CAM axonin-1 (Kuhn et al., 1991) and the GPI-anchored molecule CD24 (Kadmon et al., 1995) are also well characterized. L1 was also identified as a ligand for several RGD-binding integrins, i.e. $\alpha_5\beta_1$, $\alpha_v\beta_1$, $\alpha_v\beta_3$ as well as the platelet integrin $\alpha_{IIb}\beta_3$ (Blaess et al., 1998; Ebeling et al., 1996; Felding-Habermann et al., 1997; Montgomery et al., 1996; Ruppert et al., 1995). Integrin-mediated cell binding and migration is supported by RGDs in the six Ig-like domain of L1 (Duczmal et al., 1997; Ebeling et al., 1996; Felding-Habermann et al., 1997; Ruppert et al., 1995). Furthermore, L1 ligand binding is linked to intracellular signalling pathways. For instance, homophilic interaction of L1 promotes neurite outgrowth via activation of FGFRs and related second messenger cascades in the stimulated cells (Doherty et al., 1995). Components of the MAPK signalling pathway (Schaefer et al., 1999) and the tyrosine kinase src have been also implicated in L1 mediated responses (Ignelzi, Jr. et al., 1994; Schuch et al., 1989).

The cytoplasmic domain of L1 plays an important role in signal transduction and internalisation of L1. It contains a binding region for ankyrin, a linker protein of the spectrin cytoskeleton. The insertion of RSLE peptide into the cytoplasmic domain of L1 generates a tyrosine-based signal that results in the sorting of L1 protein to the growth cone and induces the AP-2-mediated endocytosis of L1 via clathrin-coated pits (Kamiguchi and Lemmon, 1998).

L1 is a subject of glycosylation and phosphorylation, both of which may affect its function. In addition to tyrosine phosphorylation of the ankyrin-binding domain, serine phosphorylation by specific kinase occurs at several sites (Schuch et al., 1989; Wong et al., 1996; Zisch et al., 1997). These sites are next to known binding domains for either cytoskeletal components of the AP-2 complex, suggesting that serine phosphorylation may influence cytoplasmic interactions, L1 mobility and internalization.

In addition to its function as a cell surface adhesion molecule L1 can be shed from the membrane (Montgomery et al., 1996; Richter-Landsberg et al., 1984) and deposited in the ECM (Martini and Schachner, 1986; Montgomery et al., 1996) suggesting a potential role for L1 as a matrix constituent. Thus, all homologues of L1 have been shown to be sensitive to cleavage within the third fibronectin-like domain (Burgoon et al., 1995; Faissner et al., 1985; Kayyem et al., 1992; Nybroe et al., 1990; Sadoul et al., 1988; Wolff et al., 1988), which results in an extracellular amino-terminal fragment of approximately 140 kDa (L1-140) and a transmembrane fragment of approximately 80 kDa (L1-80). Recently a matrix metalloprotease ADAM 10 and plasmin have been shown to release a 180 kDa L1 from the cell surface through cleavage at specific sites (Beer et al., 1999; Nayeem et al., 1999).

Mutation of L1 in man and mouse results in developmental defects that are consistent with a role for L1 in axonal pathfinding as well as cell migration. X-linked hydrocephalus, MASA syndrome (mental retardation, aphasia, shuffling gait, adducted thumbs), spastic paraplegia type I (SPGI), and X-linked agenesis of corpus callosum (ACC) are related neurological syndromes with X-linked recessive mode of inheritance. All these syndromes are due to mutations in the L1 gene and have therefore been summarised as L1 disease (Finckh et al., 2000). They are also referred to as CRASH syndrome, for corpus callosum hypoplasia, retardation, adducted thumbs, spastic paraplegia, and hydrocephalus (Fransen et al., 1995a; Kenwrick et al., 2000).

2.2 The neural cell adhesion molecule (NCAM)

NCAM have been the first Ig-like CAM to be isolated and characterized in detail (Brackenbury et al., 1977; Cunningham et al., 1987). The amino acid sequences of NCAM are highly conserved among vertebrate species (Edelman, 1987; Williams and Barclay, 1988), and cross-species NCAM-mediated cell aggregation has been demonstrated (Hoffman et al., 1984). All NCAM isoforms are composed of five Ig-domains followed by two Fn III repeats (Cunningham et al., 1987). NCAM is expressed as three major isoforms

via alternative splicing of a primary transcript from a single gene (Owens et al., 1987). Two isoforms are transmembrane forms with approximate molecular weights of 140 kDa and 180 kDa and the third isoform (120 kDa) is attached to the cell membrane via a GPI linkage (Figure 7). Several other isoforms result from alternative splicing in the extracellular domain, some of which are tissue or developmental stage specific (Cunningham et al., 1987; Owens et al., 1987; Santoni et al., 1987; Santoni et al., 1989; Small et al., 1988; Small and Akeson, 1990). In addition, soluble forms of NCAM can be generated by truncation, proteolysis or shedding (Olsen et al., 1993).

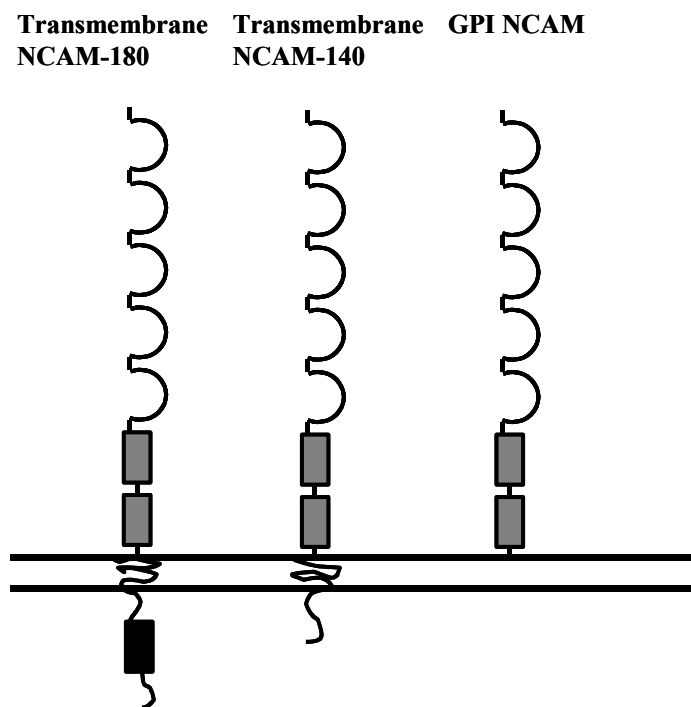


Figure 7: Schematic diagram of the three main classes of NCAM protein

Ig-like domains are indicated by horse-shoe shapes and Fn III-like repeats by grey boxes. NCAM isoforms can be either GPI-anchored or exist as transmembrane isoforms with a small or large cytoplasmic domain. Exon 18-corresponding cytoplasmic domain of NCAM is represented by black box.

Both major cytoplasmic isoforms of NCAM are phosphorylated on serine and threonine residues (Mackie et al., 1989; Sorkin et al., 1984) and are fatty acid acylated (Brackenbury et al., 1987; Little et al., 1998). The prevalence of the NCAM isoforms differs during neuronal development (Edelman, 1987). NCAM 180, for instance, is exclusively expressed on neurons. It shows a reduction of lateral mobility in the cell membrane (Pollerberg et al., 1986) and a tendency to concentrate at sites of cell contact (Pollerberg et

al., 1985; Pollerberg et al., 1987) and at postsynaptic densities (Persohn et al., 1989). However, the expression of NCAM is not restricted to neural tissue. It is expressed by several cell types in many tissues. NCAM was found to be expressed in the proliferating neuroepithelium in a position-dependent manner along the rostrocaudal axis. NCAM was found not only on neurons, it is also expressed by astrocytes and Schwann cells (Neugebauer et al., 1988; Seilheimer and Schachner, 1988). Furthermore, it is expressed within targets such as skeletal muscle with a time course that correlates with the innervation status (Moore and Walsh, 1986).

NCAM is a multivalent adhesion molecule that mediates homotypic and heterotypic cell-cell adhesion through a homophilic-binding mechanism (Crossin and Krushel, 2000; Cunningham, 1995; Rutishauser, 1993; Walsh and Doherty, 1997), and through heterophilic interactions with L1 (Horstkorte et al., 1993), heparan sulphate proteoglycans (Cole and Akeson, 1989) and collagens I-IV and IX (Probstmeier et al., 1989). It has been shown that NCAM plays important role in the formation, maintenance, and regeneration of the nervous system. NCAM mediates neurite outgrowth, fasciculation, and branching (Bixby et al., 1987; Frei et al., 1992; Landmesser et al., 1988; Landmesser et al., 1990; Rutishauser and Edelman, 1980) and is involved in retinal and tectal histogenesis and formation of the neuromuscular junction (Buskirk et al., 1980; Covault and Sanes, 1986; Fraser et al., 1984; Thanos et al., 1984). It has also been implicated in synaptic plasticity (Luthi et al., 1994; Ronn et al., 1995; Scholey et al., 1993; Rutishauser and Jessell, 1998). In addition to its role in cell adhesion, NCAM has been implicated in signal transduction. NCAM has been shown to induce neurite outgrowth in neurons and PC12 cells by stimulating FGFRs. This results in the activation of various signalling cascades, including the PLC- γ pathway and the mitogen-activated protein kinase (p42/44 MAPK) pathway (Corbit et al., 1999; Doherty and Walsh, 1994; Hall et al., 1996; Kolkova et al., 2000; Saffell et al., 1997; Schmid et al., 1999; Williams et al., 1994). NCAM also associates with other signal-transducing molecules, including focal adhesion kinase (FAK) and the src-related tyrosine kinase p59^{l^{yn}} (Beggs et al., 1997). Recently, it has been demonstrated that cosignaling of NCAM via lipid rafts and the FGR receptor is required for neurogenesis (Niethammer et al., 2002).

NCAM is a substrate for extracellular proteolysis by the tissue-type plasminogen activator (tPA), resulting in the release of 105-115 kDa fragments (Endo et al., 1998). Furthermore, the members of ADAM family are seems to be involved in extracellular cleavage of NCAM (Borman and Schachner, unpublished data).

NCAM is unique among adhesion molecules since it can carry polymers of α 2-8 linked sialic acid (PSA), varying in length from a few residues to possibly 200 residues (Hoffman et al., 1982) (Figure 8 B). These chains of PSA create a large negatively charged hydration sphere around NCAM. Polysialylation is regulated during the development of the brain. Early in development, up to 30% of the mass of NCAM can carry PSA and this is progressively reduced as the brain develops (Chuong and Edelman, 1984). NCAM's Ig domain 5 contains three potentially polysialylated asparagine (Asn) residues at positions 404, 430 and 459 (Figure 8 A). PSA has been shown to be associated with residues 430 and 459, which, according to molecular modelling, are in spatial vicinity. Although PSA is located within Ig domain 5, the Ig domain 4, the first FN-III domain and membrane attachment also play a role in polysialylation (Nelson et al., 1995). Addition of PSA to NCAM takes place in the trans-Golgi compartment as a regular step in the biosynthetic pathway of protein glycosylation in eukaryotes (Alcaraz and Goridis, 1991; Scheidegger et al., 1994).

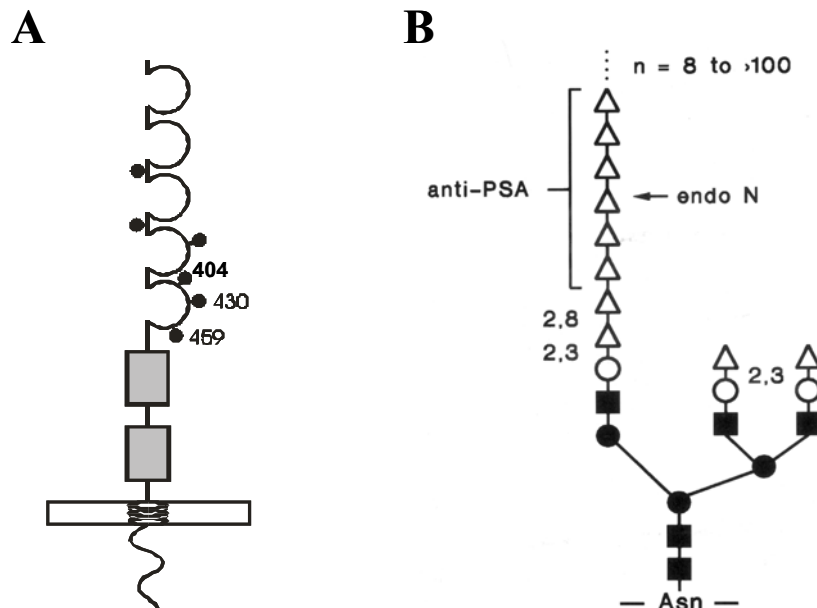


Figure 8: Structure of PSA-NCAM

(A) Schematic diagram showing N-glycosylation sites of Ig domains. The fifth Ig-like domain of NCAM contains three potentially polysialylated asparagines (Asp) residues at positions 404, 430 and 459.

(B) Structure of polysialic acid attached to NCAM via a typical N-linked core glycosylation. The unique structure of the α 2,8-linked polymer allows for its specific recognition by monoclonal antibodies and by phage-derived endoneuraminidase (endo-N). Open triangles, sialic acid; open circles, galactose; closed squares, glucosamine; closed circles, mannose.

There are two major polysialyltransferases, STX and PST, which are responsible for polysialylation (Ong et al., 1998). STX (ST8SiaII) is predominately expressed during development, whereas PST (ST8SiaIV) is the major polysialyltransferase expressed in the adult central nervous system (Angata et al., 1997; Hildebrandt et al., 1998b; Kojima et al., 1995; Kojima et al., 1996; Nakayama et al., 1995; Scheidegger et al., 1995; Tanaka et al., 2000). Mouse PST exhibits 56% amino-acid sequence identity with mouse STX. PST is a type II transmembrane protein containing a potential Golgi retention signal (Eckhardt et al., 1995), and, *in vitro* tests have shown that autopolysialylation is a prerequisite for its activity (Muhlenhoff et al., 1996). PST and STX are expressed distinctly in a tissue-and cell-specific manner. Recently, a new polysialyltransferase ST8Sia III has been described, however, it catalyze polysialylation of NCAM much less efficiently than ST8SiaII and ST8SiaIV (Angata et al., 2000).

In the adult brain polysialylation is restricted to only those regions of the central nervous system that remain plastic and is involved in processes underlying memory formation (Becker et al., 1996; Cremer et al., 1994; Fox et al., 1995; Fryer and Hockfield, 1996; Muller et al., 1996). In addition to its normal occurrence, PSA-NCAM has been associated with an increasing number of cancers, including the small cell lung carcinoma, neuroblastomas, and Wilm's tumor (Hildebrandt et al., 1998a; Tanaka et al., 2000), and its expression is associated with metastasis and poor patient prognosis (Michalides et al., 1994). Glycosylation of NCAM by PSA significantly reduces the ability of NCAM molecules to interact and as the result enhances cell migration (Doherty et al., 1990; Hu et al., 1996). Recent data also indicate that PSA may act as a global inhibitor of cell adhesion and affect a broad spectrum of cell interactions (Acheson et al., 1991; Rutishauser et al., 1988). PSA on NCAM was shown to play an important role in morphogenetic events such as axonal growth (Doherty et al., 1990; Zhang et al., 1992), cell migration (Wang et al., 1994) and muscle innervation (Landmesser et al., 1990). In recent studies, the highly sialylated embryonic form of NCAM has been found to persist in central structures capable of morphological plasticity (Aaron and Chesselet, 1989; Bonfanti et al., 1992; Kiss et al., 1993; Miragall et al., 1988; Theodosis et al., 1991). Some of these, such as the hypothalamo-neurohypophyseal system, the dentate gyrus of the hippocampal formation and the olfactory bulb, are known to undergo activity-dependent morphological remodelling in the adult (Theodosis and Poulain, 1993). A correlation of activity-dependent plasticity and PSA expression was also demonstrated in the neuromuscular

junction where the activity-dependent intramuscular nerve branching was blocked by removal of PSA (Landmesser, 1992).

2.3 Implication of CAMs in neurological disorders

As mentioned before, CAMs have been proposed to be involved in different neurological disorders. For instance, abnormal levels of different isoforms of NCAM have been reported in some psychiatric disorders. People suffering from bipolar mood disorder type 1, recurrent unipolar major depression (Poltorak et al., 1996a) and schizophrenia (Poltorak et al., 1995a) show elevated levels of the 120-kDa isoform of NCAM in their cerebral spinal fluid (CSF). In addition, an increased expression of NCAM 105-115 kDa was found in the hippocampus of patients with schizophrenia (Vawter et al., 1998) as well as NCAM VASE (variable alternative spliced exon) isoforms in CSF of these patients (Vawter et al., 2000). In contrast, the decreased level of L1 140 kDa isoform was observed in the CSF of patients with schizophrenia (Poltorak et al., 1995a). As mentioned before, a number of severe neurological disorders, known as CRASH syndrome, are caused by mutations in L1 gene. Moreover, the role of various cell adhesion molecules in brain plasticity in the adult nervous system support the idea that they can contribute to the development of age-related pathology, particularly in AD. Thus, PSA-NCAM has been implicated in long-term potentiation and learning and memory (Becker et al., 1996; Muller et al., 1996). An increased number of PSA-NCAM staining positive cells has been reported in some regions of the hippocampus of individuals with AD (Mikkonen et al., 1999). In addition to AD, cell adhesion molecules may contribute to myelin and oligodendrocyte degeneration in multiple sclerosis. The null mutant mouse deficient for MAG (myelin-associated glycoprotein) and the double knock out mutants derived from crossbreeds between MAG- and NCAM-knockout mutants show degenerative changes of myelin and myelinating cells of the peripheral and CNS, related to multiple sclerosis (Carenini et al., 1997; Fruttiger et al., 1995; Lassmann et al., 1997; Montag et al., 1994).

3. Introduction to the theory of complementary hydropathy

The theory of complementary hydropathy is based on the observation that there is a significant inverse correlation throughout the entire triplet code between the hydropathic coefficients of amino acids encoded by complementary DNA strands. Amino acids with medium hydrophobicity are generally complemented by similar ones, strongly hydrophobic amino acids by strongly hydrophilic ones and vice versa (Brentani, 1988). Transcription of complementary DNA strands in the same reading frame leads to peptides which are predicted to form amphipathic structures and thus bind one other because highly hydrophilic amino acids will be complemented by hydrophobic ones (Figure 9). These sense-antisense peptide pairs interact because hydrophilic residues turn towards the aqueous phase, leaving a space in the peptide's carbon backbone that can accommodate the hydrophobic residue from the opposing chain.

5'	-	GCT	CTT	-	3'
NH ₂		A	L		COOH
COOH		S	K		NH ₂
3'	-	CGA	GAA	-	5'

Figure 9: Complementary hydropathy

Complementary DNA strands encode amino acids with inversely correlated hydropathic coefficients.

Amphiphilic peptides with a length of 15 amino acids together with their corresponding antisense peptides separated by approximately 50 amino acid residues, termed an antisense homology box, are found in proteins which encode biologically active peptides (Baranyi et al., 1995). It has been suggested that exons coding for interacting peptides were juxtaposed and co-evolved together if both DNA strands from the same exon displayed coding capacity; it is therefore possible that functional domains of interacting proteins may have co-evolved this way (Brentani, 1988).

Complementary hydropathy has been successfully used to identify several receptor-ligand pairs, including a cellular prion protein receptor, a collagen binding site in collagenase, and an integrin receptor for fibronectin (Brentani et al., 1988; de Souza and Brentani, 1992; Martins et al., 1997).

II. Aims of the study

(Study 1)

APP has important functions in neuronal cell migration and synaptic transmission and is believed to play a critical role in the pathophysiology of Alzheimer disease (AD). Several studies deal with the search for ligands or receptors that interact with APP (Borg et al., 1996; Guenette et al., 1996; Trommsdorff et al., 1998; Ninomiya et al., 1993; Williamson et al., 1996) in order to better understand physiological roles of APP. Furthermore, the mechanisms of APP proteolysis contributing to AD remain to be elucidated. Finally, the identification of binding partners of APP might help to understand better the mechanisms of APP cleavage and to identify potential targets for drugs to treat the AD.

The aim of this study was to isolate and characterize binding partners of APP, which might be involved in the molecular processes controlling APP proteolysis, or which might be the proteases cleaving APP themselves. For this purpose, polyclonal rabbit antisera were raised against the antisense peptides of the β - and γ - cleavage sites of APP. Following the theory of complementary hydrophathy the proteins recognized by these antisera are the putative binding partners of APP. For isolation, different brain subfractions were prepared from the brain homogenate of adult mice and subjected to affinity chromatography using the antisense antibodies of the β - and γ - cleavage sites. After identification of the putative APP binding proteins, the interaction should be confirmed using alternative binding assays.

(Study 2)

A definite diagnosis of AD still relies on the presence of neuritic plaques and neurofibrillary tangles, which is mostly done in autopsied tissue. Thus, improving diagnostic accuracy or making diagnosis more specific and earlier in the course of AD becomes very important. Pathological changes in several neuropsychiatric and neurodegenerative disorders are reflected in abnormalities of the cerebral spinal fluid (CSF). Therefore, great efforts have been devoted to search for biochemical markers in the CSF, which can be used for the diagnosis of AD (Andreasen et al., 2001; Galasko, 1999; Garlind et al., 1999; Growdon, 1999; Hampel et al., 2001; Hock et al., 2000). However, the role of cell adhesion molecules as potential candidate markers for early diagnosis of AD has not been investigated. Cell adhesion molecules were shown to play a critical role in activity-dependent synaptic plasticity (Fields and Itoh, 1996; Miller et al., 1993; Murase

and Schuman, 1999; Schachner, 1997; Wheal et al., 1998) and can contribute to the development of age-related pathology, particularly in AD. Therefore, this study was focused on L1, NCAM and PSA-NCAM molecules, which have been reported to participate in the synaptic changes underlying learning and memory processes and show abnormal levels of expression in patients with different neurological and psychiatric disorders (Mikkonen et al., 1999).

The aim of the present study was to compare the levels of L1, NCAM and PSA-NCAM adhesion molecules in the CSF in healthy subjects and in patients suffering from AD and other neurological disorders. For this purpose, a sensitive, specific capture ELISA was developed. CSF from patients and healthy controls were collected, and concentrations of adhesion molecules were quantified followed by statistical analysis of the data.

III. Materials

1. Chemicals

All chemicals were obtained from the following companies in p.a. quality: GibcoBRL (Life technologies, Karlsruhe, Germany), Macherey-Nagel (Düren, Germany), Merck (Darmstadt, Germany), Serva (Heidelberg, Germany) and Sigma-Aldrich (Deisenhofen, Germany).

Restriction enzymes were obtained from New England biolabs (Frankfurt am Main, Germany) and MBI Fermentas (St. Leon-Rot, Germany), molecular weight standards were obtained from Gibco. DNA Purification kits were purchased from Life Technologies (Karlsruhe, Germany), Pharmacia Biotech (Freiburg, Germany), Macherey & Nagel and Qiagen (Hilden, Germany). Plasmids and molecular cloning reagents were obtained from Clontech, Invitrogen, Pharmacia Biotech, Promega, Qiagen and Stratagene. Biotinylated peptides were ordered from Schafer-N (Denmark). Cell culture material was ordered from Nunc (Roskilde, Denmark) or Life Technologies and PAA Laboratories GmbH (Gölbe, Germany).

2. Solutions and buffers

(in alphabetical order)

BCA-Reagent A (<i>BCA kit</i>)	1	% (w/v)	Bicincholinacid disodium salt
	1.7	% (w/v)	Na ₂ CO ₃ x H ₂ O
	0.16	% (w/v)	Natriumtartrat
	0.4	% (w/v)	NaOH
	0.95	% (w/v)	NaHCO ₃ pH 11.25
BCA-Reagent B (<i>BCA kit</i>)	4	% (w/v)	CuSO ₄ x 5 H ₂ O
Blocking buffer (<i>Immunocytochemistry</i>)	2	% (w/v)	BSA in PBS

III. Materials

Blocking buffer (<i>Western Blot, ELISA</i>)	5	% (w/v)	instant milk powder in TBS/PBS
Blotting buffer (<i>Western Blot</i>)	25	mM	Tris
	192	mM	Glycine
	10	%	Methanol
Buffer 1 (<i>Binding assay, ELISA</i>)	1	% (w/v)	BSA in TBS
	1	mM	CaCl ₂
	1	mM	MnCl ₂
	1	mM	MgCl ₂
	0.05	% (v/v)	Tween 20
Coupling buffer (<i>Affinity Purification</i>)	0.1	M	Sodium Phosphate, pH 7.0
	0.05	%	Sodium Azide
Developing solution (<i>Silver Staining</i>)	2	% (w/v)	Sodium Carbonate
	0.04	% (v/v)	Formaldehyde
Developing solution (<i>ELISA</i>)	4.75	ml	NaAc pH 5.0
	0.25	ml	ABTS 2% (w/v)
	3.5	μl	H ₂ O ₂ 30% (v/v)
DNA-sample buffer (5x) (<i>DNA-gels</i>)	20	% (w/v)	glycerol in TAE buffer
	0,025	% (w/v)	orange G
Elution buffer (<i>Affinity Chromatography</i>)	0.1	M	Glycine pH 2.7
Elution buffer (<i>Serum purification</i>)	0.1	M	Citric Acid pH 3.0
Ethidiumbromide	10	μg/ml	ethidiumbromide in 1xTAE

III. Materials

staining solution

(DNA-gels)

Fixation solution	50	% (v/v)	Methanol
<i>(Silver Staining)</i>	5	% (v/v)	Acetic Acid
	45	% (v/v)	H ₂ O
Fixing solution	20	ml	Methanol
<i>(Coomassie Staining)</i>	79	ml	H ₂ O
	1	ml	o-Phosphoric acid 85%
Homogenisation buffer	0.32	M	Sucrose
<i>(Subfraction preparation)</i>	1	mM	CaCl ₂
	1	mM	MgCl ₂
	5	mM	Tris-HCl, pH 7.4
Ligation buffer (10x)	200	mM	Tris-HCl, pH 7,9
	100	mM	MgCl ₂
	100	mM	Dithiothreitol (DTT)
	6	mM	ATP
Neutralization buffer	1	M	Tris, pH 9.5
<i>(Affinity chromatography)</i>			
Oxidizing reagent	5	mg	Sodium Meta-periodate
<i>(Affinity chromatography)</i>			
Phosphate buffered saline	150	mM	NaCl
(PBS)	20	mM	Na ₃ PO ₄ pH 7.4
Phosphate buffered saline	150	mM	NaCl
Tween (PBS-T)	20	mM	Na ₃ PO ₄ pH 7.4
	0.05	% (v/v)	Tween 20
Roti-Blue staining	20	ml	Methanol
solution			

III. Materials

<i>(Coomassie Staining)</i>	20	ml	Roti-Blue 5 x concentrate
	60	ml	H ₂ O
Running Gel 10%	3.92	ml	deionized water
<i>(Protein gels)</i>	5.26	ml	1M Tris pH 8.8
	0.14	ml	10% SDS
	4.70	ml	30%Acrylamide–Bis 29:1
	70.0	μl	10% APS
	7.00	μl	TEMED
Sample buffer (5x)	0.312	M	Tris-HCl pH 6.8
<i>(Protein-gels)</i>	10	% (w/v)	SDS
	5	% (w/v)	β-Mercaptoethanol
	50	% (v/v)	Glycerol
	0.13	% (w/v)	Bromphenol blue
Sample buffer	0.02	M	Tris-HCl, pH 8.0
(Isolation of IgG fractions)	0.028	M	NaCl
	0.02	% (v/v)	NaN ₃
SDS running buffer (10x)	0.25	M	Tris-HCl, pH 8.3
<i>(Protein-gels)</i>	1.92	M	glycine
	1	M	SDS
Silvering buffer	0.1	% (w/v)	AgNO ₃
<i>(Silver Staining)</i>			
Stabilizing solution	20	g	Ammonium sulphate
<i>(Coomassie Staining)</i>			up to 100 ml H ₂ O
Stacking Gel 5%	3.77	ml	deionized water
<i>(Protein gels)</i>	0.32	ml	1 M Tris pH 6.8
	0.05	ml	10% SDS
	0.83	ml	30%Acrylamide

—

III. Materials

			Bis29:1
	25.0	μl	10% APS
	7.00	μl	TEMED
Stopping solution (Silver staining)	5	% (v/v)	Acetic acid
Stopping solution (ELISA)	1.25	% (w/v)	Sodium fluorid
Sentitising solution (Silver Staining)	0.02	% (w/v)	Sodium thiosulfate
Storage solution (Silver Staining)	1	% (v/v)	Acetic acid
Stripping buffer (Western blots)	0.5	M	NaCl
	0.5	M	acetic acid
Stock solution 1 (Membrane solubilization)	10	% (w/v)	n-octylβ-D-glucopyranoside
Stock solution 2 (Membrane solubilization)	10	% (w/v)	DTT
Stock solution 3 (Membrane solubilization)	10	% (w/v)	SDS
Sucrose stock solution (Subfraction preparation)	80	% (w/v)	Sucrose
TAE (50x) (DNA-gels)	2	M	Tris-Acetate, pH 8,0
	100	mM	EDTA

III. Materials

TE (10x)	0,1	M	Tris-HCl, pH 7,5
Tris plus buffer	1.25	ml	Tris-HCl, pH 7.4
<i>(Subfraction preparation)</i>	0.25	ml	1M CaCl ₂
	0.25	ml	1 MMgCl ₂
Tris Buffered Saline (TBS)	10	mM	Tris-HCl, pH 8.0
Washing buffer	25	ml	Methanol 99.8%
<i>(Coomassie Staining)</i>	75	ml	H ₂ O
Washing buffer	0.1	M	Acetic acid pH 3.0
<i>(Isolation of IgG fractions)</i>	1.4	M	NaCl

3. Bacterial media

(Media were autoclaved and antibiotics were supplemented prior to use)

LB-medium pH 7,4	10	g/l	Bacto-tryptone
	10	g/l	NaCl
	5	g/l	yeast extract
LB/Amp-medium	100	mg/l	ampicilin in LB-Medium
LB/Amp-plates	20	g/l	agar in LB-Medium
	100	mg/l	ampicillin

4. Bacterial strains and cell lines

CHO-K1	<i>Chinese Hamster Ovary</i> Dehydrofolatereductase deficient hamster cell line
--------	--

<i>Escherichia coli</i> DH5 α	Clonotech <i>deoR, endA1, gyrA96, hsdR17(r_k⁻m_k⁺), recA1, relA1, supE44, thi-1, Δ(lacZYA-argFV169), Φ80lacZΔM15, F⁻</i>
--------------------------------------	--

5. Cell culture media

Media were prepared from a 10X stock solution purchased from Gibco GBL

CHO-cell Medium	Glasgow MEM (GMEM) (with nucleotides, L-Glutamine) supplemented with 10 % (v/v) fetal calf serum (FCS) 50 U/ml Penicilline/Streptomycine 4 mM L-Glutamine
-----------------	--

Versene	Gibco GBL
---------	-----------

HBSS	Gibco GBL
------	-----------

6. Molecular weight standards

1kb DNA ladder	14 bands within the range from 200-10000 bp (Gibco)
----------------	--

BenchMark™	6 μ l of the <i>BenchMark Prestained Protein Ladder</i> (Invitrogen) were loaded on the SDS-PAGE gel
------------	--

Band No.	apparent molecular weight (kDa)
1	176.5
2	113.7
3	80.9
4	63.8*
5	49.5
6	37.4
7	26.0
8	19.6
9	14.9
10	8.4
*Orientation band (pink in color)	

7. Plasmids

pcDNA3 mammalian expression vector for transfection of eukaryotic cells. Amp-resistance (Invitrogen)

NCAM-Fc PIG mammalian expression vector for transfection of eukaryotic cells. Amp-resistance (gift of Dr. Jane L. Saffell, Department of Biochemistry, Imperial College, London, England)

8. Antibodies

8.1 Primary antibodies

anti-APP	mouse monoclonal antibody, recognized amino acids 66-8 N-terminus on the APP molecule, clone 22C11 (Chemicon) IB: 1:5000 (5% milk in TBS)
anti-APP	mouse monoclonal antibody, recognized amino acids 1-16 on the A β of APP molecule, clone W02 (A beta) IP: 1:100
anti-APP	rabbit polyclonal antibody against ICD of APP Immunocytochemistry: 1:100
anti-calreticulin	affinity-purified goat polyclonal antibody (Santa Cruz, clone sc-7431), raised against a peptide mapping at the amino terminus of calreticulin of mouse origin IB: 1:100 (5% milk in TBS) Immunocytochemistry: 1:10
anti-calreticulin	affinity purified rabbit generated against peptide QAKDEL on the C-terminus of calreticulin IP: 1:15
anti-calreticulin	goat polyclonal antibody made against rabbit skeletal muscle calreticulin Immunocytochemistry: 1:50
anti-creatine kinase B	affinity-purified goat polyclonal antibody (Santa Cruz, clone sc-15160), raised against a

	peptide mapping at the carboxy terminus of creatine kinase B of human origin IB: 1:100 (5% milk in TBS) Immunocytochemistry: 1:10 IP: 1:10
anti-L1	mouse monoclonal antibody clone 4.1.1.3.3 raised against human L1 (BD Technologies) ELISA: 1:1000 in PBS IB: 1:1000 (5% milk in TBS)
anti-L1	rabbit polyclonal antibody raised against human L1 (Lab As Ltd, Tartu, Estonia) ELISA: 1:4000 in PBS IB: 1:4000 (5% milk in TBS)
anti-NCAM	monoclonal antibody clone 14.2 raised against human NCAM (BD Technologies) ELISA: 1:1000 in PBS IB: 1:1000 (5% milk in TBS)
anti-NCAM	rabbit polyclonal antibody produced against human NCAM (BD Technologies) ELISA: 1:1000 in PBS IB: 1:1000 (5% milk in TBS)
anti-PSA	monoclonal antibody clone 735 produced against PSA ELISA: 1:700 in PBS
anti-versican	rabbit polyclonal antibody raised against human recombinant versican (isoform V1, produced in the lab of Richard G. LeBaron) IB: 1:100 (5% milk in TBS) Immunocytochemistry: 1:100

IP: 1:30

anti- β -secretase cleavage site of APP	rabbit antibody raised against the synthetic antisense peptide C (generated by Frank Plöger)
---	--

IB: 1:1000 (5%Milk in TBS)

anti- γ -secretase cleavage site of APP	rabbit antibody raised against the synthetic antisense peptide D (generated by Frank Plöger)
--	--

IB: 1:1000 (5%Milk in TBS)

8.2 Secondary antibodies

All horseradish-coupled secondary antibodies were purchased from Dianova and used in a dilution of 1:7.000.

For immunocytochemistry, Cy2, Cy3 and Cy5, secondary antibodies were obtained from Dianova and used in a dilution of 1:100.

9. Peptides

9.1 Antisense peptides

Peptide C (β -cleavage site of APP) sequence:

NH₂ - Val - Met - Ser - Glu - Leu - Cys - Ile - His - Leu - His - Phe - Arg - Asp - Leu - Leu - COOH

Peptide D (γ -cleavage site of APP) sequence:

NH₂ - Gln - Gly - Asp - Asp - Asp - His - Cys - Arg - Tyr - Asp - Asn - Thr - Ala - His - His - COOH

9.2 Biotinylated peptides

Peptide APP1 (γ -cleavage site of APP) sequence:

Biotin-SNKGAIIGLMVGGVVIATVIVITLVMLKKKC-OH

Peptide APP2 (β -cleavage site of APP) sequence:

Biotin-TNIKTEEISEVKMDAEFGHDSGFEVRHQKC-OH

IV. Methods

1. Protein-biochemical methods

1.1 SDS-polyacrylamide gel electrophoresis

Separation of proteins was performed by means of the discontinuous SDS-polyacrylamide gel electrophoresis (SDS-PAGE) using the Mini-Protean III system (BioRad). The size of the running and stacking gel were as follows:

Running gel: height 4.5 cm, thickness 0.75 mm
 8 % or 10 % acrylamide solution

Stacking gel: height 0.8 cm, thickness 0.75 mm
 5% (v/v) acrylamide solution
 10 or 15-well combs

After complete polymerization of the gel, the chamber was assembled as described by the manufactures protocol. Up to 25 µl sample were loaded in the pockets and the gel was run at constant voltage at 80 V for 15 min and then for the rest at 120V. The gel run was stopped when the bromphenolblue line had reached the end of the gel. Gels were then either stained or subjected to Western Blotting.

1.2 Western Blot-analysis

1.2.1 Electrophoretic transfer

Proteins were transferred from the SDS-gel on a Nitrocellulose membrane (Protran Nitrocellulose BA 85, 0,45 µm, Schleicher & Schüll) using a MINI TRANSBLOT-apparatus (BioRad). After equilibration of the SDS-PAGE in blot buffer for 5 min, the blotting sandwich was assembled as described in the manufactures protocol. Proteins were transferred electrophoretically at 4°C in blot buffer at constant voltage (90 V for 120 min or 35 V overnight). The prestained marker BenchMark™ (Gibco BRL) was used as a molecular weight marker and to monitor electrophoretic transfer.

1.2.2 Immunological detection of proteins on Nitrocellulose membranes

After electrophoretic transfer, the membranes were removed from the sandwiches and placed protein-binding side up in glass vessels. Membranes were washed once in TBS and incubated in 10 ml blocking buffer for 1 h at room temperature. Afterwards, the primary antibody was added in the appropriate dilution either for 2 h at RT or overnight at 4°C. The primary antibody was removed by washing the membrane 5 x 5 min with TBS. The appropriate secondary antibody was applied for 1 h at RT. The membrane was washed again 5 x 5 min with TBS and immunoreactive bands were visualized using the enhanced chemiluminescence detection system (ECL).

1.2.3 Immunological detection using enhanced chemiluminescence

The antibody bound to the membrane was detected using the enhanced chemiluminescence detection system (Pierce). The membrane was soaked for 1 min in detection solution (1:1 mixture of solutions I and II). The solution was removed and the blot was placed between two saran wrap foils. The membrane was exposed to X-ray film (Biomax-MR, Kodak) for several time periods, starting with a 5 min exposure.

1.3 Coomassie staining of polyacrylamide gels

The colloidal Coomassie staining of polyacrylamide gels were performed with Roti-Blue kit (Carl Roth GmbH + Co). After SDS-PAGE, the gels were fixed in fixing solution for 60 min and subsequently incubated with Roti-Blue staining solution for 2-15 h with constant agitation. The gels were then incubated in destaining solution until the background of the gel appeared nearly transparent.

1.4 Silver staining of polyacrylamide gels

After SDS-PAGE, gels were fixed with acetic acid/methanol solution for 30 min, intensively washed and quickly rinsed with freshly prepared thiosulfate solution. Afterwards, gels were silvered for 30 min at 4°C, washed and developed with

formaldehyde/sodium carbonate solution. When a sufficient degree of staining has been obtained, reaction was stopped with 5% acetic acid.

1.5 Determination of protein concentration (BCA)

The protein concentration assay was determined using the BCA kit (Pierce). Solution A and B were mixed in a ratio of 1:50 to give the BCA solution. 10 µl of the sample were mixed with 200 µl BCA solution in microtiter plates and incubated for 30 min at 37°C. A BCA standard curve was co-incubated ranging from 0.1 mg/ml to 2 mg/ml. The extinction of the samples was determined at 560 nm in a microtiter plate reader.

1.6 Enzyme-linked immunosorbent assay (ELISA), binding assay

Several antigens were immobilized on polyvinylchloride surface in 96-well microtiter plate in concentration 5-10 µg/ml for overnight at 4°C. Non-absorbed proteins were removed, the wells were washed five times for 5 min with TBS-T and blocked for one hour at RT with 2% BSA in TBS. After washing, the wells were subsequently incubated with the putative binding proteins diluted in a wide range (70 ng/ml to 20 µg/ml) in TBS-T containing 1%BSA, 1mM CaCl₂, 1mM MgCl₂ and 1mM MnCl₂ for a further hour at RT. Non-bound proteins were removed and the wells were washed five times for 5 min at RT to remove unspecifically bound proteins. Specifically bound proteins were detected with streptavidin coupled to horseradish peroxidase or with certain primary antibodies and the appropriate HRP-linked secondary antibodies. Protein binding was visualized by the detection reaction of HRP with ABTS reagent that resulted into a coloured product that was quantified using ELISA reader at 405 nm.

1.7 Capture ELISA

Monoclonal capture antibody in appropriate concentration was pipetted into each well of 96-well microplates and incubated overnight at 4°C. The plate was washed five times with PBS-T and blocked with a 5% solution of nonfat dry milk in PBS for 1.5h at 37°C. Protein standards in appropriate concentration were prepared freshly for each test from a frozen

stock solution in serial two-fold dilutions. Each well was loaded with standard or CSF test sample and incubated for 1.5 h at RT. The detector antibodies in concentration 1.5µg/ml were loaded into each well and incubated for 20 h at RT. After washing, peroxidase-labeled goat anti-rabbit IgG antibody (0.16µg/ml) was loaded into each well and incubated for 1.5 h at RT. ABTS was added for colometric detection. The enzymatic reaction was stopped with 1.25% sodium fluoride and absorbance values were measured an ELISA reader at 405 nm.

1.8 Preparation of membrane subfractions

Brains were prepared from adult mice of different ages. Mice were decapitated, brains were removed from skulls and immediately transferred into a Dounce homogenizer (Wealton, Teflon pestle, 0.1µm). All following steps were carried out at 4⁰C. Brains were homogenized in 3 ml of homogenisation buffer applying 12 up-and-down. The homogenate was centrifuged (1.400 x g, 10 min, 4⁰C) and supernatant was further centrifuged at 17.500 x g for 15 min. The resulting pellet was resuspended in homogenisation buffer and was applied on the top of a sucrose step gradient (1.2 M, 1.0 M, 0.85 M, 0.65 M), whereas supernatant (soluble fraction) was collected and stored at -20⁰C until the further analysis was performed. The 1.400 x g-pellet was resuspended in homogenisation buffer and the sucrose concentration was adjusted to 1 M using 2.34 M sucrose stock solution. This solution was laid on 1.2 M sucrose and was overlaid with homogenisation buffer. The sucrose gradients were ultracentrifuged at 25.000 rpm for 1 h using SW 28 rotor. The bands at the 1.0/1.2 M interfaces which contained synaptosomes (Syn 1) and synaptosomes from Mossy Fibers (Syn 2) respectively were collected, diluted at least two times with homogenisation buffer and subsequently centrifuged at 25.000 rpm for 30 min. The pellets were resuspended in Tris plus buffer and incubated for 30 min on ice in order to osmotically shock the synaptosomes. Membranes were isolated by centrifugation at 25.000 rpm for 20 min, resuspended in 5mM Tris pH 7.4, applied to a sucrose step gradient (1.2 M, 1.0 M, 0.85 M, 0.65 M) and centrifuged at 25.000 rpm for 1 h. The bands at the 1.0/1.2 M interfaces which contained synaptosomal membranes were collected, diluted at least two times with 5mM Tris pH 7.4 and centrifuged at 25.000 rpm for 30 min. The membranes were resuspended in Tris plus and incubated for 30 min on ice in presence of 0.6 M NaHCO₃, pH 10 and 5mM EDTA. Treated membranes were applied to a sucrose step gradient containing 150 mM NaHCO₃ pH 10 and 5mM EDTA, and

centrifuged at 25.000 rpm for 1 h. The bands at the 1.0/1.2 M interfaces which contained synaptosomal membranes were collected, diluted at least two times with 5mM Tris pH 7.4 and centrifuged at 25.000 rpm for 30 min. The resulting pellet was resuspended in 3 ml of 5 mM Tris pH 7.4 and used for further analysis.

1.9 Solubilisation of membrane fractions

Syn 1 and Syn 2 Triton-insoluble membrane fractions were diluted in two times with 5 mM Tris pH 7.4 and incubated on ice for 1 h in presence of 1% n-octyl β -D-glucopyranoside. Afterwards fractions were centrifuged (15000 x g, 30 min, 4⁰C) and supernatant was collected. The pellet was resuspended in 5 mM Tris pH 7.4 and incubated on ice for 1 h in presence of 2% of n-octyl β -D-glucopyranoside. Fractions were centrifuged as described and supernatant was collected. The pellet was resuspended in 5 mM Tris pH 7.4 and incubated on ice for 1 h in presence of 5% of n-octyl β -D-glucopyranoside. After centrifugation supernatant was collected, pellet was resuspended in 5 mM Tris pH 7.4 and incubated at 95⁰C for 5 min in presence of 1%SDS and 1%DTT. Fractions were then cooled down, centrifuged (15000 x g, 15 min, 4⁰C), and supernatant was collected. The pellet was resuspended in 5 mM Tris pH 7.4 and treated as above in presence of 5%SDS and 2%DTT. After centrifugation supernatant was collected and pellet was resuspended in 5 mM Tris pH 7.4. All fractions were stored for further analysis.

1.10 Isolation of IgG fractions

For isolation of IgG fractions the DEAE Affi-Gel Blue Gel kit (Bio-Rad) was used according to the instruction manual. In brief, a column of DEAE Affi-Gel Blue gel with a total bed volume of 7 ml gel per milliliter of the serum to be processed was prepared. Gel was prewashed with at least 5 bed volumes of 0.1 M acetic acid, pH 3.0, containing 1.4 M NaCl and 40% (v/v) isopropanol and equilibrated with at least 12 bed volumes of sample buffer (0.02 M Tris-HCl, pH 8.0, 0.028 M NaCl, 0.02%NaN₃). Rabbit serum, dialysed against appropriate buffer (0.02 M Tris-HCl, pH 8.0, 0.028 M NaCl, 0.02%NaN₃), was applied to the column and unbound material was eluted with 3 bed volumes of buffer. The eluted fractions containing the purified IgG protein, as determined photometrically by

their absorption at 280 nm, were then pooled and their protein concentration was determined using BCA Protein Assay Kit (Pierce).

1.11 Affinity chromatography

Coupling of purified IgG fractions to CarboLink columns and subsequent affinity purification of soluble or membrane fractions of mouse brain homogenate were performed as described in the CarboLink Kit (Pierce) instruction manual. Briefly, 4-8 mg of purified IgG (derived from rabbit antiserum against antisense peptide C and D) was applied to the Desalting Column in order to perform a buffer exchange. The eluted fractions containing IgG protein in coupling buffer were concentrated until 2 ml and applied to the CarboLink columns. The coupling reaction was done overnight at 4°C.

For affinity purification 1 ml of sample was loaded into the CarboLink columns with immobilized purified IgG. The columns were then incubated for 60 min at RT, washed with appropriate sample buffer in order to remove unbound material and eluted with 0.1 M glycine pH 2.5. Fractions of 1 ml were collected and neutralized by addition of 50 µl of 1M Tris-HCl, pH 9.5. The eluted fractions containing the purified protein, as determined photometrically by their absorption at 280 nm, were then pooled, dialysed against the PBS buffer containing 0.1% of n-octyl β-D-glucopyranoside, concentrated until 200 µl and stored at -20°C.

1.12 Sample preparation for protein sequencing

Protein samples were subjected to SDS gel electrophoresis followed by Coomassie staining, but in order to avoid accidental contamination, all reagents and solutions were freshly prepared using autoclaved pipette tips, and each step requiring direct handling was performed with a new pair of disposable gloves and in closed containers, when possible. Following SDS gel electrophoresis, the gel was placed under an acrylic glass cover to allow safe handling, each stained band to be sequenced was cut out from the gel with a sterile scalpel, placed into the 1.5 ml centrifuge tube and covered with storage solution. Afterwards, the samples were sent for sequencing.

1.13 Purification of rabbit IgG using protein A

Freeze-dried Protein A sepharose was rewollen and prepared as described in the manufacture protocol. The protein A column was equilibrated with PBS (flow rate 10 to 20 ml/h). Serum diluted in PBS 1:2 was applied and passed through the protein A column. After washing with PBS bound IgGs were eluted with 0.1 M citric buffer pH 3.0 and neutralized with 1 M Tris pH 8.0. Buffer was exchanged against PBS using centricon 50 columns and protein concentration was determined using the BCA kit (Pierce).

1.14 Immunoprecipitation

For immunoprecipitations protein A/G agarose beads were used. The crude homogenate or synaptosomes were incubated for 40 min at 4°C in the presence of 1% n-octyl β -D-glucopyranoside. After centrifugation at 1000 x g the supernatant was collected and incubated with appropriate amounts of respective antibodies on a rocking platform for at least 3 hours at 4°C. Afterwards 50 μ l of the homogeneous protein A/G-suspension were added to the mixture and incubated overnight at 4°C on a rocking platform. Beads were pelleted at 1000 x g, supernatant was carefully removed and the beads were subsequently washed three times with ice-cold PBS containing 1% n-octyl β -D-glucopyranoside for 10 min, and one time with PBS. 40 μ l of gel-loading buffer was added to the beads, and the proteins were denaturated by heating at 95 °C for 5 min. The beads were pelleted by centrifugation and the supernatant was collected and applied to SDS-PAGE.

2. Molecular biology

2.1 Bacterial strains

2.1.1 Maintenance of bacterial strains

Strains were stored as glycerol stocks (LB-medium, 25% (v/v) glycerol) at –70°C.

An aliquot of the stock was streaked on an LB-plate containing the appropriate antibiotics and incubated overnight at 37°C. Plates were stored up to 6 weeks at 4°C.

2.1.2 Production of competent bacteria

DH5 α bacteria were streaked on LB-plates and grown overnight at 37°C. 50 ml of LB-medium was inoculated with 5 colonies and grown at 37°C until the culture had reached an optical density (OD₆₀₀) of 0.3-0.5.

2.1.3 Transformation of bacteria

To 100 μ l of competent DH5 α either 50-100 ng of plasmid DNA or 20 μ l of ligation mixture were added and incubated for 30 min on ice. After a heat shock (2 min, 42°C) and successive incubation on ice (3 min), 800 μ l of LB-medium were added to the bacteria and incubated at 37°C for 30 min. Cells were then centrifuged (10000 x g, 1 min, RT) and the supernatant removed. Cells were resuspended 100 μ l LB medium and plated on LB plates containing the appropriate antibiotics. Plates were incubated at 37°C overnight.

2.2 Plasmid isolation of E. coli

2.2.1 Plasmid isolation from 3 ml cultures (Minipreps)

(see Amersham Pharmacia Mini preparation kit)

3 ml LB/Amp-Medium (100 μ g/ml ampicillin) were inoculated with a single colony and incubated over night at 37°C with constant agitation. Cultures were transferred into 2 ml Eppendorf tubes and cells were pelleted by centrifugation (12,000 rpm, 1min, RT). Plasmids were isolated from the bacteria according to the manufactures protocol. The DNA was eluted from the columns by addition of 50 μ l Tris-HCl (10 mM, pH 8.0) with subsequent centrifugation (12,000 rpm, 2 min, RT).

2.2.2 Plasmid isolation from 15 ml-cultures

To obtain rapidly higher amounts of DNA, the Macherey-Nagel Nucleospin kit was used. 15 ml LB/Amp-Medium (100 μ g/ml ampicillin) were inoculated with a single colony and incubated over night at 37°C with constant agitation. Cultures were transferred into 15 ml

Falcon tubes and cells were pelleted by centrifugation (12,000 rpm, 1min, RT) in an eppendorf centrifuge. Plasmids were isolated from the bacteria according to the manufactures protocol with the exception that twice the suggested amount of buffers were used. DNA was eluted from the columns by adding twice 50 µl of prewarmed (70°C) TrisHCl (10 mM, pH 8.0) with subsequent centrifugation (12,000 rpm, 2 min, RT). Finally, the concentration was determined.

2.2.3 Plasmid isolation from 500 ml-cultures (Maxipreps)

(See Qiagen Maxiprep kit)

For preparation of large quantities of DNA, the Qiagen Maxiprep kit was used. A single colony was inoculated in 2 ml LB/amp (100 µg/ml ampicillin) medium and grown at 37°C for 8 h with constant agitation. Afterwards, this culture was added to 500ml LB/amp medium (100 µg/ml ampicillin) and the culture was incubated at 37°C with constant agitation overnight. Cells were pelleted in a Beckmann centrifuge (6,000g, 15 min, 4°C) and DNA was isolated as described in the manufactures protocol. Finally, the DNA pellet was resuspended in 600 µl of prewarmed (70°C) Tris-HCl (10 mM, pH 8.0) and the DNA concentration was determined.

2.3 Enzymatic modification of DNA

2.3.1 Digestion of DNA

For restriction, the DNA was incubated with twice the recommended amount of appropriate enzymes in the recommended buffer for 2 h. Restriction was terminated by addition of sample buffer and applied on agarose gel. If two enzymes were incompatible with each other, the DNA was digested successively with the enzymes. The DNA was purified between the two digestions using the rapid purification kit (Life technologies).

2.3.2 Dephosphorylation of Plasmid-DNA

After restriction the plasmid DNA was purified and SAP buffer (Boehringer Ingelheim) and 1 U SAP (s_{cr}imps a_lkine p_hosphatase) per 100 ng plasmid DNA were added. The reaction was incubated at 37°C for 2 h and terminated by incubation at 70°C for 10 min. The plasmid DNA was used for ligation without further purification.

2.3.3 Ligation of DNA-fragments

Ligation of DNA fragments was performed by mixing 50 ng vector DNA with the fivefold molar excess of insert DNA. 1 µl of T4-Ligase and 2 µl of ligation buffer (both Boehringer Ingelheim) were added and the reaction mix was brought to a final volume of 20 µl. The reaction was incubated either for 2 h at room temperature or overnight at 16°C. The reaction mixture was used directly for transformation without any further purification.

2.4 DNA Gel-electrophoresis

DNA fragments were separated by horizontal electrophoresis chambers (BioRad) using agarose gels. Agarose gels were prepared by heating 1-2 % (w/v) agarose (Gibco) in 1xTAE buffer, depending on the size of DNA fragments. The gel was covered with 1xTAE buffer and the DNA samples were pipetted in the sample pockets. DNA sample buffer was added to the probes and the gel was run at constant voltage (10V/cm gel length) until the orange G dye had reached the end of the gel. Afterwards, the gel was stained in an ethidiumbromide staining solution for 20 min. Finally gels were documented using a UV-light imaging system.

2.5 Extraction of DNA fragments from agarose gels

(Rapid gel extraction kit, Life technologies)

For isolation and purification of DNA fragments from agarose gels, ethidiumbromide-stained gels were illuminated with UV-light and the appropriate DNA band was excised from the gel with a clean scalpel and transferred into an Eppendorf tube. The fragment

was isolated following the manufactures protocol. The fragment was eluted from the column by addition of 50 µl prewarmed (70°C) Tris-HCl (10 mM, pH 8.0). The DNA-concentration was determined using the undiluted eluate.

2.6 Purification of DNA fragments

(Rapid PCR Purification kit, Life technologies)

For purification of DNA fragments the Rapid PCR Purification kit was used according to the manufactures protocol. The DNA was eluted from the column by addition of 50 µl prewarmed (70°C) Tris-HCl (10 mM, pH 8.0). The DNA-concentration was determined using the undiluted eluate.

2.7 Determination of DNA concentrations

DNA concentrations were determined spectroscopically using an Amersham-Pharmacia spectrometer. The absolute volume necessary for measurement was 50 µl. For determining the concentration of DNA preparations (III 1.2), the eluate was diluted 1:50 with water and the solution was pipetted into a 50 µl cuvette. Concentration was determined by measuring the absorbance at 260 nm, 280 nm and 320 nm. Absorbance at 260 nm had to be higher than 0.1 but less than 0.6 for reliable determinations. A ratio of A_{260}/A_{280} between 1,8 and 2 monitored a sufficient purity of the DNA preparation.

2.8 DNA-Sequencing

(Step-by-Step protocols for DNA-sequencing with Sequenase-Version 2.0, 5th ed., USB, 1990)

DNA sequencing was performed by the sequencing facility of the ZMNH. For preparation, 1 µg of DNA was diluted in 7µl ddH₂O and 1 µl of the appropriate sequencing primer (10 pM) was added.

3. Cell culture

3.1 CHO cell culture

CHO cells were cultured in GMEM with 10 % FCS (fetal calf serum) and 2% Penicillin/Streptomycin (P/S) 37°C, 5 % CO₂ and 90 % relative humidity in 75 cm² flasks (Nunc) with 15 ml medium or in six-well plates (d = 35 mm; area = 9,69 cm²) with 2 ml medium. Cells were passaged when they were confluent (usually after 3-4 days). Medium was removed and cells were detached by incubation with 4 ml versene for 5 min at 37°C. Cells were centrifuged (200xg, 5 min, RT) and the pellet was resuspended in 10 ml fresh medium. Cells were split 1:10 for maintenance or seeded in six-well plates for transfection (300 µl per well).

3.2 Stable transfection of CHO-cells

(Lipofectamine Plus manual, Life technologies)

For transfection of CHO cells, the Lipofectamine Plus kit (Life Technologies) was used. One day before transfection, 2×10^5 cells were seeded per 35 mm dish. When cell density had reached 60-70% (usually after 18-24 h) the cells were washed with GMEM Ø FCS and antibiotics and transfected with 2 µg total DNA (pcDNA3 expressing vector, containing NCAM gene encoding the human NCAM-Fc was used) per 35 mm well. Transfection was performed as described in the manufactures protocol. Transfection was terminated after 3 h by addition of an equal volume of GMEM, 10 % FCS and 2% PS. 24 h after transfection, cells were detached with 500 µl versene per well and seeded in bigger dish. Next day the medium was exchanged against selection medium containing gentamycin (*f.c.* 0.8 mg/ml). The cells grow during 2-3 weeks in selection medium, which was changed every 2-3 days, until the single clones appeared. Single clones were then picked and placed into the 96-wells plate. Clones were cultured as described above, frozen and stored at -80°C.

3.3 Cell culture of stable transfected CHO cells

CHO cells were cultured in GMEM with 10% FGS (fetal calf serum) and 2% Penicillin/Streptomycin (P/S) 37°C, 5 % CO₂ and 90 % relative humidity in 75 cm² flasks (Nunc) with 15 ml medium. Cells were passaged when they were confluent as described above. For production of NCAM-Fc, cells were seeded in 175 cm² flasks and medium was exchanged against GMEM containing 2% ultra low IgG FCS with gentamycin (*f.c.* 0.015 mg/ml) and L-glutamine (*f.c.* 2mM).

3.4 Preparation of dissociated hippocampal cultures

For preparation of dissociated hippocampal cultures, mice of postnatal day 1 – 4 were used. Hippocampi were prepared by Galina Dityateva. Preparations were performed as described (Brewer et al., 1993; Lochter et al., 1991)

In brief, the procedure was performed as followed:

1) Dissection

Mice were decapitated and brains removed from skull. Brains were cut out along the midline, hippocampi were prepared and split into 1mm thick pieces.

2) Digestion

Hippocampi were washed twice with dissection solution and treated with trypsin and DNaseI for 5 min at RT. Digestion solution was removed, hippocampi were washed twice and the reaction was stopped by adding trypsin inhibitor.

3) Dissociation

Hippocampi were resolved in dissection solution containing DNaseI. Titration with Pasteur pipettes having successively smaller diameters dissociated hippocampi to homogeneous suspensions.

4) Removal of cell debris and plating of cells

By subsequent centrifugation (80 x g, 15 min, 4°C) and resuspension in dissection buffer, cell debris was removed. Cells were counted in a Neubauer cell chamber and plated to provide a density of 1.000 cells/mm².

4. Immunocytochemistry

4.1 Fixation of hippocampal neurons

The medium was removed from the coverslips and cells were fixed with 1 ml of warmed 4% para-formaldehyde in PBS for 10 min at RT. Cells were washed twice with PBS and stored in PBS at 4°C.

4.2 Immunocytochemistry of fixed hippocampal neurons

Coverslips were placed on Parafilm in a humid chamber and incubated with 100 µl blocking buffer for 1 h at RT. The blocking buffer was removed by aspiration and the coverslips were covered with 100µl antibody solution containing the appropriate primary antibody and incubated overnight at 4°C in a humid chamber. Coverslips were washed three times with PBS and incubated with 100µl antibody solution containing the fluorescent dye-labeled secondary antibody (Cy2, Cy3, Cy5) for 1 h at room temperature in the dark. Finally, cells were washed three times with PBS and mounted on objectives with Aqua Poly-Mount medium (Polysciences Inc). Coverslips were stored in the dark at 4°C.

4.3 Co-capping on hippocampal neurons

The coverslips with leaving neurons were washed briefly with medium and incubated for 20 min at 37°C with 100µl solution containing the appropriate primary antibody. Afterwards the coverslips were washed for three times with medium and one time with PBS and incubated with appropriate secondary antibodies for 15 min at 37°C. After washing the neurons were fixed with 1 ml of warmed 4% para-formaldehyde and subjected for immunocytochemistry as described above.

4.4 Confocal laser-scanning microscopy

All images of hippocampal neurons were obtained with a Zeiss LSM510 argon-crypton confocal laser-scanning microscope equipped with a 60x oil-immersion objective lens. Images were scanned with a resolution of 512x512. Detector gain and pinhole were adjusted to give an optimal signal to noise ratio.

5. Clinical methods

5.1 Patients and collection of cerebrospinal fluid

CSF were collected by Dr. Buhmann, Dr. Eggers and Dr. Müller-Thomsen (Department of Neurology and Psychiatry, University Hospital Hamburg). 218 patients with different neurological diseases, including Alzheimer disease (AD), vascular dementia (VD), dementia of mixed type (MT), diffuse Lewy body dementia (DLBD), multiple system atrophy (MSA), Parkinson's disease (PD), major and minor depression, multiple sclerosis (MS), epilepsy, amyotrophic lateral sclerosis (ALS), polyneuropathy (PNP), progressive supranuclear palsy PSP, Pick's disease, hydrocephalus, schizophrenia, paranoia, epidural hematoma, cervical osteochondrosis, herpes zoster infection, spinal muscular atrophy, paraneoplastic encephalopathy were examined in this study. In addition, normal controls without any confirmed neurological or neuropsychiatric diseases were studied.

Clinical diagnoses were made according to published criteria: Alzheimer disease and dementia of mixed type (McKhann et al., 1984), vascular dementia (Roman et al., 1993), multiple sclerosis (McDonald et al., 2001), multiple system atrophy (Gilman et al., 1999), Parkinson's disease (UK Parkinson's Disease Society Brain Bank criteria (Gibb and Lees, 1988), diffuse Lewy bodies dementia (McKeith, 2002) or to general neurological practice, e.g. epilepsy, amyotrophic lateral sclerosis or polyneuropathy.

Dementia was diagnosed by standard clinical procedures and the degree defined by the score in the Mini Mental State Examine (MMSE) (Folstein et al., 1975). A score of 30 to 27 points was classified as non-demented, 26 to 20 as mildly demented, 19 to 10 points as moderately demented, and 9 to 0 points as severely demented.

Normal controls underwent lumbar puncture to collect cerebrospinal fluid (CSF) for diagnostic purpose, for instance to exclude subarachnoid hemorrhage, and revealed no signs for any disease of the central or peripheral nervous systems and were inconspicuous

for protein levels, albumin quotient, cell count, oligoclonal bands, immunoglobulins, glucose, lactate, lysozyme, neuron-specific enolase and copper.

Cerebrospinal fluids (CSF) were collected by lumbar puncture between L4 and L5. Patients were in supine position for two hours before puncture. CSF were taken in 1 ml fractions in polypropylene tubes immediately frozen and stored at -80°C until biochemical analyses were performed. Informed consent according to the declaration of Helsinki was obtained before lumbar puncture and the study was approved by the Ethical Committee of the City of Hamburg.

6. Computer analysis

6.1 Sequence analysis

Computer based sequence analysis and alignments of DNA sequences and protein sequences was performed using the Lasergene-programe (DNASTAR, *Inc.*, www.dnastar.com). The following databases were used: Medline-, BLASTN- and BLASTP-Server of NCBI (National Center for Biotechnology Information, www.ncbi.nlm.nih.gov).

6.2 Statistical analysis

Comparisons between different patients groups were performed using the non-parametric Kruskal-Wallis test. The level of statistical significance was set at 0.05. Normal distribution of CSF parameters for dementia/non-dementia and neurodegeneration/non-neurodegeneration groups was confirmed using the Kolmogorov-Smirnov test. Between-group differences in discontinuous variables were analyzed by Student's t-test for independent groups. Correlations were analyzed by Pearson Product Moment Correlations. ANOVA with age as co-variant was used to explore the extent to which values were specifically influenced by age. Post hoc analysis was done with the Scheffé-test. Additionally we estimated the influence of presence of dementia, neurodegeneration, gender and age on L1, NCAM and polysialic acid by multiple regression analysis including measurement of partial correlation of independent variables. Results are expressed as mean \pm standard error.

V. Results

Study 1: Identification and characterization of putative binding partners of Amyloid Precursor Protein (APP)

1. Identifying proteins involved in APP proteolysis

In order to exploit the concept of complementary hydrophathy to identify proteins potentially involved in the cleavage of APP, antisense peptides (Figure 1) which complement the amyloid precursor protein's amino acid structure at the β - and γ - cleavage sites have been constructed. This has been done with 15mers by Dr. Frank Plöger.

A

APP sequence

N	E	E	I	S	E	V	K	M	D	A	E	F	R	H	D	C
5'	gag	gag	atc	tct	gaa	gtg	aag	atg	gat	gca	gaa	ttc	cga	cat	gac	3'
3'	ctc	ctc	tag	aga	ctt	cac	ttc	tac	cta	cgt	ctt	aag	gct	gta	ctg	5'
C	L	L	D	R	F	H	L	H	I	C	L	E	S	M	V	N

Complementary sequence

B

APP sequence

N	M	V	G	G	V	V	I	A	T	V	I	V	I	T	L	C
5'	atg	gtg	ggc	ggc	gtt	gtc	ata	gcg	aca	gtg	atc	gtc	atc	acc	ttg	3'
3'	tac	cac	ccg	cca	caa	cag	tat	cgc	tgt	cac	tag	cag	tag	tgg	aac	5'
C	H	H	A	T	N	D	Y	R	C	H	D	D	D	G	Q	N

Complementary sequence

Figure 1: Antisense peptides constructed according to the principle of complementary hydrophathy to complement the amyloid precursor protein's amino acid structure at the β - and γ - cleavage sites

Antisense peptide C complement the β - cleavage site of the APP.

Antisense peptide D complement the γ - cleavage site of the APP.

Amino acids correspondent to cleavage sites are highlighted in boldface type.

According to the theory of complementary hydrophathy, these antisense peptides complement the APP “receptor” and should therefore mimic its binding partners and/or functionally interacting proteins. Antibodies raised against these peptides are expected to recognize ligands and binding partners of amyloid precursor protein.

2. Characterization of the antibodies

IgG fractions of the two rabbit antisera raised against antisense peptides were isolated by removing albumin and other serum proteins using Bio-Rad DEAE Affi-Gel Blue Gel. The purified antibodies were tested then by Western blot using mouse brain homogenate and the brain subfractions prepared by ultracentrifugation in sucrose gradient. In order to prepare subfractions, brain homogenate was centrifuged at 1.400 x g and supernatant was further centrifuged at 17.500 x g. The resulting pellet was resuspended and applied on the top of a sucrose step gradient (1.2 M, 1.0 M, 0.85 M, 0.65 M), whereas the 1.400 x g pellet was resuspended and the sucrose concentration was adjusted to 1 M. This solution was laid on 1.2 M sucrose and was overlaid with homogenisation buffer. After ultracentrifugation of sucrose gradients at 25.000 rpm the bands at the 1.0/1.2 M interfaces which contained synaptosomes, as well as the light fraction contained myelin, were collected. Thus, the following brain subfractions were used for Western blot analysis with purified antibodies: myelin, synaptosomal subfractions Syn 1 (prepared by applying of pellet from centrifugation at 17500g in sucrose gradient) and Syn 2 (prepared by applying of pellet from centrifugation at 1400g in sucrose gradient). The last one possibly contains synaptosomes from mossy fibers. The Western blot analysis of the whole brain homogenate using purified antisense antibody of the γ -cleavage site of APP revealed several bands (Figure 2A), whereas three bands of molecular weight around 60 kDa were specifically recognized in brain subfractions by this antibody (Figure 2B). The purified antisense antibody of the β -cleavage site of APP showed more specific reactivity and recognized the single band of approximately 40 kDa in brain subfractions (Figure 2C).

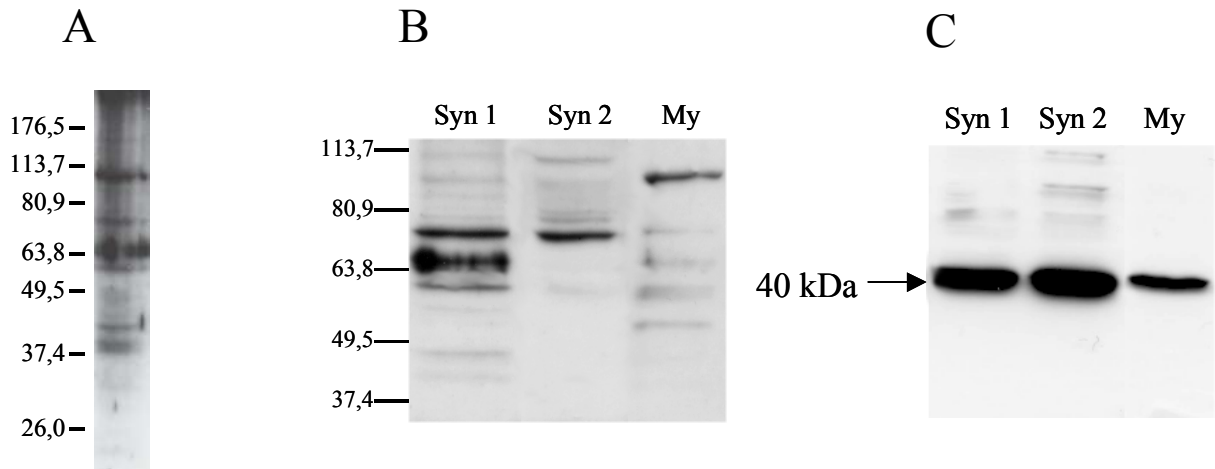


Figure 2: Specificity of the antisense antibodies of γ - and β -cleavage sites of APP after purification using Bio-Rad DEAE Affi-Gel Blue Gel

(A) Western blot of mouse brain homogenate (5mg per line) using the antisense antibody of the γ -cleavage site. (B) Western blot analysis showing the specificity of antisense antibody of the γ -cleavage site in synaptosomal and myelin fractions from brain homogenate of adult mice. (C) Western blot analysis showing the specificity of antisense antibody of the β -cleavage site in synaptosomal and myelin fractions from mouse brain homogenate. Molecular weights are indicated on the left.

3. Organ specificity of identified proteins

In order to determine the expression of the identified proteins in organs other than brain, different organs of a wild type adult mouse were homogenized and analysed by Western blot analysis. The 60 kDa protein, recognized in brain subfractions by antisense antibody of the γ -cleavage site, is expressed uniformly in all tissues (investigated data not shown). Furthermore, there was no significant difference in expression level of this protein (data not shown). Whereas the 40 kDa protein, recognized in brain subfractions by antisense antibody of the β -cleavage site, was detected exclusively in brain and to a lower degree in kidney, and traces of this protein were seen in skeletal muscle (Figure 3).

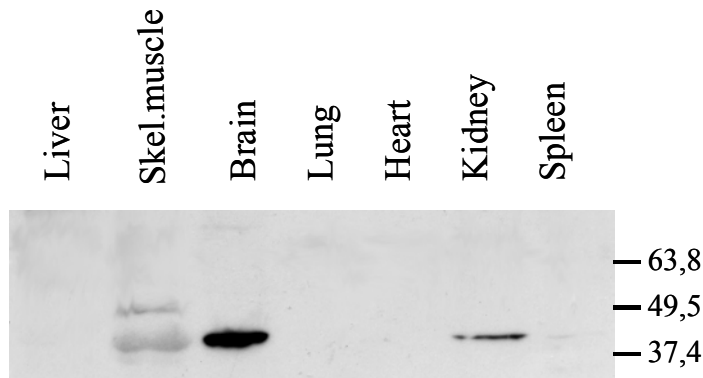


Figure 3: Organ specificity of antisense antibody of the β -cleavage site

Different organs of a wild type adult mouse were homogenized and subjected to SDS-PAGE (5 mg/ml). After transfer to nitrocellulose membrane, fractions were analysed using the antisense antibody of the β -cleavage site. Molecular weights are indicated on the right.

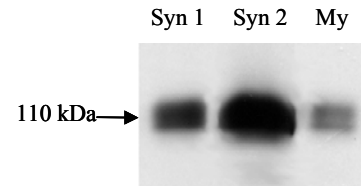


Figure 4: Distribution of APP in different membrane fractions

Western blot analysis of synaptosomal and myelin fractions from mouse brain homogenate using monoclonal anti-APP antibody 22C11.

4. Fraction co-localization of identified proteins and APP

As shown in the figures 2B and 2C, synaptosomal membranes were more enriched with the identified proteins in comparison to myelin fraction. In order to check the distribution of APP protein in different brain subfractions, Western blot analysis of investigated fractions using 22C11 anti-APP antibody was performed. The band of approximately 110 kDa, corresponding to the molecular weight of APP (Figure 4) was observed in all investigated fractions, however, the intensity of staining was higher in synaptosomal membranes than in myelin. This data suggest the synaptosomal co-localization of identified proteins and APP. Therefore, for the next experiments it was decided to use Syn1 and Syn 2 subfractions.

5. Solubilization of synaptosomal membranes with Triton X-100

Non-ionic detergent Triton X-100 (1%) was used for solubilization of membranes. Afterwards Triton soluble and Triton insoluble fractions were analysed on immunoblots using the antisense antibody of the γ -cleavage site (Figure 5A). The Triton X-100 appears to be not very effective in solubilizing of these synaptosomal membranes, since the amount of protein present in soluble and insoluble fractions was approximately equal. In addition, some physical properties of Triton X-100 (for instance tendency to increase viscosity at low temperature) would make the following affinity purification more complicated.

6. Optimisation of solubilization process

In order to optimize efficiency of membranes solubilization, three different detergents were tested: the non-ionic detergents n-octyl β -D-glucopyranoside and deoxycholate as well as the zwitterionic detergent CHAPS. After treatment of the membranes with these detergents (1%) the amount of protein in soluble and insoluble fractions was analysed by Western blots (Figure 5B). In result, n-octyl β -D-glucopyranoside was found the best solubilizing agent among all detergents were tested. Lower efficiency was achieved when deoxycholate was used, whereas CHAPS was almost ineffective. Therefore, n-octyl β -D-glucopyranoside was preferred for further solubilization of synaptosomal membranes, and also was used as the appropriate detergent in the sample buffer for the following affinity chromatography. The solubilization of membranes was performed with subsequent increase in detergent concentration from 1% up to 5 %. The efficiency of solubilization with different amounts of detergent has been controlled by Western blot analysis using the antisense antibodies of the γ -and β cleavage site (Figure 5C, D).

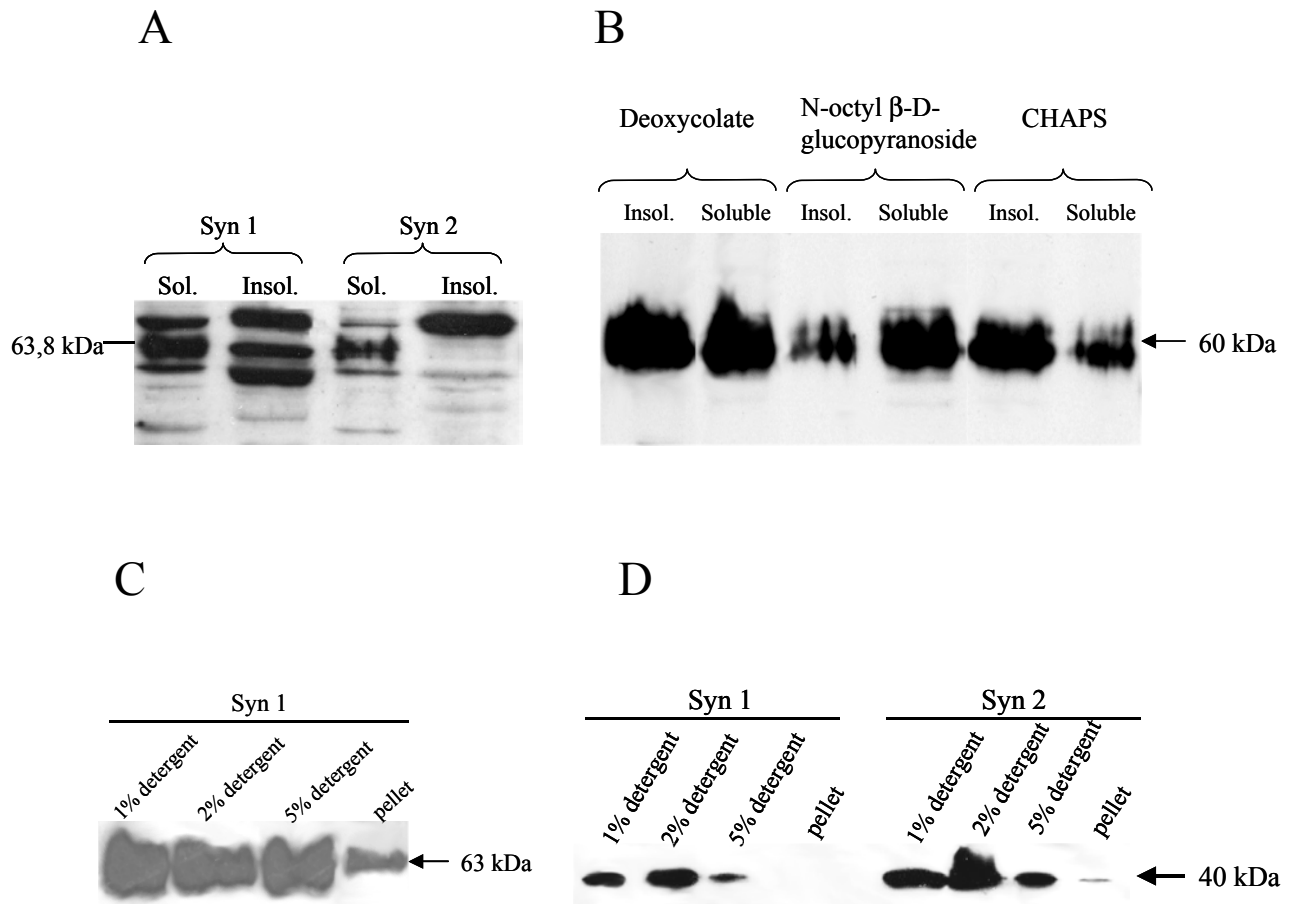


Figure 5: Solubilization of synaptosomal membranes

(A) Solubilization of synaptosomal membranes with Triton X-100 (1%). As a control for solubilization efficiency, Western blot analysis of Triton soluble and Triton insoluble fractions using the antisense antibody of the γ -cleavage site was performed. (B) Solubilization of synaptosomal membranes with different detergents. After treatment with (1%) of n-octyl β -D-glucopyranoside, deoxycholate or CHAPS, the efficiency of solubilization has been checked by Western blot using the antisense antibody of the γ -cleavage site. (C and D) Western blot analysis of synaptosomal membranes after treatment with 1%, 2% or 5% of β -D-glucopyranoside using antisense antibodies of the γ - or β -cleavage site respectively.

7. Affinity chromatography

In order to isolate the identified proteins, affinity columns with the respective antibodies were prepared and loaded with detergent soluble membrane fractions of mouse brain

homogenate. In addition soluble membrane fraction S3 was also used for affinity purification in the column with antisense antibody of the β -cleavage site. After extensive washing, the binding proteins were eluted from the column with acetate buffer at pH 2.5 and neutralized. After buffer exchange and concentration until the small volume, eluted fractions were subjected to SDS-PAGE and silver/Coomassie staining was performed after separation (Figure 6).

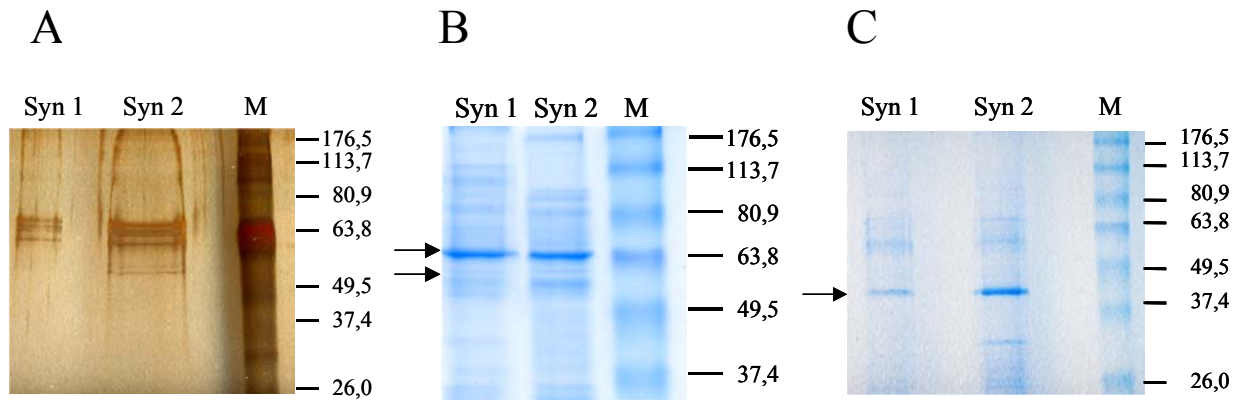


Figure 6: Affinity chromatography of detergent soluble membrane fractions from mouse brain homogenate using immobilized antisense antibodies of the γ - and β -cleavage site

Detergent soluble brain membranes were prepared for the isolation of putative APP binding proteins. (A) Fractions were applied to the column with immobilized antisense antibody of the γ -cleavage site. After extensive washing, bound proteins were eluted and concentrated until the small volumes. The eluates were subjected to SDS-PAGE and silver staining was performed after separation. (B) The eluates were separated on SDS gel and the proteins were visualized by Coomassie staining. The proteins corresponding to the bands specifically recognized by antisense antibody of the γ -cleavage site (indicated by arrows) were cut out from the gel and sent for sequence analysis. (C) Fractions were applied to the column with immobilized antisense antibody of the β -cleavage site. After extensive washing, bound proteins were eluted and concentrated until the small volumes. The eluates were subjected to SDS-PAGE and Coomassie staining was performed after separation. The proteins corresponding to the bands specifically recognized by antisense antibodies of the β -cleavage site (indicated by arrows) were cut out from the gel and sent for sequencing. The molecular weights are indicated on the right.

8. Protein sequencing

The Coomassie stained proteins corresponding to the bands recognized by antisense antibodies of the γ - and β -cleavage site respectively were cut out from the SDS gel (Figure

6) and sequenced using the matrix-assisted laser desorption/ionisation – mass spectroscopy (MALDI-MS) (Jensen et al., 1997; Mortz et al., 1994). The protein sequencing was performed by Dr. Buck from the Institute für Zellbiochemie und Klinische Neurobiologie, UKE, Hamburg. Sequence analysis of bands recognized by antisense antibody of the γ -cleavage site revealed two proteins. One of them was calreticulin, an acidic protein of 55-60 kDa on SDS-polyacrylamide gel. Another one was identified as versican (V3 splice variant), a protein with molecular mass of 60-70 kDa. Whereas the sequence of band recognized by antisense antibody of the β -cleavage site revealed creatine kinase B (brain specific form), a protein of approximately 45 kDa.

9. Confirmation of the presence of identified proteins in fractions purified by affinity chromatography

To verify that the fractions purified by affinity chromatography (eluates) contain the proteins identified by sequence analysis, the eluates were subjected for SDS-PAGE and analysed by Western blot analysis using the respective antibodies. The fraction purified using the antisense antibody of the γ -cleavage site was analysed by Western blot using the antibodies against calreticulin and versican (Figure 7A, B), which indeed revealed the bands corresponding to the calreticulin and versican respectively. As positive controls, a recombinant rabbit calreticulin or purified bovine versican (a mixture with V0 and V1 isoforms) respectively were used. Additionally this fraction was analysed using the antisense antibody of the γ -cleavage site, which obviously recognized both calreticulin and versican (Figure 7A). To be sure that the signal was not due to the unspecific staining of secondary antibody, the fraction was analysed using peroxidase-labeled goat anti-rabbit IgG antibody alone, which did not reveal some bands (Figure 7A). In parallel the fraction purified using the antisense antibody of the β -cleavage site was analysed using the antibody against creatine kinase B. As a positive control, recombinant human creatine kinase B was applied on the gel. The Western blot analysis revealed a band of approximately 45 kDa, corresponding to creatine kinase B, confirming the presence of this protein in purified fraction (Figure 7 C).

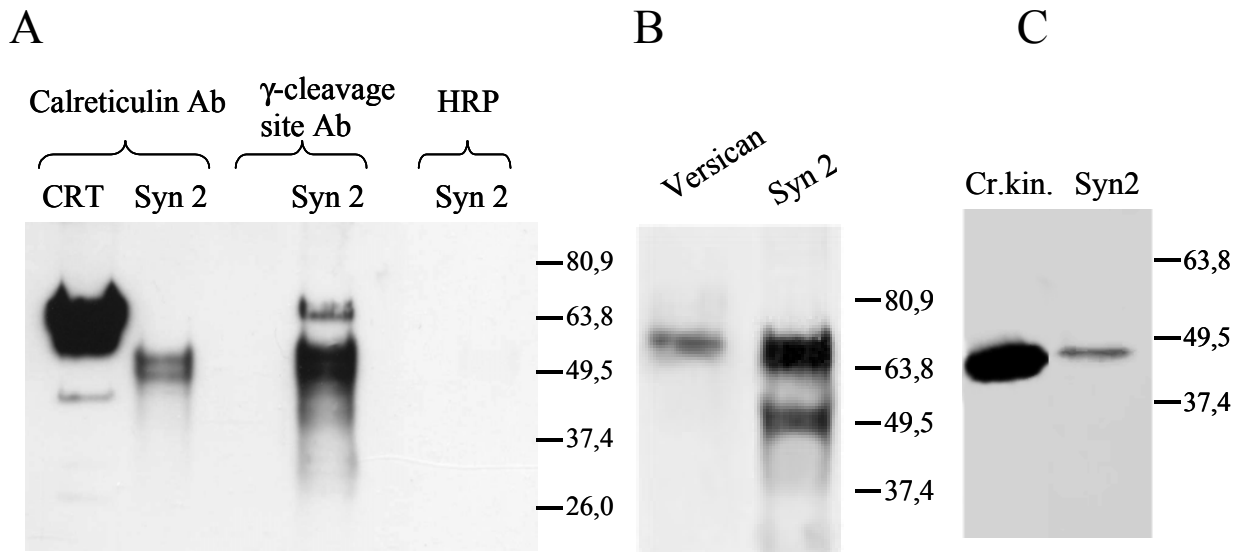


Figure 7: Confirmation of the presence of identified proteins in fractions purified by affinity chromatography

Fractions purified by affinity chromatography (eluates) were analysed by Western blot. (A) Syn 2 purified using the antisense antibody of the γ -cleavage site and recombinant calreticulin were subjected to SDS-PAGE, followed by transfer to nitrocellulose membrane and staining using either the antibody against calreticulin or the antisense antibody of the γ -cleavage site, or stained using peroxidase-labeled goat anti-rabbit IgG antibody. (B) Syn 2 purified using the antisense antibody of the γ -cleavage site and purified versican were subjected to SDS-PAGE, transferred to nitrocellulose membrane and stained using the antibody against versican. (C). Syn 2 purified using the antisense antibody of the β -cleavage site or recombinant creatine kinase B were subjected to SDS-PAGE, followed by transfer to nitrocellulose membrane and staining using the antibody against creatine kinase B.

10. Distribution of calreticulin, versican and creatine kinase B in brain subfractions

To investigate the localization of identified proteins in brain subfractions, synaptosomal and myelin fractions were analysed by Western blot analysis using the antibodies against calreticulin, versican and creatine kinase B respectively. Calreticulin, versican and creatine kinase B were detected in all investigated fractions (Figure 8). However, the amount of these proteins in synaptosomes was higher in comparison to the myelin fraction. This suggests predominantly synaptosomal localization of investigated proteins.

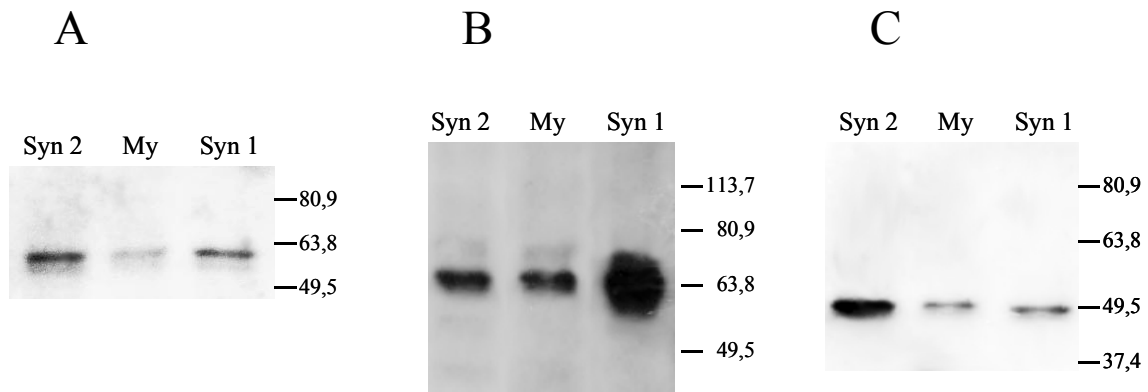


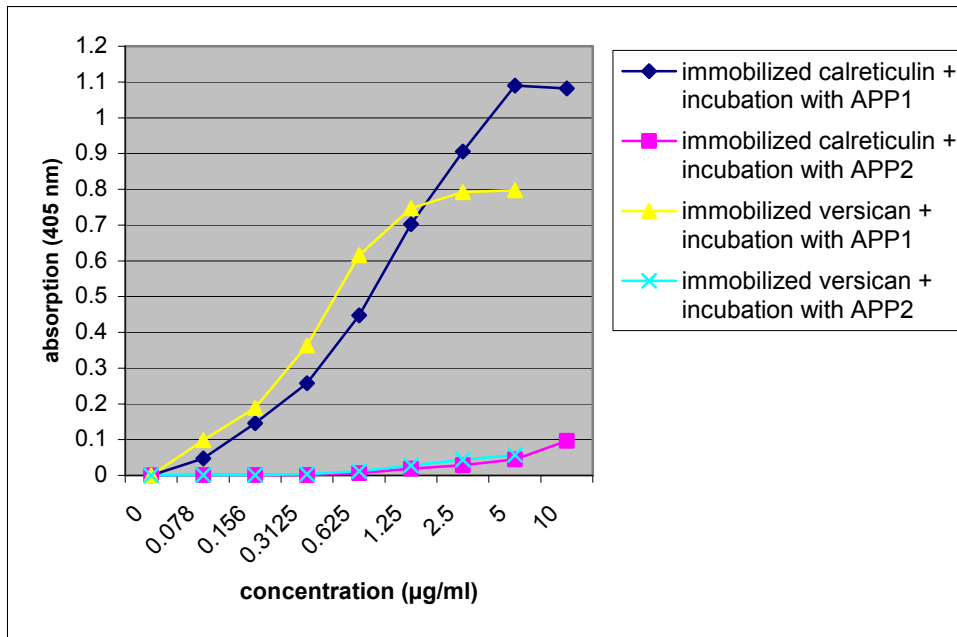
Figure 8: Distribution of calreticulin, versican and creatine kinase B in brain subfractions

Western blot analysis of synaptosomal and myelin fractions from mouse brain homogenate. All fractions were subjected to SDS-PAGE. After transfer to nitrocellulose membrane, fractions were analysed using the antibody against calreticulin (A), versican (B) or creatine kinase B (C).

11. Binding study of identified proteins and APP using an ELISA approach

To prove a direct binding of calreticulin or versican and APP, synthetic biotinylated peptides APP1 and APP2 mimicking the γ - and β -cleavage sites of APP respectively were used. Recombinant rabbit calreticulin, basically identical to human and mouse protein, or purified bovine versican (a mixture with V0 and V1 isoforms) were coated on absorbent plastic surfaces and incubated with APP1, or as a negative control, with APP2. Detection of the potential interaction partner was carried out using the streptavidin coupled with HRP. The interaction of calreticulin and APP as well as versican and APP were confirmed in the ELISA assay. Binding of the calreticulin was observed in the dose dependent manner in the range of 80 ng/ml – 5 μ g/ml, while dose dependent interaction of versican and APP was detected in the range of 40 ng/ml – 1.5 μ g/ml (Figure 9A). Vice versa, binding of soluble calreticulin or versican to immobilized APP1 was detected using the antibodies against calreticulin or versican respectively. The interaction of calreticulin and APP was detectable in this assay, showing near-linear quantitative binding in the range of 30 ng/ml – 5 μ g/ml, however when APP1 was coated and incubated with soluble versican, no interaction was observed (Figure 9B).

A



B

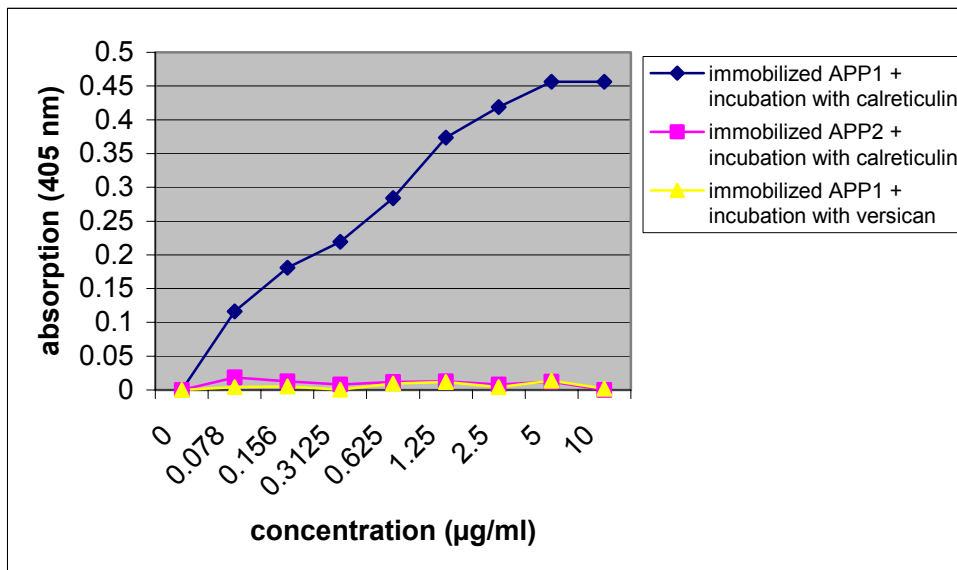


Figure 9: ELISA binding assay for evaluation of calreticulin – APP and versican – APP interactions

(A) Immobilized calreticulin (10 µg/ml) or versican (10 µg/ml) were incubated with APP1 (78 ng/ml – 10 µg/ml) or with APP2 (78 ng/ml – 10 µg/ml). Detection of bound proteins was carried out using the streptavidin coupled with HRP. (B) Immobilized APP1 (5 µg/ml) or APP2 (5 µg/ml) were incubated with calreticulin (78 ng/ml – 10 µg/ml) or with versican (78 ng/ml – 10 µg/ml). The binding proteins were detected with a polyclonal antibody against calreticulin or with a polyclonal antibody against versican respectively.

To prove a direct binding of creatine kinase B and APP, recombinant human creatine kinase B was immobilized to a plastic surface and incubated with APP2 diluted in a wide range (78 ng/ml – 20 µg/ml). Detection of the potential interaction partner was carried out using the streptavidin coupled with HRP. However, the interaction of creatine kinase B and APP could not be confirmed in the ELISA assay since binding of soluble APP2 to immobilized creatine kinase B was not observed. Vice versa, binding of soluble creatine kinase B to immobilized APP2 followed by incubation with antibody against creatine kinase B was also not detectable.

12. Verification of the interaction of identified proteins and APP by co-immunoprecipitation

For co-immunoprecipitation the detergent extract of a brain homogenate was incubated with antibody against calreticulin, versican or creatine kinase B respectively. As a positive control, the antibody against APP (mouse monoclonal antibody WO2) was applied for precipitation. Immunocomplexes were isolated using agarose protein A/G beads. As a negative control, the detergent extract was incubated with beads alone. Bound proteins were eluted by boiling at 95 °C in sample buffer and analysed for co-precipitation of APP. The analysis of the immunoprecipitates revealed that after precipitation of creatine kinase B a co-precipitation of APP occurred, while a co-precipitation of APP was not detectable after precipitation of calreticulin or versican (Figure 10 A). However, when the detergent extract of synaptosomes (prepared as described above) was used instead of the whole brain homogenate, APP was detected after precipitation of calreticulin or versican, while after precipitation with creatine kinase B no co-precipitation of APP occurred (Figure 10 B).

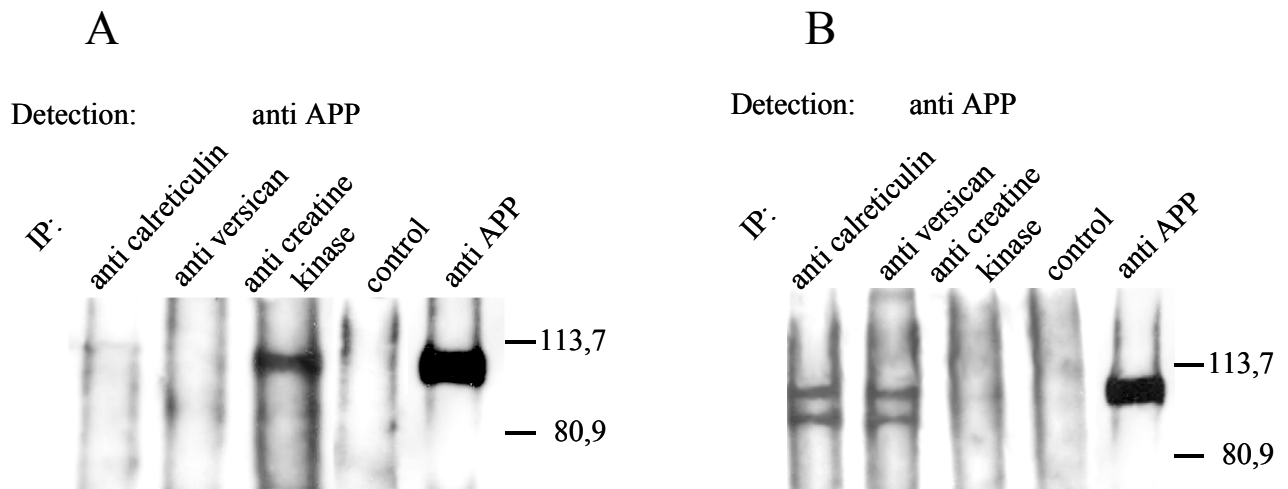


Figure 10: Analysis of co-immunoprecipitation of APP and identified proteins

(A) A detergent extract of brain homogenate was incubated with anti calreticulin, anti versican or anti creatine kinase B antibodies, or as positive control, with monoclonal antibody WO2 against APP. Immunocomplexes were isolated using agarose protein A/G beads. As a negative control, a detergent extract was incubated with beads alone. The eluates from the agarose beads were subjected for SDS-PAGE, transferred to nitrocellulose membrane and stained using the monoclonal antibody 22C11 against APP. (B) A detergent extract of synaptosomes was incubated with antibodies against calreticulin, versican or creatine kinase B, or as positive control, with monoclonal antibody WO2 against APP. Immunocomplexes were isolated using agarose protein A/G beads. As a negative control, a detergent extract was incubated with beads alone. The eluates from the agarose beads were subjected for SDS-PAGE, transferred to nitrocellulose membrane and stained using the monoclonal antibody 22C11 against APP.

13. Co-localization and co-capping of identified proteins and APP in primary hippocampal cultures

Since a co-localization of proteins is a prerequisite for functional interaction *in vivo*, the localization of calreticulin, versican, creatine kinase B and APP in primary cell cultures was analysed. Hippocampal neurons of 3-day-old mice were dissociated and cultured for one week. Afterwards, cells were fixed and co-immunostained with antibody to APP and one of its putative binding partners. The co-immunostaining with polyclonal goat antibody against calreticulin and with polyclonal antibody against APP showed a strong overlap, suggesting a co-localization of calreticulin and APP (Figure 11 A, yellow areas). In parallel, cultures were stained with a polyclonal antibody against versican and the monoclonal antibody 22C11 against APP. However, no apparent co-localization of

versican and APP could be observed (data not shown). To investigate a co-localization of creatine kinase B and APP cells were stained with the polyclonal antibody against creatine kinase B and the polyclonal antibody against APP. Although a widespread expression of creatine kinase B all over the cell was observed, only small amounts of immunoreactive creatine kinase B overlapped with the immunostaining for APP (Figure 11 B).

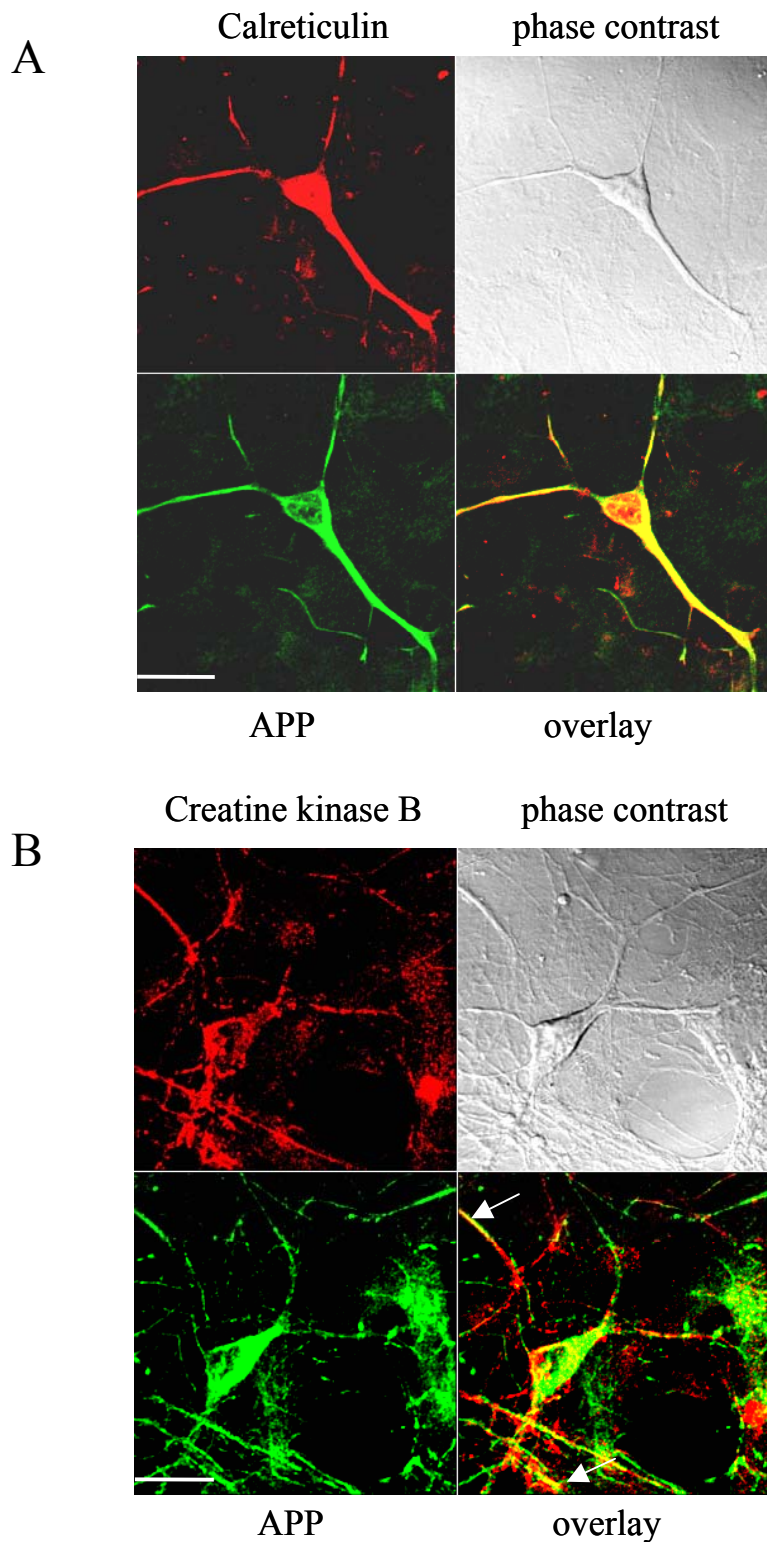


Figure 11: Co-localization of APP and its putative binding partners in primary hippocampal cultures

(A) Hippocampal cultures prepared from 3-day-old mice and maintained for one week in vitro were fixed and co-immunostained with anti-calreticulin antibody (red) and anti-APP antibody (green). Superposition of immunostainings is shown in an overlay image, in which yellow areas indicate co-localization of calreticulin and APP. Phase contrast shows the cellular structures. Scale bar, 20 μm . (B) As in (A) but cultures were co-immunostained with antibody against creatine kinase B (red), or with antibody against APP (green). Scale bar, 20 μm .

Furthermore, the interaction between APP and its putative binding partners was tested using a co-capping assay. In this method, clustering of a protein is induced by application of antibodies to live cultures and co-clustering (co-capping) of its binding partners is expected to be observed. For co-capping of calreticulin and APP, the cells were pre-incubated with polyclonal rabbit antibody against APP. Primary antibodies were clustered with the secondary anti-rabbit antibody and afterwards cells were fixed and stained with polyclonal goat anti-calreticulin antibody. Clustering of APP appeared to induce accumulations of calreticulin on the cell surface. Co-localization of clusters indicating a co-redistribution of calreticulin and APP was nicely observed in cell soma, axons and dendrites (Figure 12 A, yellow areas). For co-capping of creatine kinase B and APP, the cells were pre-incubated with polyclonal rabbit antibody against APP and clustered with the secondary anti-rabbit antibody. Afterwards, cells were fixed and stained with polyclonal goat antibody against creatine kinase B. Apparently, only small amounts of overlapped clusters, indicated by yellow staining, could be observed in this case (Figure 12 B).

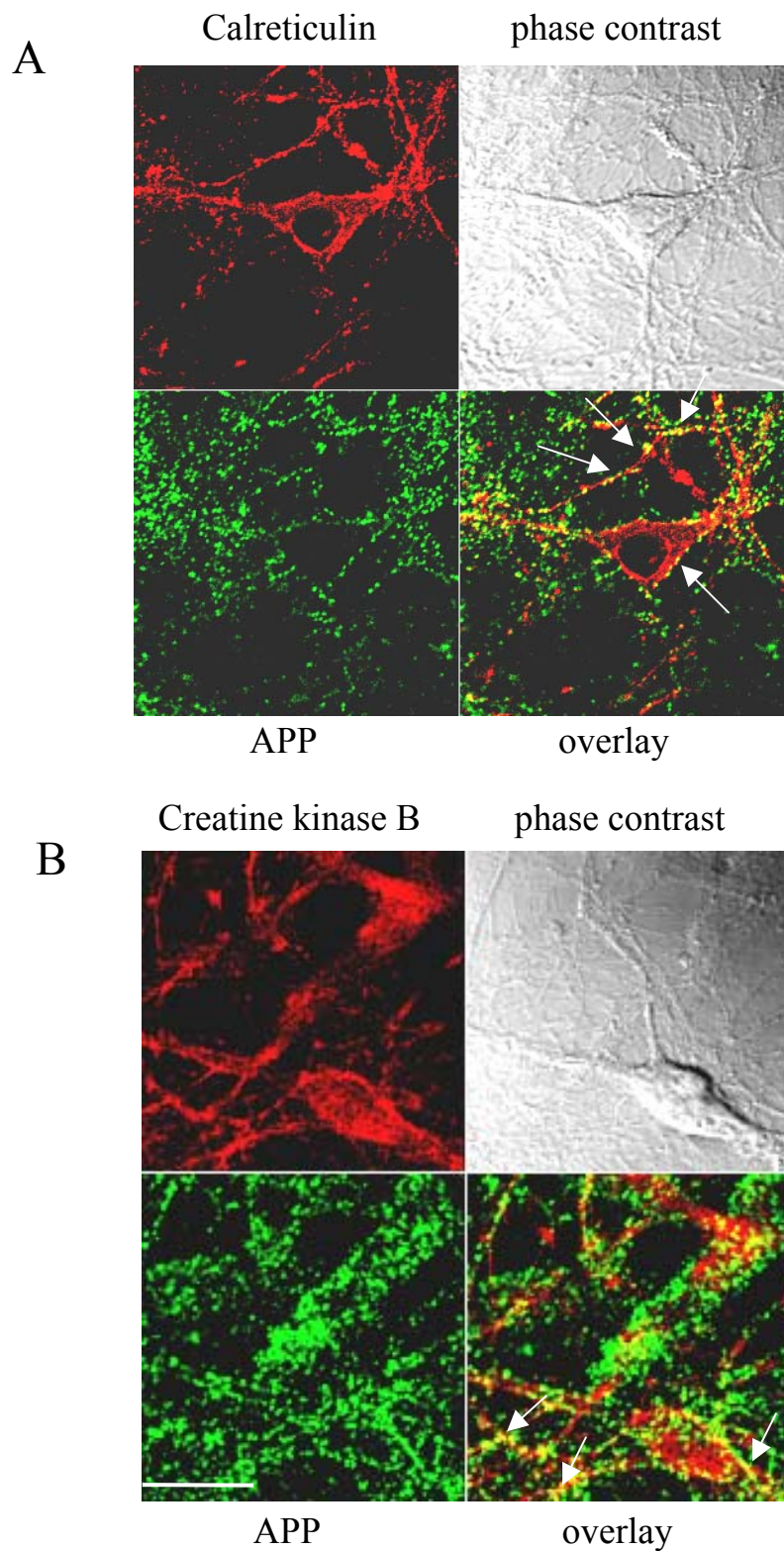


Figure 12:Co-capping of APP and its putative binding partners in primary hippocampal cultures

(A) Hippocampal cultures prepared from 3-day-old mice and maintained for one week in vitro were pre-incubated with polyclonal rabbit anti-APP antibody that was clustered with a secondary anti-rabbit antibody

V. Results

(green). Afterwards, cells were immunostained with anti-calreticulin antibody (red). Co-localization of calreticulin and APP is indicated by yellow staining (arrows). Phase contrast shows the cellular structures. Scale bar, 20 μm . (B) As in (A) but after clustering of APP hippocampal cultures were immunostained with antibody against creatine kinase B (red). Yellow staining indicates co-localization of creatine kinase B and APP (arrows). Scale bar, 20 μm .

Study 2: Cell adhesion molecules as biochemical markers for Alzheimer disease

1. Introduction in “Capture” ELISA

The primary advantage of the antigen-capture ELISA is the ability of this test to detect antigen in the course of the disease. The main component of the capture ELISA (Figure 1) is a specific monoclonal antibody. Antigens from the test sample are first captured by monoclonal antibody, supported on a solid phase, and a polyclonal detection antibody, which can be recognized then by secondary enzyme-labelled antibody, detects their presence. The desired characteristics of the capture antibody are strong binding to the antigen and the ability to attach to an ELISA plate without loss of reactivity. In addition, detection polyclonal antibody recognizes other epitopes than that recognized by the capture monoclonal antibody. Therefore, it is generally thought, that this test provides high specificity.

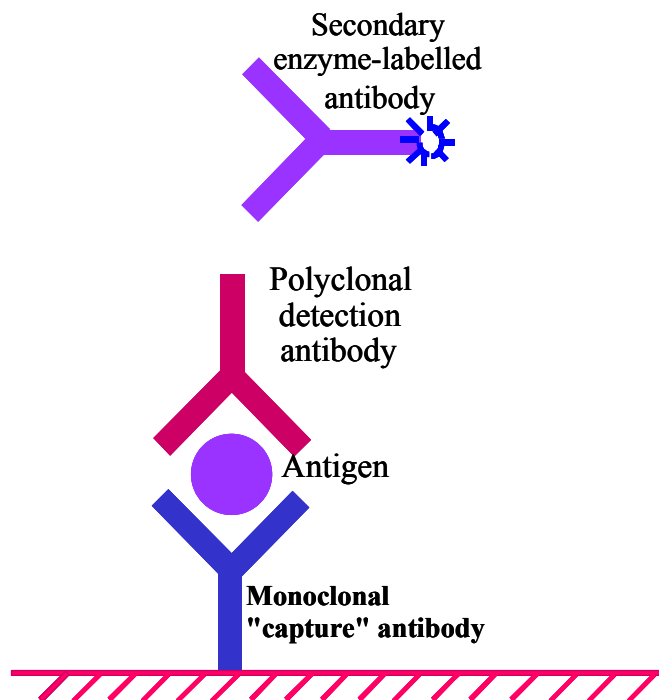


Figure 1: Principle of the antigen-capture ELISA

2. Establishment of a capture ELISA for quantification of L1 level in the CSF

2.1 Checking of the specificity and working titre of the detection polyclonal anti-human L1 antibodies

Determination of the working dilution of the detection polyclonal antibodies was performed using the standard direct antigen ELISA on the solid phase. Two-fold serial dilutions of the standard (purified human L1-Fc; 2 – 256 ng/ml) were absorbed on the microwell plate and incubated with different concentrations of polyclonal anti-human L1 antibodies, followed by incubation with HRP conjugated antibody and substrate reaction. As a negative control, some wells were coated with other antigens, such as human NCAM-Fc and mouse PSA. Uncoated wells were used as a blank control. The HRP conjugated antibody has been used in dilution of 1:5000 (followed by manufacture's protocol). The dilution curves (Figure 2A) represent increasing of the O.D. with increasing amounts of antigens and the other parameters being constant. The optimal working dilution of the polyclonal anti-human L1 antibodies was accepted as 1:4000. It provides a wide working diapason (linear part), which allows detecting the antigen in range 8 – 60 ng/ml, and gives low background. When the lower concentration of the polyclonal antibodies was used the linear part of the curve was set in the field of lower O.D. allowing to detect antigen in range 12-48 ng/ml. Whereas the higher antibodies concentration leads to higher background, and, in addition, it is not economically advantageous. The testing antibody was highly specific for L1 and did not show the crossreactivity with other antigens.

2.2 Establishment of the optimal coating concentration of the capture monoclonal anti-human L1 antibody (Neuro 4.1.1.3.3)

The optimal working dilution of the capture monoclonal antibody was determined from the titration against homologous antigen. The dilution curve (Figure 2 B) reflects decrease of the O.D. with increasing of antibody dilution when the other parameters, established in the previous test, were constant. Namely, detection polyclonal antibodies diluted 1:4000 and antigen (L1-Fc protein) in concentration of 20 ng/ml were used for this test. The

working dilution of the capture antibody 1:1000 appear to be appropriate, as it gives the O.D. around 1.0 and set in the middle of the saturation field (upper plateau) of the curve, suggesting that the maximal coating of the wells with the primary antibody should abolish non-specific antigens binding with a surface of microwell plate and therefore, has not influence on the test results.

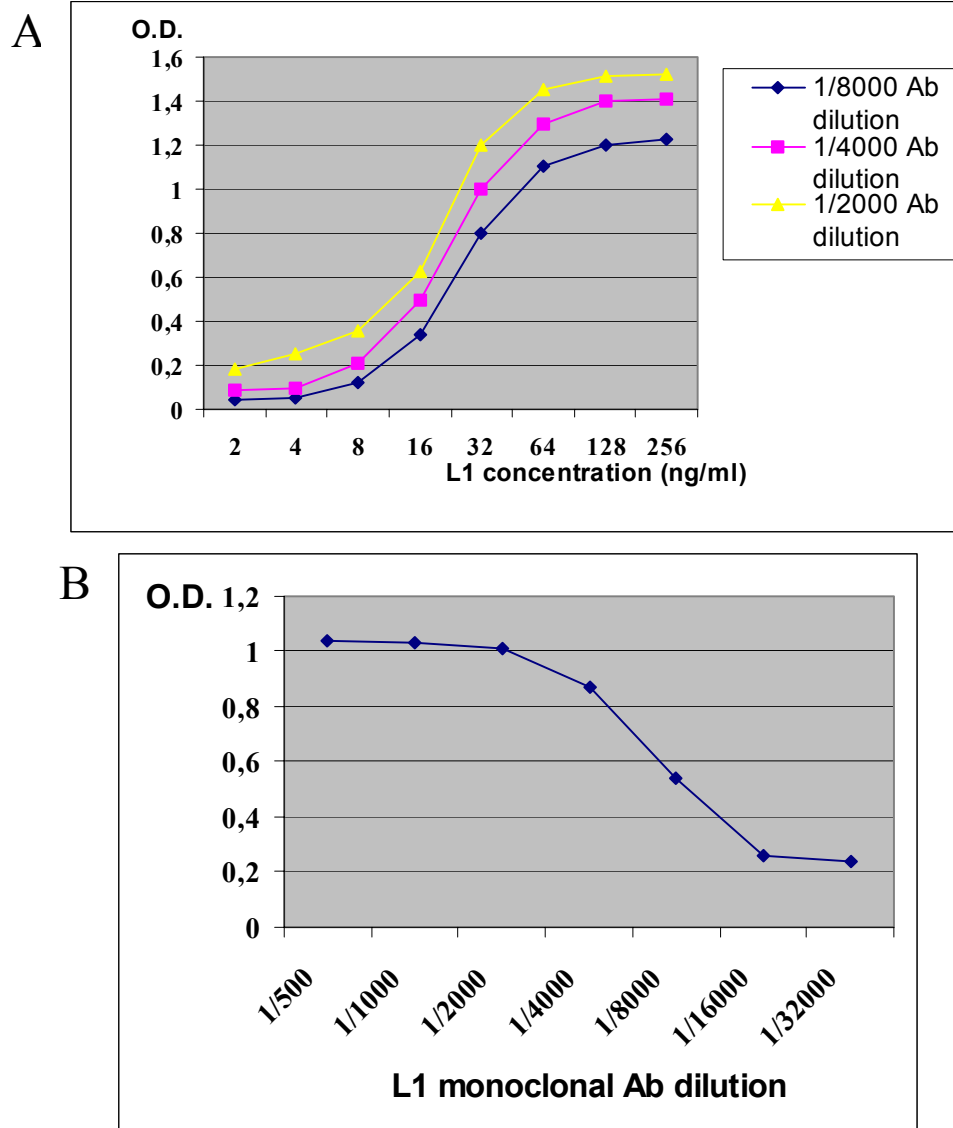


Figure 2: Establishment of the L1 antibodies working concentrations

(A) Dilutions curves of the detection polyclonal anti-human L1 antibody. Two-fold serial dilutions of the purified human L1-Fc (2 – 256 ng/ml) were absorbed on the microwell plate and incubated with different concentrations of polyclonal anti-human L1 antibodies (1/2000, 1/4000 or 1/8000 dilution were tested), followed by incubation with HRP conjugated antibody and substrate reaction. (B) Titration of the capture monoclonal anti-human L1 antibody 4.3.3.1.1. Two-fold serial dilutions of the monoclonal antibody (1/500 – 1/32000) were used whereas the other parameters (antigen concentration 20 ng/ml and detection antibody dilution 1/4000) have been constant.

2.3 Standard antigen-binding curve

Under the optimized conditions, described above, a standard antigen-binding curve was prepared (Figure 3). The assay shows near-linear quantitative binding of antigen in the range 2 – 50 ng/ml. Greatest accuracy in determining test samples is achieved in readings falling between O.D. 0.2 and 1.2. Test samples can be quantitated for antigen against this curve.

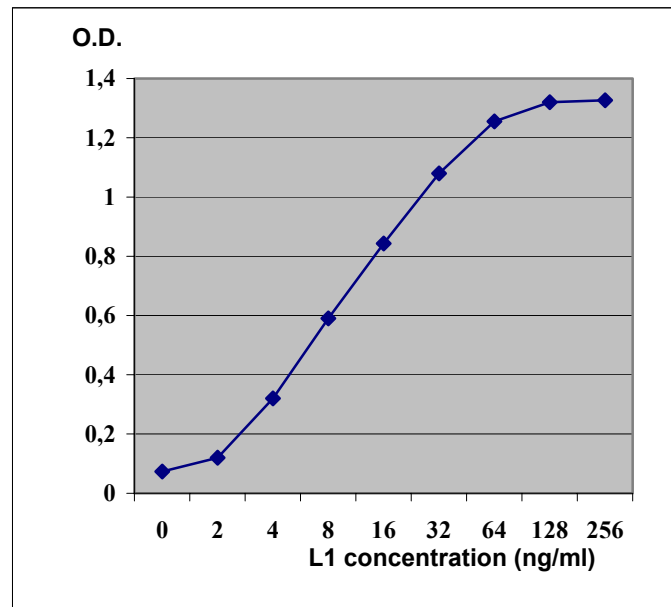


Figure 3: Standard antigen (L1-Fc) binding curve

The purified human L1-Fc protein was titrated on ELISA plate in two-fold serial dilutions (2 – 256 ng/ml) when the other parameters (capture monoclonal antibody dilution 1/1000 and detection polyclonal antibody dilution 1/4000) were constant.

2.4 Determination of the optimal test sample (CSF) dilution

Optimal CSF dilutions were determined by titration of three different CSF, containing presumably low, middle or high amount of L1 protein (as was detected by Western blot analysis) in order to except the possibility being out of the working range for the testing CSF with very low or very high L1 concentration. The CSF were titrated in two-fold serial dilutions and analysed under the appropriate conditions, chosen previously, which are: the

dilution of the capture monoclonal antibody 1:1000, dilution of the detection polyclonal antibody 1:4000. The dilution curves (Figure 4) show that the undiluted CSF set in the optimal working range, described above, whereas already 1:2 CSF dilution leads to significant O.D. decrease in case of all tested CSF.

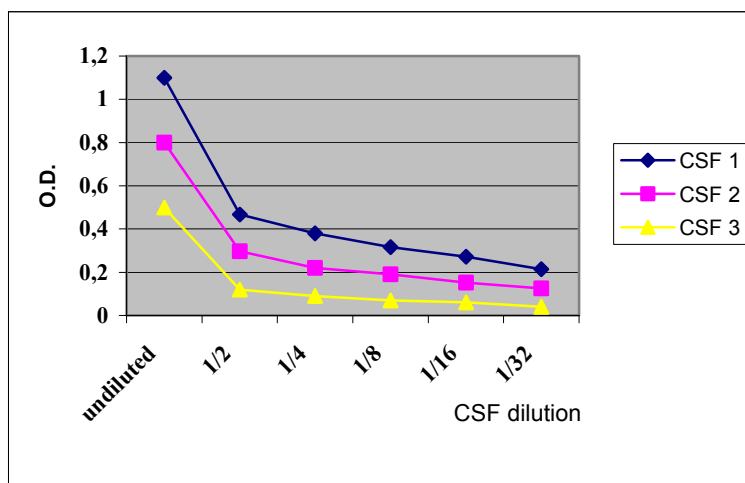


Figure 4: CSF dilution curves in L1-Fc ELISA

Three different CSF with low, middle or high amount of L1 protein were titrated in two-fold serial dilutions when the other parameters (capture monoclonal antibody dilution 1/1000 and detection polyclonal antibody dilution 1/4000) were constant.

2.5 Optimizing the ELISA

Optimisation of ELISA to fit a high specificity involved the manipulation of temperature, incubation time and blocking agents. To provide maximum specificity, a comparison was made between three different blocking agents commonly used in ELISA: 5% dried skim milk, 2% gelatin and 2% BSA. No large variations were observed in the absorbance with the blocking agents used, although the background level was lower with 5% dried skim milk, which finally was used in quantitative ELISA. In addition, the different incubation times and temperatures for all steps were investigated. Finally, the following optimal conditions were determined: coating step was performed at 4°C overnight, blocking at 37°C for 2 h, the incubation with detection antibody was optimal at RT for 20 h, and incubation with HRP conjugated antibody was performed at RT for 1.5 h.

2.6 Sensitivity of the L1-Fc ELISA test

Sensitivity, or Minimum Detectable Concentration (MDC), was confirmed by assaying of 20 replicates of the zero standard in a single assay. The concentration extrapolated from the standard curve of the average O.D. for the standard 0 replicates + 2 SD is the MDC. Sensitivity calculated for this test was 1.5 ng/ml, which represents the lowest value read from the standard curve that can be statistically differentiated from zero.

3. Establishment of a capture ELISA for quantification of NCAM and PSA-NCAM levels in the CSF

3.1 Checking of the specificity and working titre of the detection polyclonal anti-human NCAM antibodies (3731)

Determination of the working dilution of the detection polyclonal antibodies was performed using the standard direct antigen ELISA on the solid phase, as described above (see 2.1). Purified human NCAM-Fc and mouse PSA-NCAM proteins were used as standards to establish NCAM and PSA-NCAM ELISA. To check the antibody specificity, some wells were coated with other antigens, like human L1-Fc or CHL1-Fc. Uncoated wells were used as a blank. The dilution curves are represented on the Figure 5A and Figure 5B, respectively for NCAM and PSA-NCAM ELISA. In both cases the optimal dilution of the detection antibody was 1:1000, providing the wide working diapason (linear part) and low background. The analysed antibodies were highly specific for NCAM and did not show the crossreactivity with other antigens.

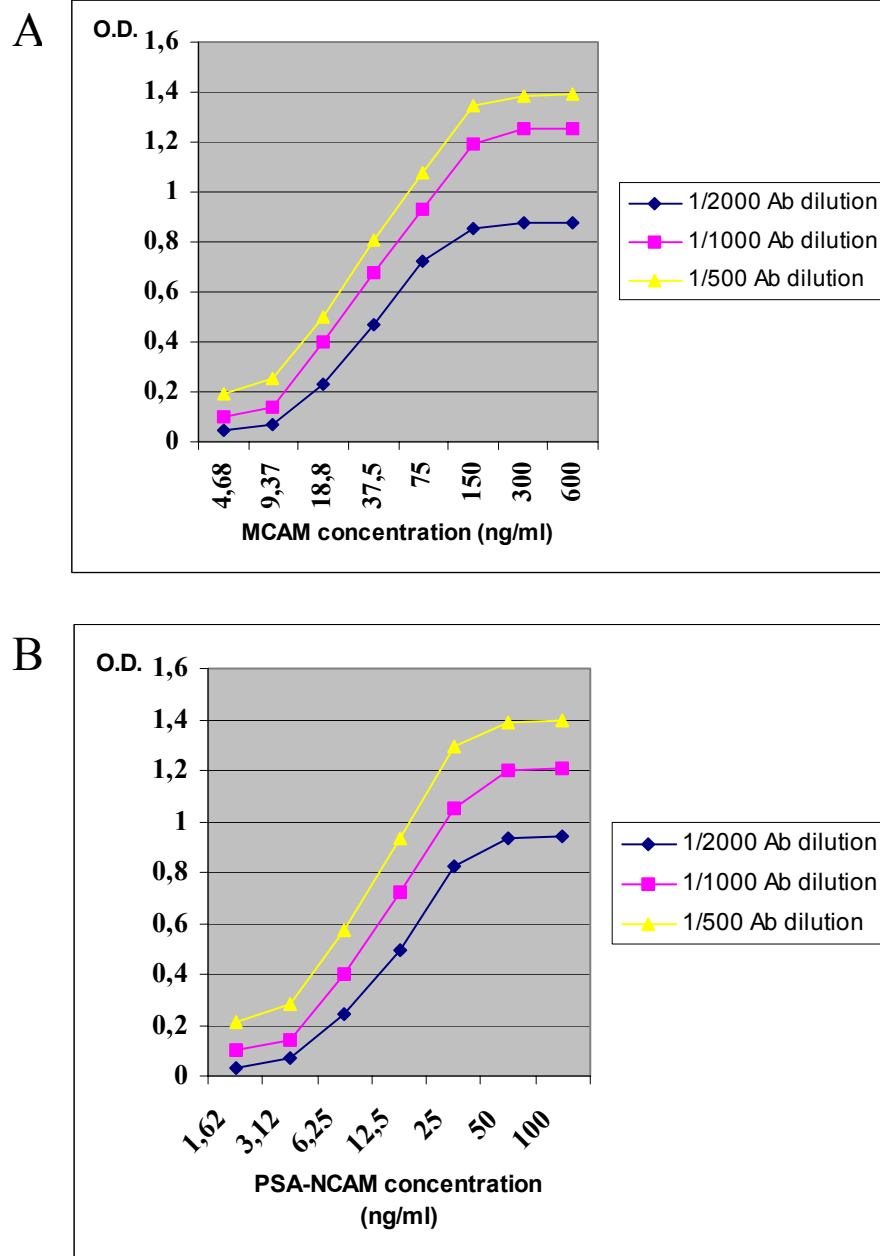


Figure 5: Establishment of the polyclonal anti-human NCAM antibodies 3731 working concentrations
 (A) Dilutions curves of the detection polyclonal anti-human NCAM antibodies in NCAM-ELISA test. Two-fold serial dilutions of the purified human NCAM-Fc protein (4.68 – 600 ng/ml) were absorbed on the microwell plate and incubated with different concentrations of polyclonal anti-human NCAM antibodies (1/500, 1/1000 or 1/2000 dilution were used), followed by incubation with HRP conjugated antibody and substrate reaction. (B) Dilutions curves of the detection polyclonal anti-human NCAM antibodies in PSA-NCAM-ELISA test. Two-fold serial dilutions of the purified mouse PSA-NCAM-Fc protein (1.62–100 ng/ml) were absorbed on the microwell plate and incubated with different concentrations of polyclonal anti-human NCAM antibodies (1/500, 1/1000 or 1/2000 dilution were used), followed by incubation with HRP conjugated antibody and substrate reaction.

3.2 Establishment of the optimal coating concentrations of the capture monoclonal anti-human NCAM antibody (14.2) and monoclonal anti-PSA antibody (735)

The optimal working dilutions of the capture monoclonal antibodies were determined from the titration against homologous antigens. The dilution curves (Figure 6A and 6B respectively for NCAM and PSA antibodies) are represented. Based on the same principle, as in case with monoclonal anti-L1 antibody (see 2.2), the working dilution of the monoclonal anti-human NCAM antibody 1:1000 has been chosen, whereas for anti-PSA antibody the working dilution 1:700 was accepted.

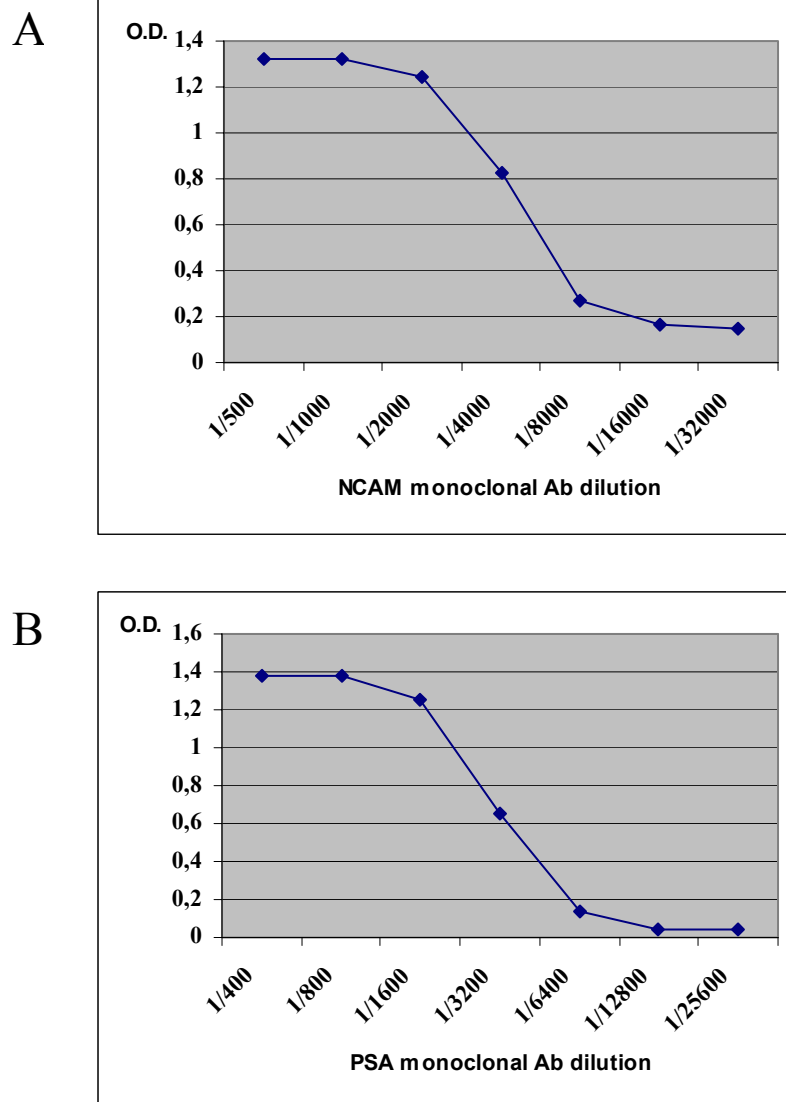
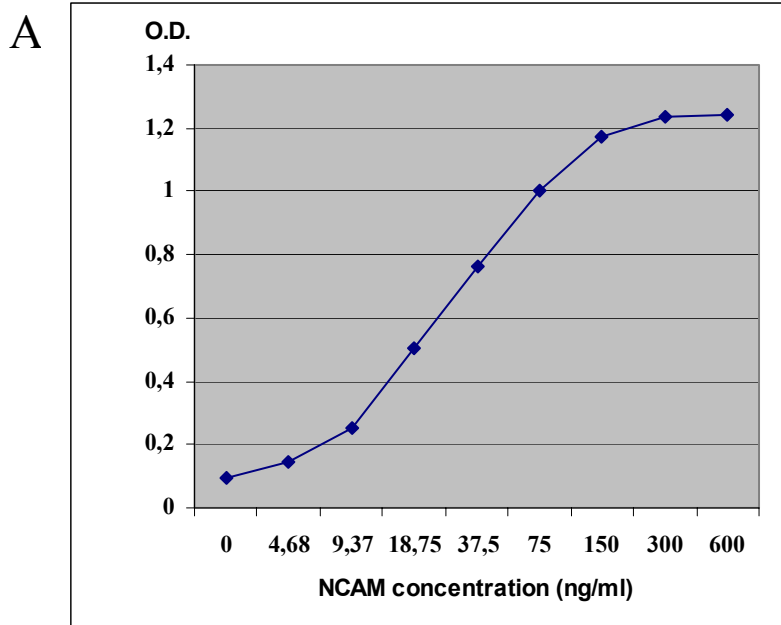


Figure 6: Determination of the coating concentrations of the capture monoclonal anti-human NCAM antibody (14.2) and monoclonal anti-PSA antibody (735)

(A) Titration of the capture monoclonal anti-human NCAM antibody 14.2. Two-fold serial dilutions of the monoclonal antibody (1/500 – 1/32000) were used when the other parameters (antigen concentration 50 ng/ml and detection antibody dilution 1/1000) have been constant. (B) Titration of the capture monoclonal anti-PSA antibody 735 in two-fold serial dilutions (1/500 – 1/32000) under the other parameters (antigen concentration 13 ng/ml and detection antibody dilution 1/1000) being constant.

3.3 Standard antigen binding curves

Under the optimized conditions, described above, a standard antigen binding curves were generated (Figure 7A and 7B respectively for NCAM and PSA-NCAM ELISA). The NCAM assay shows near-linear quantitative binding of antigen in the range of 9.37 – 150 ng/ml with greatest accuracy in determining test samples between O.D. 0.3 and 1.1. Whereas for PSA-NCAM assay the linear binding range of 3.12 – 25 ng/ml was observed, providing the maximum accuracy in determining test samples between O.D. 0.25 and 1.0. Test samples can be quantitated for antigens against these curves.



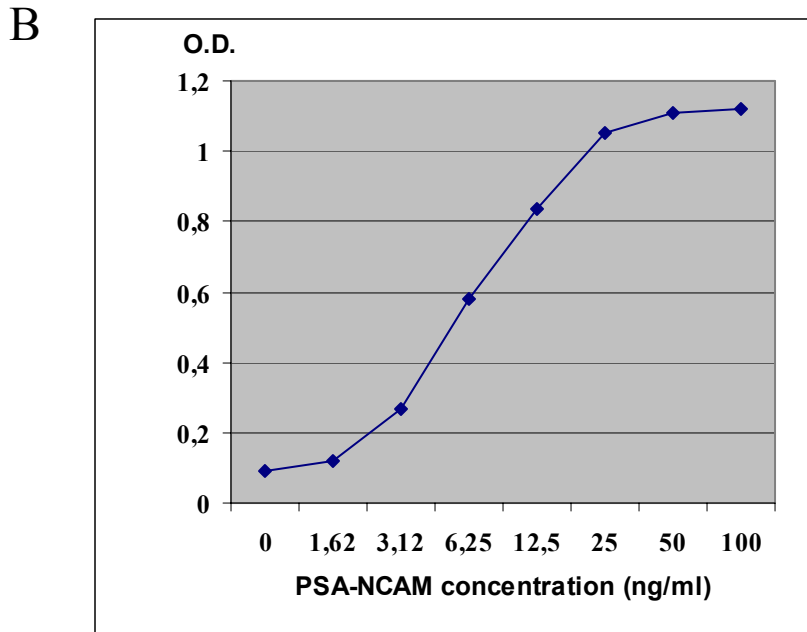


Figure 7: Standard antigen (NCAM-Fc and PSA-NCAM-Fc) binding curves

(A) The purified human NCAM-Fc protein was titrated on ELISA plate in two-fold serial dilutions (4.68–600 ng/ml) when the other parameters (capture monoclonal antibody dilution 1/1000 and detection polyclonal antibody dilution 1/1000) were constant. (B) Titration of the purified mouse PSA-NCAM protein on ELISA plate (1.62 – 100 ng/ml) under the other constant parameters (capture monoclonal antibody dilution 1/700 and detection polyclonal antibody dilution 1/1000).

3.4 Determination of the optimal test sample (CSF) dilutions

Optimal CSF dilutions were determined by titration of three different CSF, containing presumably low, middle or high amount of NCAM or PSA-NCAM protein (as was detected by Western blot analysis) in order to except the possibility being out of the working range for the testing CSF with very low or very high analysed protein concentration. The CSF were titrated in two-fold serial dilutions and analysed under the appropriate conditions, described previously, respectively for NCAM and PSA-NCAM ELISA (see 3.1 and 3.2). The optimal CSF dilution 1:15 was accepted for NCAM assay (Figure 8A) which set in the middle of the linear part of the curves. This dilution provides a good signal and in addition, allows to work in a big diapason and therefore, to analyze the CSF with different concentrations. In case of PSA-NCAM ELISA the optimal CSF dilution 1:8 has been chosen (Figure 8B).

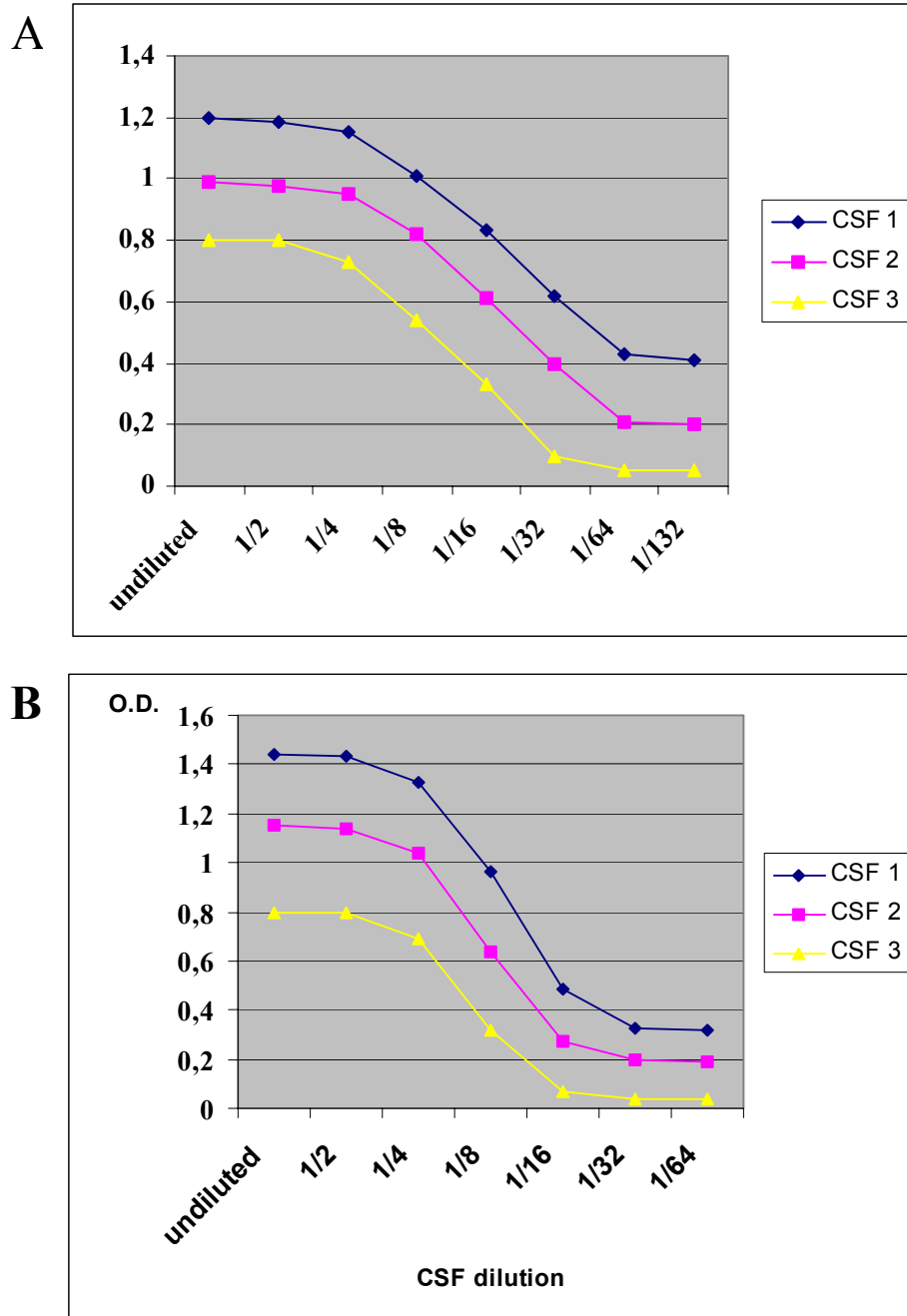


Figure 8: CSF dilution curves in NCAM-Fc and PSA-NCAM-Fc ELISA

(A) Three different CSF with low, middle or high amount of NCAM protein were titrated in two-fold serial dilutions when the other parameters: capture monoclonal antibody dilution 1/1000, detection polyclonal antibody dilution 1/1000 were constant. (B) Three different CSF with low, middle or high amount of PSA-NCAM protein were titrated in two-fold serial dilutions when the other parameters: capture monoclonal antibody dilution 1/700 and detection polyclonal antibody dilution 1/1000 were constant.

3.5 Optimizing the ELISA

The optimisation of NCAM and PSA-NCAM ELISA was performed as described previously (see 2.5).

3.6 Sensitivity of the NCAM-Fc and PSA-NCAM-Fc ELISA tests

Sensitivity of the NCAM-Fc and PSA-NCAM-Fc tests was determined as described above (see 2.6). MDC calculated for NCAM-Fc ELISA test was 5.5 ng/ml, whereas this value for PSA-NCAM-Fc ELISA test was 2.5 ng/ml.

4. Levels of L1, NCAM and PSA-NCAM in the cerebrospinal fluids of different patient groups

There was an increase ($p < 0.0001$) in mean levels of L1 in the cerebrospinal fluid CSF of Alzheimer disease (AD) patients (18.2 ± 0.7 ng/ml, $n=76$) when compared to normal controls (12.2 ± 0.6 ng/ml, $n=46$) (Figure 9). There was also an increase ($p < 0.01$ and $p < 0.05$ respectively) in L1 levels in patients with vascular dementia (19.6 ± 2.7 ng/ml, $n=9$) and dementia of mixed type (17.8 ± 1.8 ng/ml, $n=8$) in comparison to normal controls. Elevated L1 levels in the CSF of these groups were observed irrespective of age and gender. Other groups: multiple system atrophy ($n=4$), Parkinson's disease ($n=6$), diffuse Lewy body dementia ($n=4$), epilepsy ($n=15$), amyotrophic lateral sclerosis ($n=7$), polyneuropathy ($n=10$), multiple sclerosis ($n=9$), did not show any difference in comparison to the normal control group.

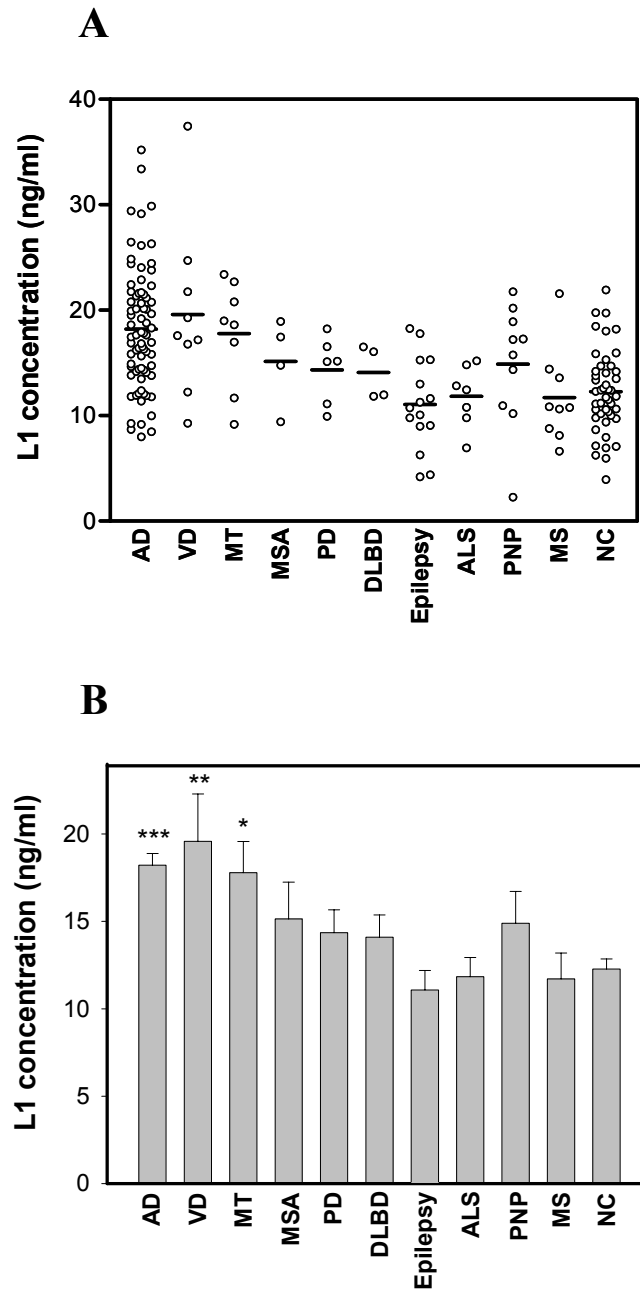


Figure 9: L1 concentrations in the CSF of different patients groups

(A) Individual values (circles) represent L1 concentration in the cerebrospinal fluid (CSF) of patients with Alzheimer disease (AD), vascular dementia (VD), dementia of mixed type (MT), multiple system atrophy (MSA), Parkinson's disease (PD), diffuse Lewy body dementia (DLBD), epilepsy, amyotrophic lateral sclerosis (ALS), polyneuropathy (PNP), multiple sclerosis (MS) and normal controls (NC). Each horizontal line represents the mean value of L1 concentration. (B) Mean values of L1 concentration \pm standard error. Statistical analysis (with age correlation) showed increased (***) levels in the CSF of Alzheimer disease patients in comparison to normal controls. The concentrations of L1 were also increased (** $p < 0.01$ and * $p < 0.05$ respectively) in the CSF of patients with vascular dementia and dementia of mixed type in comparison to normal controls.

V. Results

Levels of NCAM were increased ($p < 0.0001$) in the CSF of Alzheimer disease patients (845.4 ± 39.7 ng/ml, $n=76$), when compared to normal controls (551.3 ± 33.3 ng/ml, $n=46$). Furthermore, levels of NCAM were higher ($p < 0.05$) in patients with vascular dementia (852.1 ± 146.2 , $n=9$) and dementia of mixed type (937.5 ± 177.4 , $n=8$) in comparison to normal controls (Figure 10). NCAM concentration was independent of gender, but correlated with age. When corrected for age as co-variable, the association of higher NCAM concentrations in the patients with Alzheimer disease remained significant ($p < 0.05$). However, when patients with vascular dementia and dementia of mixed type were compared to the normal controls with correction for age, the difference was not anymore significant. NCAM level was decreased ($p < 0.05$) in the CSF from patients with multiple sclerosis (342.2 ± 16.7 ng/ml, $n=9$) in comparison to normal controls, and the difference remained significant after correction for age.

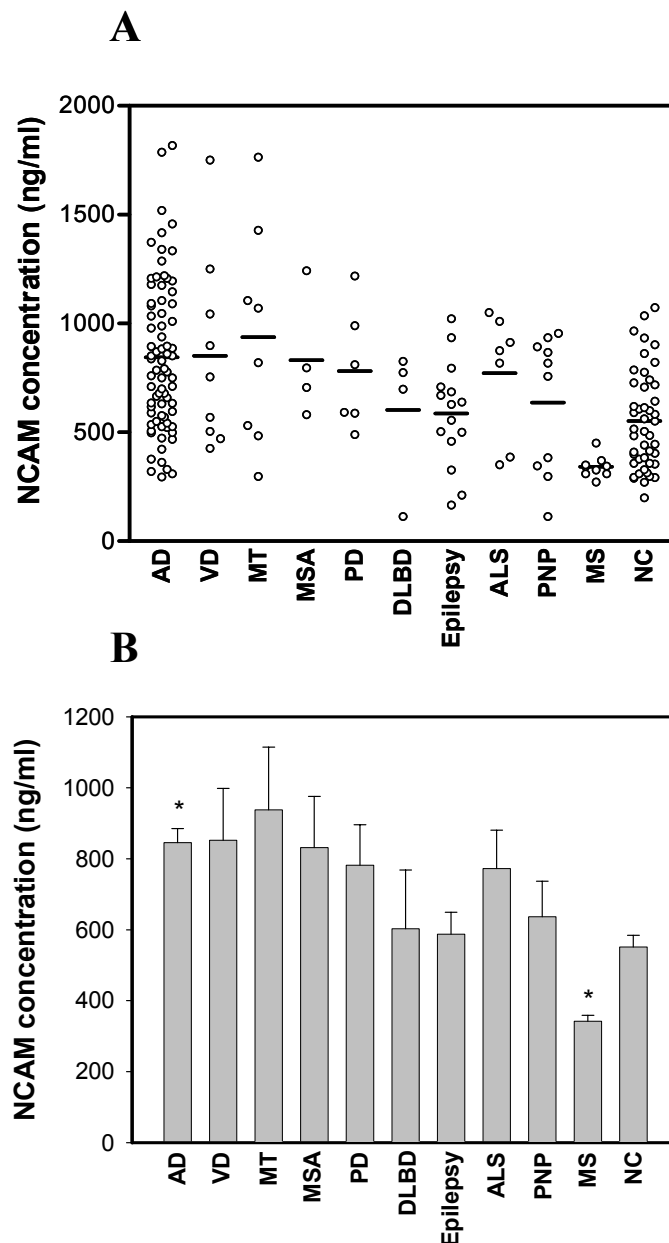


Figure 10: NCAM concentrations in the CSF of different patients groups

(A) Individual levels (circles) represent NCAM concentration in the cerebrospinal fluid (CSF) of patients with Alzheimer disease (AD), vascular dementia (VD), dementia of mixed type (MT), multiple system atrophy (MSA), Parkinson's disease (PD), diffuse Lewy body dementia (DLBD), epilepsy, amyotrophic lateral sclerosis (ALS), polyneuropathy (PNP), multiple sclerosis (MS) and normal controls (NC). Each horizontal line represents the mean value of NCAM concentration. (B) Mean values of NCAM concentration \pm standard error. Statistical analysis (with age correlation) showed higher ($*p<0.05$) levels in the CSF of Alzheimer disease patients when compared to normal controls. The level of NCAM was decreased ($*p<0.05$) in the CSF of patients with multiple sclerosis (MS).

Levels of PSA-NCAM in the CSF did not differ among the groups (Figure 11). The mean concentration of PSA-NCAM in normal control group was 56.9 ± 2.8 ng/ml ($n=46$).

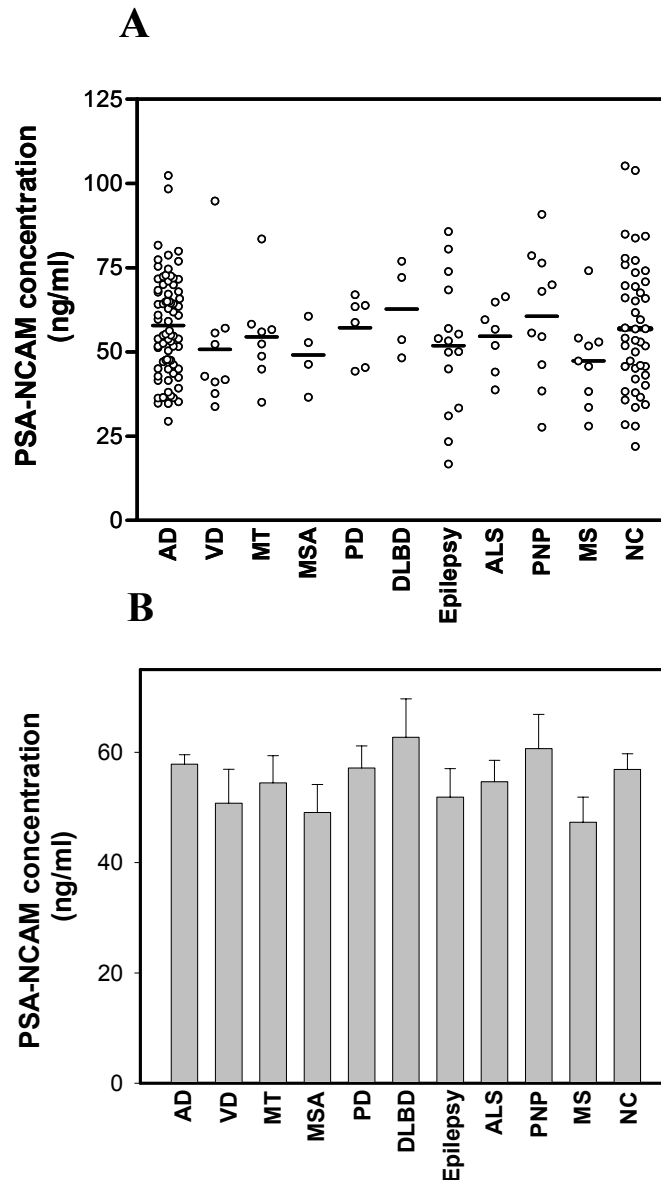


Figure 11: PSA-NCAM concentrations in the CSF of different patients groups

(A) Individual levels (circles) represent PSA-NCAM concentration in the cerebrospinal fluid (CSF) of patients with Alzheimer disease (AD), vascular dementia (VD), dementia of mixed type (MT), multiple system atrophy (MSA), Parkinson's disease (PD), diffuse Lewy body dementia (DLBD), epilepsy, amyotrophic lateral sclerosis (ALS), polyneuropathy (PNP), multiple sclerosis (MS) and normal controls (NC). Each horizontal line represents the mean value of PSA-NCAM concentration. (B) Mean values of PSA-NCAM concentration \pm standard error. Statistical analysis did not show any significant difference in PSA-NCAM levels between the groups.

5. L1, NCAM and PSA-NCAM levels in cerebrospinal fluid of dementia and non-dementia groups

To investigate whether the levels of adhesion molecules are associated with all forms of dementia, the concentrations of L1, NCAM and PSA-NCAM were further analysed in patients after their assignment to dementia and non-dementia groups. There was an increase ($p < 0.000001$) in mean of L1 levels in the CSF of patients with dementia (17.2 ± 0.6 ng/ml, $n=117$) in comparison to the non-dementia group (13.2 ± 0.5 ng/ml, $n=101$) (Figure 12A). The L1 concentration in these groups was independent of gender but correlated with age ($r=0.28$; $p < 0.05$). However, the association of higher L1 concentrations in patients with all forms of dementia remained when corrected for age as co-variable ($p < 0.00001$).

When corrected for age within the group of demented patients, the severity of dementia as defined by the Mini Mental State Examine (MMSE) as a discontinuous variable (stepwise regression), or the assignment of patients to groups of mildly ($n=68$), moderately ($n=42$) and severely ($n=7$) demented patients did not correlate with the L1 concentration.

NCAM concentration was higher ($p < 0.00001$) in the CSF of patients with dementia (830.3 ± 33.3 ng/ml, $n=117$) when compared to the non-dementia group (603.5 ± 26.0 ng/ml, $n=101$) (Figure 12B). NCAM concentrations were independent of gender but correlated with age ($r=0.37$; $p < 0.05$). The association of higher NCAM concentrations with dementia remained when corrected for age as co-variable ($p < 0.05$).

When corrected for age within the group of demented patients, the degree of dementia as defined by the MMSE as a discontinuous variable (stepwise regression) or the assignment of patients to groups of mildly ($n=71$), moderate ($n=42$) and severely ($n=7$) demented did not correlate with the NCAM concentration.

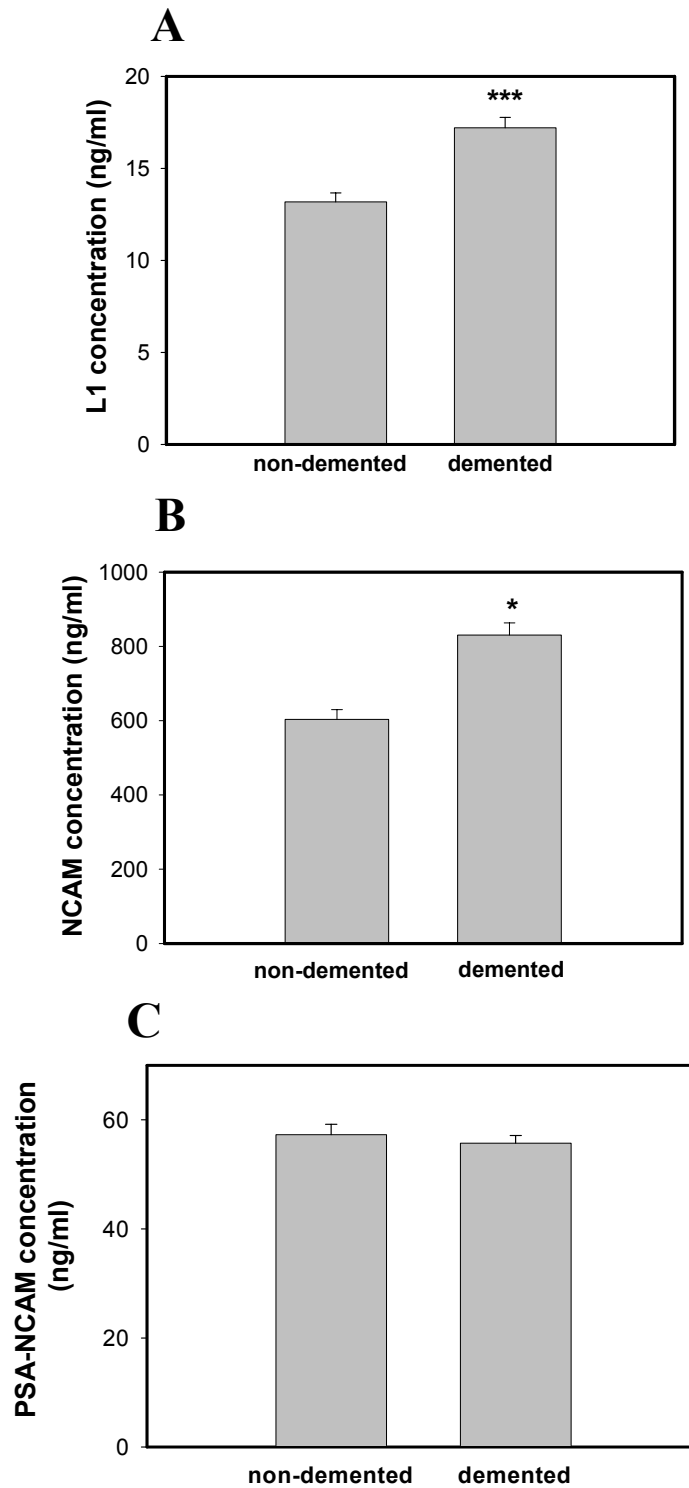


Figure 12: L1, NCAM and PSA-NCAM concentrations in the CSF of demented and non-demented patients

(A) Mean values of L1 concentrations \pm standard error in dementia and non-dementia groups. Statistical analysis (with correction for age) revealed increased (***) levels of L1 in the CSF of patients with dementia in comparison to the non-dementia group. (B) Mean values of NCAM concentrations \pm standard error in dementia and non-dementia groups. Statistical analysis (with correction for age) showed

that NCAM concentration was higher (* $p < 0.05$) in the CSF of patients with dementia when compared to the non-dementia group. (C) Mean values of PSA-NCAM concentrations \pm standard error in dementia and non-dementia groups. Statistical analysis did not reveal any difference in PSA-NCAM levels between the dementia and non-dementia groups.

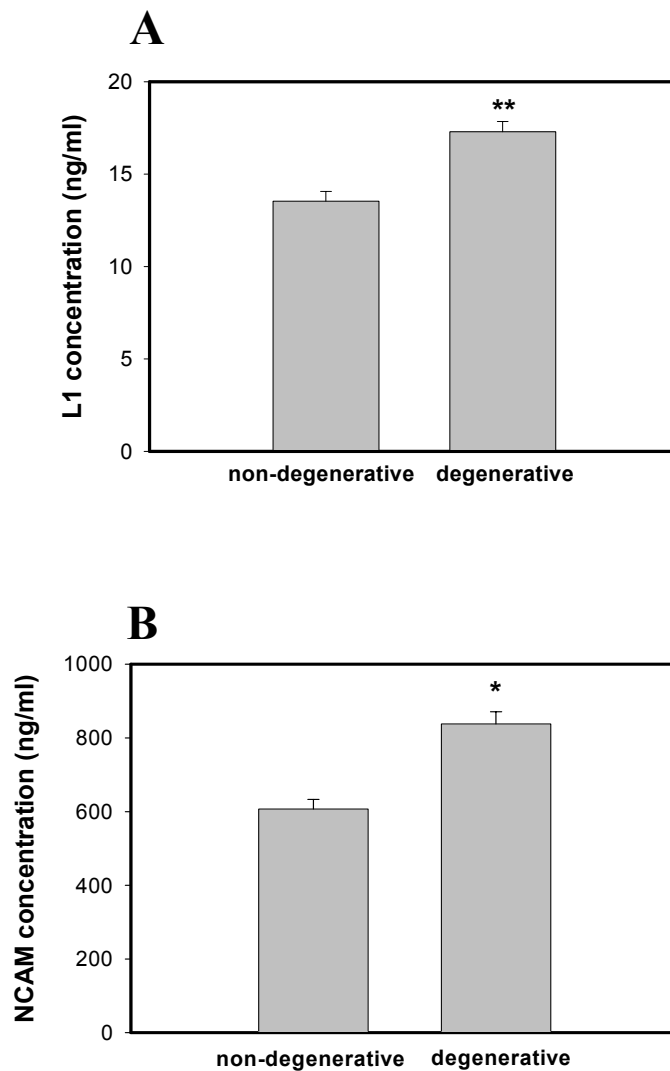
The mean concentration of PSA-NCAM in patients without dementia was 57.3 ± 1.9 ng/ml ($n=102$), while the mean concentration of PSA-NCAM in patients with dementia was 55.7 ± 1.4 ng/ml ($n=116$). Statistical analysis did not reveal any difference in the concentration of PSA-NCAM in the CSF of demented and of non-demented patients (Figure 12C). Concentrations of PSA-NCAM were independent of gender and did not correlate with age.

6. Levels of L1, NCAM and PSA-NCAM in the CSF of patients with neurodegenerative disorders and non-degenerative diseases

Because in most patients the condition causing dementia is associated with neurodegeneration, it was decided to explore whether neurodegenerative processes in the central nervous system are associated with elevated L1 and NCAM concentrations. Indeed, the group of patients with neurodegenerative diseases (Alzheimer disease; $n=76$, dementia of mixed type; $n=8$, Parkinson's disease; $n=6$, diffuse Lewy body dementia; $n=4$, multiple system atrophy; $n=4$, amyotrophic lateral sclerosis; $n=7$, progressive supranuclear palsy; $n=1$ and Pick's disease; $n=2$) had significantly higher ($p < 0.000001$) concentrations of L1 in the CSF (17.3 ± 0.5 ng/ml, $n=108$) compared to the group of patients with non-degenerative diseases (vascular dementia; $n=9$, multiple sclerosis; $n=9$, epilepsy; $n=15$, polyneuropathy; $n=10$, normal pressure hydrocephalus; $n=2$, psychosis; $n=3$, alcoholism; $n=3$, major depression; $n=6$, paraneoplastic encephalopathy; $n=1$, rheumatoid arthritis; $n=1$, epidural hematoma; $n=2$, varicella zoster neuritis; $n=2$, spinal muscle atrophy, $n=1$), including normal controls ($n=46$), (13.5 ± 0.5 ng/ml, $n=110$) (Figure 13A). This difference remained significant with correction for age ($p < 0.001$). However, when only those patients with neurodegenerative diseases were compared to the group of patients with non-degenerative diseases without dementia the difference was not anymore significant.

The levels of NCAM were higher ($p<0.000001$) in the CSF of patients with neurodegenerative disorders (837.8 ± 33.1 ng/ml, $n=108$) compared to the group of patients with non-degenerative diseases, including normal controls (606.9 ± 26.2 ng/ml, $n=106$) (Figure 13B). This difference remained significant ($p<0.05$) with correction for age. As shown for L1, NCAM values were not different between non-demented patients with neurodegenerative diseases and non-demented patients with non-degenerative diseases.

The concentrations of PSA-NCAM in the group of patients with neurodegenerative diseases (57.3 ± 1.3 ng/ml) were not different from the group of patients with non-degenerative diseases, including controls (55.8 ± 1.9 ng/ml) (Figure 13C).



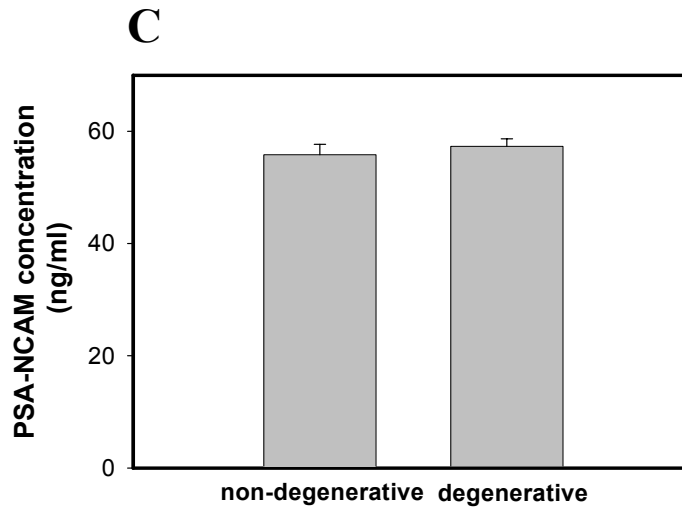


Figure 13: L1, NCAM and PSA-NCAM concentrations in the CSF of patients with degenerative and non-degenerative disorders

(A) Mean values of L1 concentrations \pm standard error in the patients with neurodegenerative and non-degenerative disorders. Statistical analysis (with correction for age) showed increased (** $p < 0.001$) levels of L1 in the CSF of patients with neurodegenerative disorders in comparison to the non-degenerative disorders group. (B) Mean values of NCAM concentrations \pm standard error in the patients with neurodegenerative and non-degenerative disorders. Statistical analysis (with correction for age) revealed that NCAM concentration was higher (* $p < 0.05$) in the CSF of patients with neurodegenerative disorder group when compared to the patients without neurodegeneration. (C) Mean values of PSA-NCAM concentrations \pm standard error in the patients with or without neurodegeneration. Statistical analysis did not show any difference in PSA-NCAM levels between the patients in neurodegenerative and non-degenerative groups.

7. Stepwise multiple regression analysis with L1, NCAM or PSA-NCAM as dependent and age, gender, presence of dementia and neurodegenerative etiology as independent variables

Additionally a stepwise multiple regression analysis with L1 as dependent and age, gender, dementia and neurodegenerative etiology as independent variables was performed. This confirmed the significant influence of dementia (beta 0.175, correlation 0.30) and

neurodegeneration (beta 0.165, correlation 0.29) but not of age (beta 0.085, correlation 0.26) and gender (beta -0.01, correlation 0.05) on levels of L1. Partial correlation indicates that L1 was almost equally influenced by dementia (beta 0.14, $p=0.049$) and neurodegeneration (beta 0.14, $p=0.047$) without influence by age (beta 0.07, $p=0.34$) and gender (beta -0.01, correlation 0.05, $p=0.9$).

The stepwise multiple regression analysis for NCAM confirmed a significant influence of age (beta 0.23, correlation 0.35) and neurodegeneration (beta 0.18, correlation 0.33) but with this statistical tool no influence of dementia (beta 0.112, correlation 0.30) and gender (beta -0.07, correlation 0.01) on NCAM values was obtained. Partial correlation indicates that NCAM was influenced more by age (beta 0.21, $p=0.004$) and neurodegeneration (beta 0.17, $p=0.02$) than by the presence of dementia (beta 0.10, $p=0.18$) and gender (beta -0.07, $p=0.32$).

For PSA-NCAM, stepwise multiple regression analysis did not reveal any influence of age, gender, dementia or neurodegeneration on levels of this molecule in the CSF.

VI. Discussion

Study 1

In the present study, the identification and characterization of putative binding partners of APP were carried out. For this purpose, polyclonal rabbit antisera were raised against the antisense peptides of the β - and γ -cleavage sites of APP. Following the theory of complementary hydrophathy the proteins recognized by these antisera are the putative binding partners of APP. For isolation, different brain subfractions were prepared from the brain homogenate of adult mice and subjected to affinity chromatography using the antibodies against antisense of the β - and γ -cleavage sites of APP. The isolation of the proteins recognized by γ -cleavage site antibody from the Coomassie gel and the subsequent analysis of the protein sequence by MALDI-MS identified one of the proteins as calreticulin, a protein of 55-60 kDa. Another one was identified as V3 (the splice variant of versican), a protein with molecular mass of 60-70 kDa. Whereas the sequence of protein recognized by β -cleavage site antibody revealed creatine kinase B (brain specific form), a protein of approximately 45 kDa.

1. Characterization of the APP - calreticulin interaction

Calreticulin (CRT) is an acidic protein of 55-60 kDa on SDS-polyacrylamide gel electrophoresis (Sontheimer et al., 1995). Although CRT was initially identified as a Ca^{2+} - binding protein residing in the ER lumen, its presence in a number of additional cellular compartments has been reported. In some cells CRT is perinuclear, intranuclear, cytosolic or at the cell surface (Matsuoka et al., 1994; Michalak et al., 1992; Opas et al., 1991; Sontheimer et al., 1995). The CRT structure has been highly conserved during evolution, indicating that it has an important role in cellular function. Analysis of the primary sequence of the protein showed that it consists of three domains. The N-terminal part of the molecule is predicted to form a globular β -sheet structure. The N-domain interacts with the DNA-binding domain of the glucocorticoid receptor *in vitro*, α -integrin, protein disulphide-isomerase (PDI) and with ER protein 57 (ERp57) and other ER proteins (Baksh et al., 1995; Burns et al., 1994; Corbett et al., 1999; Rojiani et al., 1991). The P-domain is rich in proline and contains two sets of repeated amino acid sequences unique to

CRT and its molecular homologues calnexin and calmeglin (Watanabe et al., 1994). The P-domain binds Ca^{2+} and acts as the high-affinity Ca^{2+} -binding site of CRT (Baksh and Michalak, 1991). The C-terminal region of the protein (C-domain) is highly acidic and terminates with KDEL ER retrieval sequence (Fliegel et al., 1989; Smith and Koch, 1989). It binds to Ca^{2+} with low affinity but high capacity and plays a regulatory role in the control of CRT interaction with PDI, ERp57 and perhaps other chaperons (Baksh and Michalak, 1991; Corbett et al., 1999; Fliegel et al., 1989).

CRT implicates several functional features providing a variety of interesting opportunities with regard to the function of the APP-CRT interaction. Thus, various functions have been described for CRT, including the action of CRT as a heat shock protein (Fliegel et al., 1989; Jethmalani and Henle, 1998), a lectin chaperon (Hebert et al., 1996; Nauseef et al., 1995; Pipe et al., 1998), a steroid hormone receptor (Burns et al., 1994). It has also been suggested that CRT may influence cell adhesion or cell spreading (Coppolino et al., 1997; Wada et al., 1997). Furthermore, it plays a role in intracellular Ca^{2+} - homeostasis (Bass et al., 1998; Camacho and Lechleiter, 1995), in the normal immune response and in autoimmunity (McCauliffe et al., 1990; Yokoi et al., 1993). It is not surprising therefore, that any changes in CRT expression and function have profound effects on many cellular functions.

Regarding the functional features of the calreticulin, presented above, its putative interaction with APP becomes likely and interesting since CRT has been shown to function as an ER chaperon, especially for glycoproteins, which include APP. In the present study the interaction between CRT and APP was confirmed using the ELISA binding assay. Since A β protein has a tendency to aggregate and form insoluble complexes due to its hydrophobic properties, the interaction between CRT and APP was revealed in this approach using synthetic biotinylated peptide APP1 mimicking the γ -cleavage site of APP. However, when another peptide APP2 mimicking the β -cleavage site of APP was used, no interaction was observed. These results demonstrate that CRT binds exclusively to γ -cleavage site within the APP, suggesting the high specificity of this interaction.

Furthermore, it was possible to show that APP can be co-immunoprecipitated using the antibody against CRT from mouse brain extract. Interestingly, that co-immunoprecipitation of CRT and APP was exclusively observed in synaptosomal membranes, but not in crude homogenate fractions. That is in consistence with results of distribution analysis of CRT and APP in brain subfractions, which showed an overlapping

distribution pattern in synaptosomes. In addition to this, recent data revealed that APP can be co-immunoprecipitated with the antibody against CRT from HEK 293 cells overexpressing APP₆₉₅ after their lysis in a mild detergent (Johnson et al., 2001). This study could demonstrate that CRT and APP form a transient, detergent-stable complex that appears to require divalent cations and neutral pH and N-linked glycosylation-dependent.

Finally, the immunocytochemical analysis of localization of CRT and APP in the primary hippocampal cultures was performed. Thus, the co-immunostaining with antibody against CRT and the antibody against APP showed the strong overlap, suggesting the co-localization of CRT and APP. Moreover, the interaction between these proteins was demonstrated in co-capping assay. Clustering of APP induced accumulations of calreticulin on the cell surface and co-localization of clusters indicated a co-redistribution of calreticulin and APP that was nicely observed in cell soma, axons and dendrites.

Although the association of CRT and APP is quite obvious, the precise nature of this interaction is not clear. The one possibility is lectin-mediated interaction of CRT, which is specific for monoglycosylated, high mannose containing proteins (Peterson et al., 1995; Spiro et al., 1996; Tatu and Helenius, 1997). But there are also documented examples of CRT binding via protein-protein interaction (Andrin et al., 1998; Kinoshita et al., 1998; Oliver et al., 1996). The previous study (Johnson et al., 2001) did not reveal Ca^{2+} - dependency on the APP/CRT interaction suggesting that APP and CRT may not interact through lectin-like mechanism (since lectin interactions are Ca^{2+} - dependent). Therefore, it is more likely that a protein-protein interaction is involved, although N-linked glycosylation is necessary for binding. In addition to this, it has been shown that APP/CRT complex is a part of a larger protein complex that may include other molecular chaperons as well as CRT. It is also possible that CRT may be a component of the γ -secretase complex. As mentioned before, presenilins are the major components of γ -secretase complex. Recent data indicate that this complex contains nicastrin, PEN-2, APH-1 and additional so far unidentified components.

The association of APP and CRT may have significant implications with respect to the pathogenesis of Alzheimer disease. Indeed, recently a decrease in CRT expression in neurons from AD brain has been found (Taguchi et al., 2000). Because A β 1-42 generated primarily in the ER, one might speculate that CRT binds to APP and facilitates correct folding of nascent APP. If so, impaired maturation of APP due to decreased CRT expression may affect amyloidogenic A β 1-42 production in the ER. Another possible

way in which decreased CRT levels may influence AD pathology is by damage to Ca^{2+} - homeostasis. It has been proposed that an early increase in intracellular free Ca^{2+} exacerbates oxidative stress, damages mitochondria, activates Ca^{2+} - dependent degradative enzymes, and disrupts the cytoskeleton, which play a central role in oxidant-induced cell death (Liu et al., 1998).

Thus, in the present study the *in vitro* interaction between CRT and APP was verified by several biochemical methods, such as direct binding ELISA assay and co-immunoprecipitation, and by immunocytochemical analysis. The physiological interaction between CRT and APP seems to be interesting with regard to Alzheimer disease pathology. The further functional analysis of this interaction would provide insights into better understanding the mechanisms involved in APP cleavage, and therefore, in development of AD.

2. Characterization of the APP - versican interaction

Versican is an extracellular matrix proteoglycan, which belongs to the chondroitin sulfate proteoglycan (CSPG) group. Versican is synthesized as multiple splice variants. In mammals, four different isoforms of versican have been identified. Three of these variants (V0, V1 and V2) include one or both (α and β) of the glycosaminoglycan (GAG) attachment domains and thus differ in the length of the central domain and in number of CS chains attached (Ito et al., 1995; Zimmermann et al., 1994). A fourth variant, V3, consists only of the amino – and carboxy-terminal domains and is therefore predicted to be a small glycoprotein, lacking CS chains (Zako et al., 1995). The V2, V1 and V0 splice variants of versican are very large molecules, with molecular masses between 6×10^5 and 1.5×10^5 Da (Dours-Zimmermann and Zimmermann, 1994; Schmalfeldt et al., 1998). Like all proteoglycans they are heterogeneous in size due to the variability of their glycosaminoglycan side chains. After chondroitinase ABC digestion, versicans V0, V1 and V2 migrate on SDS-polyacrylamide gels at about 550, 500 and 400 kDa, respectively. The discrepancy from the core protein sizes predicted from the amino acid sequences (370, 362 and 180 kDa, respectively) may partly result from the presence of N- and O-linked oligosaccharides. The smallest form of versican V3 is a protein of approximately 60-70 kDa by SDS-PAGE.

Immunohistochemical studies have revealed a relatively wide distribution of versican V0 and V1 in adult human tissues in the central and peripheral nervous system (Bode-Lesniewska et al., 1996). Thus, versican V0/ V1 is present in the loose connective tissues of various organs, in most smooth muscle tissues, in fibrous and elastic cartilage, as well as in blood vessels. RT-PCR experiments show a similarly wide expression pattern for the shortest splice variant V3. In contrast, versican V2 seems to be restricted to the CNS (Paulus et al., 1996; Schmalfeldt et al., 1998).

The amino-terminal domain of versican is responsible for the binding of versican to the glycosaminoglycan hyaluronan (HA) (LeBaron et al., 1992). The carboxy-terminal domain consists of EGF-like, lectin-like and complement regulatory protein-like domains (Zimmermann and Ruoslahti, 1989). The EGF-like domain has been shown to be pro-proliferative and lectin-like domain binds to tenascin-R and fibulin-1 (Aspberg et al., 1995; Aspberg et al., 1999; Zhang et al., 1998a). The CS chains are highly negatively charged and contribute anti-adhesive properties to the molecule. However, a recent study showed that the V3 isoform in contrast to larger forms increases adhesion and inhibits migration and proliferation (Lemire et al., 2002). It is conceivable, that the selective expression of a particular versican splice variant regulates conjointly with hyaluronan, link protein, and CD44, the hydration properties of hyaluronan-rich pericellular matrices and thereby modulates cell-cell and cell-matrix interactions during migration and proliferation processes.

In the present study the interaction between versican and APP was confirmed by ELISA. As described above for calreticulin, synthetic biotinylated peptide APP1 mimicking the γ -cleavage site of APP was used to prove the possible interaction. Since the commercial versican V3 is not available currently, the mixture of V0 and V1 isoforms was used for this assay. Although a relatively small amount of V3 isoform is present in larger versican isoforms, strong binding of versican and APP was observed. The specificity of the versican – APP binding was checked using the APP2 peptide, mimicking the β -cleavage site of APP, as a negative control.

Moreover, the interaction between versican and APP was verified in an alternative binding approach by a co-immunoprecipitation of these proteins from mouse brain extract. The co-immunoprecipitation of versican and APP was detected only in synaptosomal membranes, whereas the co-immunoprecipitation was not observed when crude homogenate was used. This is in principle in accordance with the results showing the co-distribution of versican and APP in synaptosomes.

However, the immunocytochemical analysis of localization of versican and APP, failed to show the co-localization and co-capping of these proteins. But taking into account that the antibody against V1 isoform of versican was used in this assay, one could suggest that it was not possible to detect V3 isoform of versican (present in minor amount), using this antibody. The V1 isoform of versican, detectable by this antibody, is apparently not co-localized with APP.

The specific binding of APP to ECM molecules was described previously. It has been demonstrated, that APP interacts mainly with heparan sulfate proteoglycans (HSPG), but also has binding sites for laminin and collagen (Beher et al., 1996; Caceres and Brandan, 1997; Small et al., 1993). It has been proposed that this interaction may be important for the function of APP. Substratum-bound APP was found to dramatically increase neurite outgrowth and survival of chick sympathetic neurons in vitro (Small et al., 1993). This effect was dependent upon the presence of substratum-bound HSPG. These results suggest that normally, when bound to the ECM, APP functions to promote neurite outgrowth and cell survival, whereas the loss of this normal trophic function might occur in AD, when APP is proteolytically processed via the amyloidogenic pathway. Moreover, it has been shown that laminin, collagen and heparin influence the level of an amyloidogenic A β in Neuro 2A neuronal cells, without a significant change in the neuronal marker acetylcholinesterase (Bronfman et al., 1996). These observations provide evidence that ECM molecules influence APP biogenesis, including the generation of A β . Taking into account these observations, the interaction between APP and versican seems to be interesting and reasonable. In the present study it was possible to prove the binding of versican and APP by ELISA assay and by co-immunoprecipitation. However, the functional role of this interaction should be investigated further.

3. Characterization of the APP - creatine kinase B interaction

Creatine kinase (CK) B is a member of the CK gene family and is a predominant cytosolic isoform in the brain. CKs are the family of enzymes that catalyze the reversible transfer of a phosphoryl group between ATP and creatine (Bessman and Carpenter, 1985) playing an important role in maintenance of energy homeostasis in the brain. It has been shown that B-CK is expressed on both neural and glial cell types across the CNS (Jost et al., 2002). The enzyme has a rather broad expression distribution in all vertebrates and is found not

only in brain, but also in kidney and smooth muscle-containing organs (Wallimann et al., 1992).

Since altered energy metabolism and oxidative stress implicated in the pathogenesis of AD (Beal, 1995; Smith et al., 1991), one can suggest a possible role of B-CK in this disorder. Indeed, recent study revealed reduced level of this enzyme in brain regions affected by neurodegeneration in AD (Aksenov et al., 2000). Interestingly, this reduction was not a result of decreased mRNA levels, demonstrating that posttranslational modification of B-CK plays a role in the decrease of enzyme activity in AD brain. Accumulating evidence supports increased oxidative modification of proteins in AD, which may disturb neuronal functions by decreasing activities of key metabolic enzymes, such as B-CK, and affecting cellular signalling system (Malorni et al., 1994). Therefore, a decrease in B-CK activity might be one of the biochemical markers of the CNS cell damage in age-related neurodegenerative disorders, including AD (Aksenov et al., 1997; Hensley et al., 1995). In addition, the studies of B-CK knock-out mice have demonstrated that animals lacking B-CK display diminished open-field habituation and slower spatial learning acquisition, which persisted upon ageing (Jost et al., 2002).

In the present study, the interaction between APP and its putative binding partner B-CK has been investigated. Immunocytochemical analysis in primary cultures revealed only small amounts of immunoreactive B-CK overlapping with immunostaining for APP, although widespread expression of B-CK all over the cell was observed. As well as co-capping experiments showed only small amounts of overlapped clusters on the cell surface.

The ELISA binding assay that was carried out in the present study failed to confirm interaction between APP and B-CK. The binding was not observed neither when B-CK was immobilized on a plastic surface and soluble APP was added, nor after immobilization of APP and incubation with soluble B-CK, although the antibody against B-CK worked well. However, it has been shown, that binding of some proteins might be observed exclusively in the presence of some co-factors, for instance, ADP or ATP. Therefore, one can propose that the putative interaction between APP and B-CK is required some substrates that can mediate this binding. However, the attempts to perform the ELISA in the presence of ADP or ATP failed to demonstrate the binding between APP and B-CK.

It was possible to co-immunoprecipitate APP with the antibody against B-CK from mouse brain extract. The co-immunoprecipitation was remarkably pronounced only in the crude

brain homogenate, but not in synaptosomal membranes. Although the co-immunoprecipitation does not prove the direct binding of the proteins, it speaks for a possible interaction. Taking these results together, one can suggest that, if there is interaction between B-CK and APP it is rather indirect, and probably requires some assisting proteins. However, this should be identified in further analysis.

Study 2

To assess a possible correlation between the levels of the immunoglobulin superfamily adhesion molecules L1 and NCAM and its associated polysialic acid, with Alzheimer disease and other forms of dementia, a capture ELISA with high specificity and sensitivity not previously attained in other studies has been developed. The choice to measure the levels of these molecules in the cerebrospinal fluids (CSF) and not in serum of the patients has been made in order for the analysis to be as close as possible to the site of action of the disease in patients that could be followed over longer periods of time. The results were evaluated in terms of concentration of the molecules measured as a function of Alzheimer disease, and also as a function of other forms of dementia, neurodegenerative etiology, age and gender, to allow for the analysis of several variables that may influence the levels of the molecules on the study. L1, NCAM and the polysialated form of NCAM, (PSA-NCAM) were chosen, because these molecules play important roles during ontogenetic development, regeneration and synaptic plasticity in the adult, as evidenced by observations on constitutively and conditionally deficient L1 and NCAM mutant mice and mice that become deficient in synthesis of PSA at weaning age (Cremer et al., 1998; Eckhardt et al., 2000; Kamiguchi et al., 1998; Runker et al., 2003; Thelin et al., 2003). Furthermore, mutations in the human L1 gene attests the importance of L1 in pathological conditions, such as X-linked hydrocephalus, X-linked spastic paraplegia, agenesis of corpus callosum and MASA syndrome (Fransen et al., 1995b; Jouet et al., 1994; Rosenthal et al., 1992). Observations on the conditionally L1 and NCAM deficient animals show that the two molecules and the NCAM associated polysialic acid play important roles in synaptic plasticity in the adult, thus demonstrating a positive direct or indirect role of these molecules in the appropriate function of the adult nervous system in learning and memory.

Previous studies have shown abnormal levels of NCAM and L1 in association with some psychiatric disorders. People suffering from bipolar mood disorder type I, recurrent unipolar major depression (Poltorak et al., 1996), schizophrenia (Poltorak et al., 1995) and autism (Purcell et al., 2001) show different levels of particular isoforms of NCAM in the CSF or in post-mortem brain tissue. Patients with bipolar mood disorder type II show normal levels of NCAM in the CSF. Interestingly, medication does not affect the concentrations of NCAM in the CSF of patients with abnormal levels of NCAM. Furthermore, it has been found a significant decrease in L1 concentration in the CSF of schizophrenic patients (Poltorak et al., 1995). Post-mortem examination of the hippocampal region of schizophrenic patients showed a significant reduction in the number of polysialic acid immunoreactive cells (Barbeau et al., 1995). Abnormalities of NCAM and L1 suggest that pathogenesis may be related to neurodevelopmental defects. However, correlation with age or gender and neurodegenerative versus non-neurodegenerative diseases have previously not been attempted. In such analysis it remains an open question, however, whether abnormal levels of recognition molecules are the cause rather the consequence of the pathological etiology.

The neural cell adhesion molecule L1 shows a prominent correlation with Alzheimer and non-Alzheimer forms of dementia. It is elevated in patients with Alzheimer disease, vascular dementia and dementia of the mixed type. A correlation with diffuse Lewy body disease was not possible because of the low number of samples. Interestingly, L1 does not correlate with a neurodegenerative etiology in general in the sense that only in demented patients that invariably have neurodegenerative processes occurring as a cause or as a result of the disease levels of L1 are increased. L1 is not elevated in patients with neurodegenerative diseases, such as Parkinson and Pick's disease and others without dementia. Importantly also, neither age nor gender are associated with abnormal levels of L1.

Different results were obtained for the protein backbone of NCAM. This is noteworthy, since NCAM and L1 have been shown to cooperate with each other functionally and share many functions in common, such as mediating neurite outgrowth and fasciculation, migration of neurons and involvement in synaptic plasticity. NCAM levels in the CSF are elevated in patients with Alzheimer disease and other forms of dementia. However, NCAM levels increased generally with age and correlate positively with neurodegenerative etiology. Thus, elevated levels of NCAM are rather related to

increasing age and neurodegeneration than with dementia as such. As for L1, no association was found relating to gender.

Strikingly, no difference in the levels of the PSA-containing isoforms of NCAM was seen under any pathological conditions, nor any correlation with age and gender. Since levels of NCAM protein are elevated under certain conditions and PSA remained constant, it must be assumed that non-polysialylated NCAM isoforms are preferentially released into the CSF when compared to polysialylated isoforms. This observation is interesting with regard to involvement of PSA in development and in synaptic plasticity and regeneration. It should be noted in this context that PSA does not protect NCAM from proteolysis (I. Kalus, R. Kleene and M. Schachner, unpublished observations).

Since the mechanisms underlying the occurrence of abnormal levels of L1 do not correlate with those of NCAM, the question remains as to the underlying mechanisms of this phenomenon. L1 is released on the cell surface by a disintegrin and metalloproteinase 10 (ADAM 10), (Kalus et al., 2003) while NCAM is released on the cell surface by ADAM 17, also called TACE (I. Kalus, R. Kleene and M. Schachner, unpublished observations). This is interesting in this respect that the α -secretase activity associated with proteolytic processing of the amyloid precursor protein (APP) has been associated with ADAM 10 (Lammich et al., 1999). Thus, both L1 and APP may respond similarly to the regulation of ADAM 10 activity. Since ADAM 10 has been discussed as abnormally regulated in AD patients, it is possible that L1 and APP are susceptible to similar mechanisms of proteolysis, different from those of NCAM. Since elevated levels of NCAM do not correspond to the etiology of dementia, but L1 and APP do, it is possible that L1 and APP may share a common mechanism of processing in dementia. Functional consequences of proteolysis with regard to neurite outgrowth have been investigated for L1 in that proteolysis, particularly in association with lipid rafts in conjunction with endocytosis as a prerequisite for neurite outgrowth. How this phenomenon may be related to L1 and APP and Alzheimer disease remains to be investigated. Finally, the relationship between reduced levels of NCAM and multiple sclerosis deserves further attention.

VII. Summary

(Study 1)

In the present study, putative binding partners of APP (amyloid precursor protein) were identified and further characterized. Since APP is believed to play a critical role in the pathophysiology of Alzheimer disease (AD), the identification of binding partners of APP would provide novel insights into understanding the mechanisms involved in APP cleavage and, therefore, help to identify potential targets for drugs to treat the AD.

For this purpose, polyclonal rabbit antisera were raised against peptides whose amino acid sequence was derived from the reverse complement nucleotide sequence corresponding to the β - and γ - cleavage sites within APP. Following the theory of complementary hydrophathy the proteins recognized by these antisera are the putative binding partners of APP. Different brain subfractions were prepared from brain homogenate of adult mice and subjected to affinity chromatography using the antisense antibodies to the β - and γ - cleavage sites. Proteins eluted from the column containing the antisense antibody of the γ - cleavage site were isolated from the Coomassie gel and subsequently analyzed by MALDI-MS. By this method, the amino acid sequence of two proteins was identified, namely calreticulin, a protein of 55-60 kDa and V3 (a splice variant of versican), a protein with the molecular mass of 60-70 kDa. In parallel, the protein eluted from the column containing the antisense antibody of the β -cleavage site was identified as creatine kinase B (brain specific form), a protein of approximately 45 kDa.

The interaction between calreticulin and APP was verified by ELISA binding assay using a synthetic biotinylated peptide that resembles the γ -cleavage site within APP. Furthermore, APP co-immunoprecipitated with the antibody against calreticulin from mouse brain extract. Co-immunoprecipitation of calreticulin and APP was exclusively observed in synaptosomal membranes, but not in crude homogenate fractions. In addition, immunocytochemical analysis revealed the co-localization of calreticulin and APP in primary hippocampal cultures. Finally, the interaction between these proteins was demonstrated in a co-capping assay. Clustering of APP induced accumulations of calreticulin on the cell surface and co-localization of clusters indicated a co-redistribution of calreticulin and APP that was observed in cell soma, axons and dendrites.

Thus, in the present study the *in vivo* interaction between calreticulin and APP was verified by several biochemical and immunocytochemical methods.

Moreover, the interaction between versican and APP was also confirmed by ELISA binding assay using the same biotinylated peptide as for calreticulin. Furthermore, the interaction between versican and APP was verified in an alternative binding approach by a co-immunoprecipitation of these proteins from extracts of synaptosomal membranes of mouse brain. The immunocytochemical analysis of localization of versican and APP failed to show the co-localization and co-capping of these proteins, which might be due to the different splice variants of versican.

The same methods were used to prove the interaction between APP and creatine kinase B. However, the ELISA binding assay that was carried out in the present study failed to confirm an interaction between these proteins. Immunocytochemical analysis in primary cultures revealed only small amounts of immunoreactive creatine kinase B overlapping with immunostaining for APP. In accordance, co-capping experiments showed only small amounts of APP clusters overlapping with creatine kinase B clusters on the cell surface. However, it was possible to co-immunoprecipitate APP from mouse brain extract using the antibody against creatine kinase B. These results suggest that if there is any interaction between APP and creatine kinase B, it is probably not a direct interaction but requires some assisting proteins or co-factors.

(Study 2)

In this study a total of 218 cerebrospinal fluid (CSF) samples from patients with different neurological diseases including Alzheimer disease, non-Alzheimer forms of dementia, other neurodegenerative diseases and normal controls were surveyed to quantitate the concentrations of the immunoglobulin superfamily adhesion molecules L1, NCAM and its associated polysialic acid. For this purpose, a sensitive, specific capture ELISA was developed and concentrations of adhesion molecules in the CSF were quantified followed by statistical analysis of the data.

L1 concentration was significantly elevated in the CSF of Alzheimer disease patients in comparison to the normal controls. L1 levels were also higher in the CSF of patients with vascular dementia and dementia of mixed type when compared to normal controls. Elevated L1 levels in the CSF in these groups were observed irrespective of age and gender. However, no significant differences in L1 concentration were seen in the CSF from patients with diffuse Lewy body dementia, multiple system atrophy, Parkinson's disease, multiple sclerosis, epilepsy, amyotrophic lateral sclerosis and polyneuropathy in comparison to normal controls. NCAM level was elevated in the CSF of Alzheimer

disease patients in comparison to normal controls. NCAM concentration was independent of gender, but correlated with age. NCAM level was significantly decreased in the CSF from patients with multiple sclerosis in comparison to normal controls, while the concentration of NCAM in the CSF from the patients with diffuse Lewy body dementia, multiple system atrophy, Parkinson's disease, epilepsy, amyotrophic lateral sclerosis and polyneuropathy did not significantly differ when compared to normal controls. There was no significant difference in PSA-NCAM levels in the CSF between the different groups.

In order to investigate whether the level of adhesion molecules is associated with dementia, the concentration of L1, NCAM and PSA-NCAM was analyzed further in patients after their assignment to dementia and non-dementia groups. The presence of dementia was explored by standard clinical procedures and the degree defined by the score in the Mini Mental State examine (MMSE). The L1 and NCAM concentrations were higher in the CSF of patients with dementia in comparison to non-dementia group, while there was no significant difference in PSA-NCAM levels in the CSF in demented and non-demented subjects. The association of higher L1 levels in patients with dementia was independent of severity of dementia and gender, but correlated with age.

Because in most patients the condition causing dementia is associated with neurodegeneration, it was further explored whether neurodegenerative processes in the central nervous system are associated with elevated L1 and NCAM concentrations. In fact, the group of patients with neurodegenerative diseases had significantly higher L1 and NCAM concentrations in the CSF compared to the group of patients with non-degenerative diseases and normal subjects.

Additionally stepwise multiple regression analysis with L1, NCAM or PSA-NCAM as dependent and age, sex, presence of dementia and neurodegenerative etiology as independent variables was performed. This confirmed a significant influence of dementia and neurodegeneration, but not of age on L1 concentrations in the CSF. Whereas a significant influence of age and neurodegeneration, but no influence of dementia on NCAM values was observed. For PSA-NCAM, stepwise multiple regression analysis did not reveal any significant influence of age, gender, presence of dementia or neurodegeneration on the level of this molecule in the CSF.

VII. Zusammenfassung

(Erster Teil)

Im Rahmen dieser Arbeit wurden potentielle extrazelluläre Interaktionspartner des Amyloid Precursor Proteins (APP) identifiziert und die Interaktion näher charakterisiert. APP spielt eine wichtige Rolle in der Pathophysiologie der Alzheimer Krankheit (AD). Daher könnte die Charakterisierung von APP-Interaktionspartnern wichtige Einblicke in die zugrundeliegenden molekularen Mechanismen der Krankheit liefern und weiterhin potentielle Angriffspunkte für neue Medikamente aufzeigen.

Um solche Interaktionspartner zu isolieren, wurden polyklonale Antikörper hergestellt, die eine Immunoreaktivität für jene Peptidsequenzen zeigen, die von der revers complementären Nucleotidsequenz der β - und γ -Schnittstelle innerhalb des APP codiert werden. Der Theorie der complementären Hydropathie folgend müssen die Proteine, welche von diesen polyclonalen Antikörpern erkannt werden, putative Interaktionspartner des APPs sein.

Gehirnhomogenate von adulten Mäusen wurden subfraktioniert und die Fraktionen über Affinitätssäulen gegeben, an die zuvor jeweils die weiter oben beschriebenen polyklonalen Antikörper gekoppelt worden waren. Die Proteine, welche spezifisch an die Antikörper gebunden hatten, wurden von den Säulen eluiert, aus Coomassie-gefärbten Gelen isoliert und mittels MALDI-MS analysiert. Zwei der Proteine, die von den polyclonalen Antikörpern gegen die complementäre Sequenz der APP γ -Schnittstelle erkannt wurden, konnten als Calreticulin (~55-60 kDa) und als eine Spleißisoform des Versicans, genannt V3 (~60-70 kDa) identifiziert werden. Parallel dazu konnte ein Protein, das von den polyclonalen Antikörpern gegen die complementäre Sequenz der APP β -Schnittstelle erkannt wurde, als Kreatin kinase B (gehirnspezifische Isoform) identifiziert werden.

Die Interaktion zwischen APP und Calreticulin konnte mittels ELISA bestätigt werden, in dem ein biotinyliertes Peptid mit der gleichen Aminosäuresequenz wie die γ -Schnittstelle verwendet wurde. Ausserdem konnte APP mit Calreticulin aus Fraktionen von Maus Gehirnhomogenaten co-immunopräzipitiert werden. APP co-präzipitierte mit Calreticulin nur aus der Synaptosomen-Fraktion, während keine Copräzipitation in crudem Gehirnhomogenat auftrat. Ferner konnte eine Colokalisation und ein Cocapping von APP und Calreticulin an kultivierten primären hippocampalen Neuronen gezeigt werden. Ein

Clustern von APP mittels anti-APP Antikörpern auf der Zelloberfläche führte zu einer Redistribution von Calreticulin auf der Zelloberfläche und einer Akkumulation von Calreticulin in den APP Clustern im Zellsoma, den Dendriten und Axonen. Die *in vivo* gefundene Interaktion von APP und Calreticulin konnte daher mittels biochemischer und immunocytochemischer Methoden verifiziert werden.

Die Interaktion von Versican und APP konnte ebenfalls im ELISA-Assay bestätigt werden. Zusätzlich konnte Versican mit APP aus der synatosomalen Fraktion von Maus Gehirnhomogenat copräzipitiert werden. Immuncytochemisch konnte allerdings weder eine Colokalisation noch ein Cocapping der beiden Proteine auf primären hippocampalen Neuronen nachgewiesen werden. Ein Grund dafür könnte die Abwesenheit der V3 Spleissform des Versicans auf hippocampalen Neuronen sein.

Die Interaktion zwischen APP und der Kreatin kinase B wurde ebenfalls mit den oben genannten Methoden untersucht. Allerdings konnte die Interaktion von APP und Kreatin kinase B im ELISA nicht bestätigt werden. Übereinstimmend damit zeigten die beiden Moleküle in der Immuncytochemie nur eine schwache Colokalisation auf primären hippocampalen Neuronen. Im Cocapping Assay zeigten die beiden Moleküle ebenfalls nur eine schwache Überlappung. Erstaunlicherweise konnte APP mit der Kreatin kinase B aus Maus Gehirnhomogenat copräzipitiert werden. Diese Ergebnisse könnten darauf hindeuten, dass APP und Kreatin kinase B nicht direkt miteinander interagieren, sondern dass weitere Proteine oder andere cofaktoren die Interaktion vermitteln.

(Zweiter Teil)

Im zweiten Teil dieser Arbeit wurden die Konzentrationen der Zelladhäsionsmoleküle aus der Immunglobulin-Superfamilie wie L1, NCAM und PSA-NCAM in der cerebrospinalen Flüssigkeit (CSF) von Patienten mit verschiedenen neurodegenerativen Erkrankungen wie z. B. Alzheimer und nicht-Alzheimer Formen der Demenz bestimmt. Dafür wurde ein sensitiver „capture“ ELISA-Assay entwickelt und die Konzentrationen der Zelladhäsionsmoleküle wurden im Vergleich zur Normalgruppe quantifiziert.

Die L1 Konzentrationen waren signifikant erhöht in den CSF von Patienten mit Alzheimer, vaskulärer Demenz und Demenz von Mischtyp im Vergleich zur Kontrollgruppe. Dabei waren die erhöhten L1 Level unabhängig von Alter und Geschlecht der Patienten. Im Gegensatz dazu zeigten Patienten mit diffuser Lewy Körper Demenz, multipler System Atrophie, Parkinson Krankheit, Multipler Skleroses, Epilepsie,

amyotropher lateraler Skleroses und Polyneuropathie keine Unterschiede in L1 Konzentrationen im Vergleich zur Kontrollgruppe.

Die Konzentration von NCAM war in der CSF von Patienten mit Alzheimer Krankheit im Vergleich zur Kontrollgruppe erhöht. Im Gegensatz dazu war die Konzentration von NCAM in Patienten mit Multipler Skleroses im Vergleich zur Kontrollgruppe reduziert. Die NCAM Konzentration zeigte in der CSF von Patienten mit diffuser Lewy Körper Demenz, multipler System Atrophie, Parkinson Krankheit, Multipler Skleroses, Epilepsie, amyotropher lateraler Skleroses und Polyneuropathie keine Abweichung zur Kontrollgruppe.

Um die Frage näher zu erörtern, ob die Konzentrationen der Zelladhäsionsmoleküle L1, NCAM und PSA-NCAM in der CSF mit dem Krankheitsbild der Demenz korreliert werden können, wurden die Konzentrationen dieser Moleküle in dem Demenz - Patientenkollektiv und dem Nicht-Demenz Patientenkollektiv näher analysiert. Der Grad der Demenz wurde nach klinischen Standards mittels des Mini Mental State Examine (MMSE) bestimmt.

Die Konzentrationen von L1 und NCAM waren in der Demenzgruppe im Vergleich zur Kontrollgruppe erhöht, während die PSA-NCAM Konzentration keine signifikanten Unterschiede zwischen den Gruppen zeigte. Die L1 Konzentration war unabhängig vom Grad der Demenz und vom Geschlecht, korrelierte aber mit dem Alter der Patienten.

Da in den meisten Fällen Demenz mit Neurodegeneration einhergeht, wurde weiter untersucht, ob neurodegenerative Erkrankungen mit den L1 und NCAM Level korrelieren. Tatsächlich hatten Patienten mit neurodegenerativen Erkrankungen erhöhte L1 und NCAM Konzentrationen in der CSF im Vergleich zur Nicht-Demenz Kontrollgruppe.

Zusätzlich wurde eine schrittweise multiple Regressionsanalyse mit L1, NCAM und PSA-NCAM als abhängigen Variablen und Alter, Geschlecht sowie Anwesenheit von Demenz und neurogenerativer Etiologie als unabhängigen Variablen durchgeführt. Dabei bestätigte sich ein signifikanter Einfluss von Demenz und Neurodegeneration, nicht aber des Alters, auf die L1 Konzentration in der CSF. Die NCAM Konzentration wurde signifikant durch Alter und Neurodegeneration, nicht aber durch Demenz, bestimmt. Die Konzentration von PSA-NCAM in der CSF zeigte sich unabhängig von Alter, Geschlecht, Demenz und Neurodegeneration der Patienten.

VIII. APPENDIX

1. ABBREVIATIONS

Ø	“without”, diameter
μ	micro (10 ⁻⁶)
× g	g-force
°C	grad celsius
aa	amino acid
A	adenine
Acc.	accession number
Amp	ampicillin
APS	ammoniumperoxodisulfate
ATP	adenosine triphosphate
bp	base pairs
BSA	bovine serum albumine
C	Cytosine
cDNA	complementary deoxyribonucleic acid
CHO	Chinese Hamster Ovarian
CSF	cerebrospinal fluid
Da	dalton
dATP	2'-desoxyadenosinetriphosphate
dCTP	2'-desoxycytidinetriphosphate
DEPC	diethylpyrocarbonate
dGTP	2'-desoxyguanosinetriphosphate
DMSO	dimethylsulfoxide
DNA	deoxyribonucleic acid
DNase	desoxyribonuclease
dNTP	2'-desoxyribonucleotide-5'-triphosphate
DTT	dithiothreitol
E. coli	escherichia coli
EDTA	ethylendiaminetetraacetic acid
ELISA	enzyme-linked immunosorbent assay

VIII. Appendix

f.c.	final concentration
FCS	fetal calf serum
g	gram
G	guanosine
h	human, hour
HEPES	2-(4-(2-Hydroxyethyl)-piperzino)-ethansulfonic acid
IP	immunoprecipitation
IPTG	isopropyl- β -D-thiogalactoside
kb	kilo base pairs
l	litre
LB	Luria Bertani
m	milli (10^{-3})
MEM	minimal essential medium
MESNa	2-mercaptoethanesulfonic acid
min	minute
MOPS	(4-(N-morpholino)-propan)-sulfonic acid
n	nano (10^{-9}), number
Nt	nucleotide(e)
OD _x	optic density
p	pico (10^{-12})
PAGE	polyacrylamide gel electrophoresis
PBS	phosphat-buffered saline
PEG	polyethylenglycol
PMSF	phenylmethanesulfonylfluoride
rpm	rounds per minute
p	statistical significance
psi	pounds per square inch
r	corralation coefficient
RNA	ribonucleic acid
RNase	ribonuclease
RT	room temperature
s	second
SDS	sodium dodecyl sulfate
T	thymine

VIII. Appendix

Tab.	table
TE	tris-EDTA
TEMED	N,N,N',N'-tetraethylenamine
T _m	melting temperature
TM	transmembrane segment
Tris	tris(-hydroxymethyl)-aminomethane
U	unit (enzymatic)
V	volt
v/v	volume per volume
Vol.	volume
w/v	weight per volume
ZMNH	Zentrum für Molekulare Neurobiologie Hamburg

Amino acids were abbreviated using the one letter code

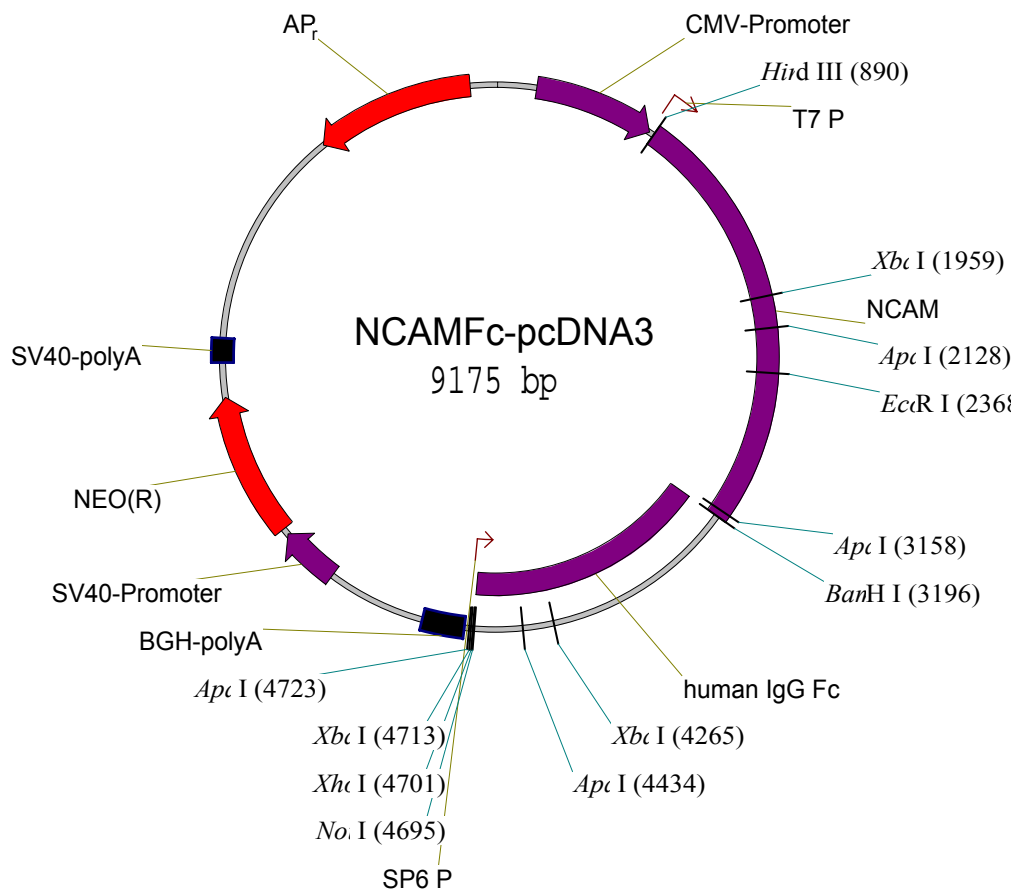
2. Accessionnumbers

Protein	Organism	Accession N°
APP	mouse	P12023
Calreticulin	rabbit	P15253
Creatine kinase B	human	P12277
Versican	bovine	P81282
L1	human	P32004
NCAM	human	O15394

3. Plasmids

3.1 NCAM-Fc in pcDNA3

NCAM and human IgG Fc were cut out of NCAM-PIG (gift of Dr. Jane L. Saffell, Department of Biochemistry, Imperial College, London, England) by digestion with the appropriate restriction enzymes BamHI/HindIII/NotI. The target vector pcDNA3 was digested with the corresponding restriction enzymes BamHI/HindIII and ligated with the insert encoding human NCAM. Human IgG Fc was subcloned into NCAMpcDNA3 intermediate construct via BamHI/NotI.



IX. Bibliography

1. Aaron L. I., Chesselet M. F. (1989) Heterogeneous distribution of polysialylated neuronal-cell adhesion molecule during post-natal development and in the adult: an immunohistochemical study in the rat brain. *Neuroscience* 28: 701-710.
2. Acheson A., Sunshine J. L., Rutishauser U. (1991) NCAM polysialic acid can regulate both cell-cell and cell-substrate interactions. *J Cell Biol* 114: 143-153.
3. Aksenov M., Aksenova M., Butterfield D. A., Markesbery W. R. (2000) Oxidative modification of creatine kinase BB in Alzheimer's disease brain. *J Neurochem* 74: 2520-2527.
4. Aksenov M. Y., Aksenova M. V., Payne R. M., Smith C. D., Markesbery W. R., Carney J. M. (1997) The expression of creatine kinase isoenzymes in neocortex of patients with neurodegenerative disorders: Alzheimer's and Pick's disease. *Exp Neurol* 146: 458-465.
5. Alcaraz G., Goridis C. (1991) Biosynthesis and processing of polysialylated NCAM by AtT-20 cells. *Eur J Cell Biol* 55: 165-173.
6. Allinquant B., Hantraye P., Mailleux P., Moya K., Bouillot C., Prochiantz A. (1995) Downregulation of amyloid precursor protein inhibits neurite outgrowth in vitro. *J Cell Biol* 128: 919-927.
7. Ando K., Oishi M., Takeda S., Iijima K., Isohara T., Nairn A. C., Kirino Y., Greengard P., Suzuki T. (1999) Role of phosphorylation of Alzheimer's amyloid precursor protein during neuronal differentiation. *J Neurosci* 19: 4421-4427.
8. Andreasen N., Minthon L., Davidsson P., Vanmechelen E., Vanderstichele H., Winblad B., Blennow K. (2001) Evaluation of CSF-tau and CSF-Aβ42 as diagnostic markers for Alzheimer disease in clinical practice. *Arch Neurol* 58: 373-379.
9. Andrin C., Pinkoski M. J., Burns K., Atkinson E. A., Krahenbuhl O., Hudig D., Fraser S. A., Winkler U., Tschopp J., Opas M., Bleackley R. C., Michalak M. (1998) Interaction between a Ca²⁺-binding protein calreticulin and perforin, a component of the cytotoxic T-cell granules. *Biochemistry* 37: 10386-10394.
10. Angata K., Nakayama J., Fredette B., Chong K., Ranscht B., Fukuda M. (1997) Human STX polysialyltransferase forms the embryonic form of the neural cell adhesion molecule. Tissue-specific expression, neurite outgrowth, and chromosomal localization in comparison with another polysialyltransferase, PST. *J Biol Chem* 272: 7182-7190.
11. Angata K., Suzuki M., McAuliffe J., Ding Y., Hindsgaul O., Fukuda M. (2000) Differential biosynthesis of polysialic acid on neural cell adhesion molecule (NCAM) and oligosaccharide acceptors by three distinct α 2,8-sialyltransferases, ST8Sia IV (PST), ST8Sia II (STX), and ST8Sia III. *J Biol Chem* 275: 18594-18601.
12. Aspberg A., Adam S., Kostka G., Timpl R., Heinegard D. (1999) Fibulin-1 is a ligand for the C-type lectin domains of aggrecan and versican. *J Biol Chem* 274: 20444-20449.

13. Aspberg A., Binkert C., Ruoslahti E. (1995) The versican C-type lectin domain recognizes the adhesion protein tenascin-R. *Proc Natl Acad Sci U S A* 92: 10590-10594.
14. Baksh S., Burns K., Andrin C., Michalak M. (1995) Interaction of calreticulin with protein disulfide isomerase. *J Biol Chem* 270: 31338-31344.
15. Baksh S., Michalak M. (1991) Expression of calreticulin in *Escherichia coli* and identification of its Ca²⁺ binding domains. *J Biol Chem* 266: 21458-21465.
16. Baranyi L., Campbell W., Ohshima K., Fujimoto S., Boros M., Okada H. (1995) The antisense homology box: a new motif within proteins that encodes biologically active peptides. *Nat Med* 1: 894-901.
17. Barbeau D., Liang J. J., Robitalille Y., Quirion R., Srivastava L. K. (1995) Decreased expression of the embryonic form of the neural cell adhesion molecule in schizophrenic brains. *Proc Natl Acad Sci U S A* 92: 2785-2789.
18. Bass J., Chiu G., Argon Y., Steiner D. F. (1998) Folding of insulin receptor monomers is facilitated by the molecular chaperones calnexin and calreticulin and impaired by rapid dimerization. *J Cell Biol* 141: 637-646.
19. Beal M. F. (1995) Aging, energy, and oxidative stress in neurodegenerative diseases. *Ann Neurol* 38: 357-366.
20. Becker C. G., Artola A., Gerardy-Schahn R., Becker T., Welzl H., Schachner M. (1996) The polysialic acid modification of the neural cell adhesion molecule is involved in spatial learning and hippocampal long-term potentiation. *J Neurosci Res* 45: 143-152.
21. Beer S., Oleszewski M., Gutwein P., Geiger C., Altevogt P. (1999) Metalloproteinase-mediated release of the ectodomain of L1 adhesion molecule. *J Cell Sci* 112 (Pt 16): 2667-2675.
22. Beggs H. E., Baragona S. C., Hemperly J. J., Maness P. F. (1997) NCAM140 interacts with the focal adhesion kinase p125 (fak) and the SRC- related tyrosine kinase p59 (fyn). *J Biol Chem* 272: 8310-8319.
23. Beher D., Hesse L., Masters C. L., Multhaup G. (1996) Regulation of amyloid protein precursor (APP) binding to collagen and mapping of the binding sites on APP and collagen type I. *J Biol Chem* 271: 1613-1620.
24. Bennett B. D., Babu-Khan S., Loeloff R., Louis J. C., Curran E., Citron M., Vassar R. (2000) Expression analysis of BACE2 in brain and peripheral tissues. *J Biol Chem* 275: 20647-20651.
25. Bessman S. P., Carpenter C. L. (1985) The creatine-creatine phosphate energy shuttle. *Annu Rev Biochem* 54: 831-862.
26. Bieber A. J., Snow P. M., Hortsch M., Patel N. H., Jacobs J. R., Traquina Z. R., Schilling J., Goodman C. S. (1989) *Drosophila neuroglian*: a member of the immunoglobulin superfamily with extensive homology to the vertebrate neural adhesion molecule L1. *Cell* 59: 447-460.

27. Bixby J. L., Pratt R. S., Lilien J., Reichardt L. F. (1987) Neurite outgrowth on muscle cell surfaces involves extracellular matrix receptors as well as Ca^{2+} -dependent and -independent cell adhesion molecules. *Proc Natl Acad Sci U S A* 84: 2555-2559.
28. Blacker D., Wilcox M. A., Laird N. M., Rodes L., Horvath S. M., Go R. C., Perry R., Watson B., Jr., Bassett S. S., McInnis M. G., Albert M. S., Hyman B. T., Tanzi R. E. (1998) Alpha-2 macroglobulin is genetically associated with Alzheimer disease. *Nat Genet* 19: 357-360.
29. Blaess S., Kammerer R. A., Hall H. (1998) Structural analysis of the sixth immunoglobulin-like domain of mouse neural cell adhesion molecule L1 and its interactions with $\alpha(v)\beta3$, $\alpha(\text{IIb})\beta3$, and $\alpha5\beta1$ integrins. *J Neurochem* 71: 2615-2625.
30. Bode-Lesniewska B., Dours-Zimmermann M. T., Odermatt B. F., Briner J., Heitz P. U., Zimmermann D. R. (1996) Distribution of the large aggregating proteoglycan versican in adult human tissues. *J Histochem Cytochem* 44: 303-312.
31. Bonfanti L., Olive S., Poulain D. A., Theodosis D. T. (1992) Mapping of the distribution of polysialylated neural cell adhesion molecule throughout the central nervous system of the adult rat: an immunohistochemical study. *Neuroscience* 49: 419-436.
32. Borg J. P., Ooi J., Levy E., Margolis B. (1996) The phosphotyrosine interaction domains of X11 and FE65 bind to distinct sites on the YENPTY motif of amyloid precursor protein. *Mol Cell Biol* 16: 6229-6241.
33. Braak H., Braak E. (1991) Neuropathological staging of Alzheimer-related changes. *Acta Neuropathol (Berl)* 82: 239-259.
34. Brackenbury R., Sorkin B. C., Cunningham B. A. (1987) Molecular features of cell adhesion molecules involved in neural development. *Res Publ Assoc Res Nerv Ment Dis* 65: 155-167.
35. Brackenbury R., Thiery J. P., Rutishauser U., Edelman G. M. (1977) Adhesion among neural cells of the chick embryo. I. An immunological assay for molecules involved in cell-cell binding. *J Biol Chem* 252: 6835-6840.
36. Brentani R. R. (1988) Biological implications of complementary hydrophathy of amino acids. *J Theor Biol* 135: 495-499.
37. Brentani R. R., Ribeiro S. F., Potocnjak P., Pasqualini R., Lopes J. D., Nakaie C. R. (1988) Characterization of the cellular receptor for fibronectin through a hydrophathic complementarity approach. *Proc Natl Acad Sci U S A* 85: 364-367.
38. Brewer G. J., Torricelli J. R., Evege E. K., Price P. J. (1993) Optimized survival of hippocampal neurons in B27-supplemented Neurobasal, a new serum-free medium combination. *J Neurosci Res* 35: 567-576.
39. Bronfman F. C., Soto C., Tapia L., Tapia V., Inestrosa N. C. (1996) Extracellular matrix regulates the amount of the beta-amyloid precursor protein and its amyloidogenic fragments. *J Cell Physiol* 166: 360-369.

40. Burgoon M. P., Grumet M., Mauro V., Edelman G. M., Cunningham B. A. (1991) Structure of the chicken neuron-glia cell adhesion molecule, Ng-CAM: origin of the polypeptides and relation to the Ig superfamily. *J Cell Biol* 112: 1017-1029.
41. Burgoon M. P., Hazan R. B., Phillips G. R., Crossin K. L., Edelman G. M., Cunningham B. A. (1995) Functional analysis of posttranslational cleavage products of the neuron-glia cell adhesion molecule, Ng-CAM. *J Cell Biol* 130: 733-744.
42. Burns K., Duggan B., Atkinson E. A., Famulski K. S., Nemer M., Bleackley R. C., Michalak M. (1994) Modulation of gene expression by calreticulin binding to the glucocorticoid receptor. *Nature* 367: 476-480.
43. Buskirk D. R., Thiery J. P., Rutishauser U., Edelman G. M. (1980) Antibodies to a neural cell adhesion molecule disrupt histogenesis in cultured chick retinæ. *Nature* 285: 488-489.
44. Buxbaum J. D., Liu K. N., Luo Y., Slack J. L., Stocking K. L., Peschon J. J., Johnson R. S., Castner B. J., Cerretti D. P., Black R. A. (1998) Evidence that tumor necrosis factor alpha converting enzyme is involved in regulated alpha-secretase cleavage of the Alzheimer amyloid protein precursor. *J Biol Chem* 273: 27765-27767.
45. Caceres J., Brandan E. (1997) Interaction between Alzheimer's disease beta A4 precursor protein (APP) and the extracellular matrix: evidence for the participation of heparan sulfate proteoglycans. *J Cell Biochem* 65: 145-158.
46. Cai X. D., Golde T. E., Younkin S. G. (1993) Release of excess amyloid beta protein from a mutant amyloid beta protein precursor. *Science* 259: 514-516.
47. Camacho P., Lechleiter J. D. (1995) Calreticulin inhibits repetitive intracellular Ca²⁺ waves. *Cell* 82: 765-771.
48. Cao X., Sudhof T. C. (2001) A transcriptionally [correction of transcriptively] active complex of APP with Fe65 and histone acetyltransferase Tip60. *Science* 293: 115-120.
49. Capell A., Grunberg J., Pesold B., Diehlmann A., Citron M., Nixon R., Beyreuther K., Selkoe D. J., Haass C. (1998) The proteolytic fragments of the Alzheimer's disease-associated presenilin-1 form heterodimers and occur as a 100-150-kDa molecular mass complex. *J Biol Chem* 273: 3205-3211.
50. Carenini S., Montag D., Cremer H., Schachner M., Martini R. (1997) Absence of the myelin-associated glycoprotein (MAG) and the neural cell adhesion molecule (N-CAM) interferes with the maintenance, but not with the formation of peripheral myelin. *Cell Tissue Res* 287: 3-9.
51. Chang S., Rathjen F. G., Raper J. A. (1990) Neurite outgrowth promoting activity of G4 and its inhibition by monoclonal antibodies. *J Neurosci Res* 25: 180-186.
52. Chen S., Mantei N., Dong L., Schachner M. (1999) Prevention of neuronal cell death by neural adhesion molecules L1 and CHL1. *J Neurobiol* 38: 428-439.
53. Chuong C. M., Edelman G. M. (1984) Alterations in neural cell adhesion molecules during development of different regions of the nervous system. *J Neurosci* 4: 2354-2368.

54. Cohen N. R., Taylor J. S., Scott L. B., Guillery R. W., Soriano P., Furley A. J. (1998) Errors in corticospinal axon guidance in mice lacking the neural cell adhesion molecule L1. *Curr Biol* 8: 26-33.
55. Cole G. J., Akeson R. (1989) Identification of a heparin binding domain of the neural cell adhesion molecule N-CAM using synthetic peptides. *Neuron* 2: 1157-1165.
56. Cook D. G., Sung J. C., Golde T. E., Felsenstein K. M., Wojczyk B. S., Tanzi R. E., Trojanowski J. Q., Lee V. M., Doms R. W. (1996) Expression and analysis of presenilin 1 in a human neuronal system: localization in cell bodies and dendrites. *Proc Natl Acad Sci U S A* 93: 9223-9228.
57. Coppelino M. G., Woodside M. J., Demareux N., Grinstein S., St Arnaud R., Dedhar S. (1997) Calreticulin is essential for integrin-mediated calcium signalling and cell adhesion. *Nature* 386: 843-847.
58. Corbett E. F., Oikawa K., Francois P., Tessier D. C., Kay C., Bergeron J. J., Thomas D. Y., Krause K. H., Michalak M. (1999) Ca²⁺ regulation of interactions between endoplasmic reticulum chaperones. *J Biol Chem* 274: 6203-6211.
59. Corbit K. C., Foster D. A., Rosner M. R. (1999) Protein kinase Cdelta mediates neurogenic but not mitogenic activation of mitogen-activated protein kinase in neuronal cells. *Mol Cell Biol* 19: 4209-4218.
60. Cotman C. W., Hailer N. P., Pfister K. K., Soltesz I., Schachner M. (1998) Cell adhesion molecules in neural plasticity and pathology: similar mechanisms, distinct organizations? *Prog Neurobiol* 55: 659-669.
61. Coulson E. J., Paliga K., Beyreuther K., Masters C. L. (2000) What the evolution of the amyloid protein precursor supergene family tells us about its function. *Neurochem Int* 36: 175-184.
62. Covault J., Sanes J. R. (1986) Distribution of N-CAM in synaptic and extrasynaptic portions of developing and adult skeletal muscle. *J Cell Biol* 102: 716-730.
63. Cremer H., Chazal G., Carleton A., Goridis C., Vincent J. D., Lledo P. M. (1998) Long-term but not short-term plasticity at mossy fiber synapses is impaired in neural cell adhesion molecule-deficient mice. *Proc Natl Acad Sci U S A* 95: 13242-13247.
64. Cremer H., Lange R., Christoph A., Plomann M., Vopper G., Roes J., Brown R., Baldwin S., Kraemer P., Scheff S., . (1994) Inactivation of the N-CAM gene in mice results in size reduction of the olfactory bulb and deficits in spatial learning. *Nature* 367: 455-459.
65. Crossin K. L., Krushel L. A. (2000) Cellular signaling by neural cell adhesion molecules of the immunoglobulin superfamily. *Dev Dyn* 218: 260-279.
66. Cunningham B. A. (1995) Cell adhesion molecules as morphoregulators. *Curr Opin Cell Biol* 7: 628-633.
67. Cunningham B. A., Hemperly J. J., Murray B. A., Prediger E. A., Brackenbury R., Edelman G. M. (1987) Neural cell adhesion molecule: structure, immunoglobulin-like domains, cell surface modulation, and alternative RNA splicing. *Science* 236: 799-806.

68. Dahme M., Bartsch U., Martini R., Anliker B., Schachner M., Mantei N. (1997) Disruption of the mouse L1 gene leads to malformations of the nervous system. *Nat Genet* 17: 346-349.
69. de Souza S. J., Brentani R. (1992) Collagen binding site in collagenase can be determined using the concept of sense-antisense peptide interactions. *J Biol Chem* 267: 13763-13767.
70. Debiec H., Christensen E. I., Ronco P. M. (1998) The cell adhesion molecule L1 is developmentally regulated in the renal epithelium and is involved in kidney branching morphogenesis. *J Cell Biol* 143: 2067-2079.
71. Doherty P., Cohen J., Walsh F. S. (1990) Neurite outgrowth in response to transfected N-CAM changes during development and is modulated by polysialic acid. *Neuron* 5: 209-219.
72. Doherty P., Walsh F. S. (1994) Signal transduction events underlying neurite outgrowth stimulated by cell adhesion molecules. *Curr Opin Neurobiol* 4: 49-55.
73. Doherty P., Williams E., Walsh F. S. (1995) A soluble chimeric form of the L1 glycoprotein stimulates neurite outgrowth. *Neuron* 14: 57-66.
74. Dours-Zimmermann M. T., Zimmermann D. R. (1994) A novel glycosaminoglycan attachment domain identified in two alternative splice variants of human versican. *J Biol Chem* 269: 32992-32998.
75. Duczmal A., Schollhammer S., Katich S., Ebeling O., Schwartz-Albiez R., Altevogt P. (1997) The L1 adhesion molecule supports alpha v beta 3-mediated migration of human tumor cells and activated T lymphocytes. *Biochem Biophys Res Commun* 232: 236-239.
76. Ebeling O., Duczmal A., Aigner S., Geiger C., Schollhammer S., Kemshead J. T., Moller P., Schwartz-Albiez R., Altevogt P. (1996) L1 adhesion molecule on human lymphocytes and monocytes: expression and involvement in binding to alpha v beta 3 integrin. *Eur J Immunol* 26: 2508-2516.
77. Eckhardt M., Bukalo O., Chazal G., Wang L., Goridis C., Schachner M., Gerardy-Schahn R., Cremer H., Dityatev A. (2000) Mice deficient in the polysialyltransferase ST8SiaIV/PST-1 allow discrimination of the roles of neural cell adhesion molecule protein and polysialic acid in neural development and synaptic plasticity. *J Neurosci* 20: 5234-5244.
78. Eckhardt M., Muhlenhoff M., Bethe A., Koopman J., Frosch M., Gerardy-Schahn R. (1995) Molecular characterization of eukaryotic polysialyltransferase-1. *Nature* 373: 715-718.
79. Eckman C. B., Mehta N. D., Crook R., Perez-tur J., Prihar G., Pfeiffer E., Graff-Radford N., Hinder P., Yager D., Zenk B., Refolo L. M., Prada C. M., Younkin S. G., Hutton M., Hardy J. (1997) A new pathogenic mutation in the APP gene (I716V) increases the relative proportion of A beta 42(43). *Hum Mol Genet* 6: 2087-2089.
80. Edelman G. M. (1987) CAMs and Igs: cell adhesion and the evolutionary origins of immunity. *Immunol Rev* 100: 11-45.

81. Endo A., Nagai N., Urano T., Ihara H., Takada Y., Hashimoto K., Takada A. (1998) Proteolysis of highly polysialylated NCAM by the tissue plasminogen activator-plasmin system in rats. *Neurosci Lett* 246: 37-40.
82. Esch F. S., Keim P. S., Beattie E. C., Blacher R. W., Culwell A. R., Oltersdorf T., McClure D., Ward P. J. (1990) Cleavage of amyloid beta peptide during constitutive processing of its precursor. *Science* 248: 1122-1124.
83. Esler W. P., Kimberly W. T., Ostaszewski B. L., Diehl T. S., Moore C. L., Tsai J. Y., Rahmati T., Xia W., Selkoe D. J., Wolfe M. S. (2000) Transition-state analogue inhibitors of gamma-secretase bind directly to presenilin-1. *Nat Cell Biol* 2: 428-434.
84. Faissner A., Teplow D. B., Kubler D., Keilhauer G., Kinzel V., Schachner M. (1985) Biosynthesis and membrane topography of the neural cell adhesion molecule L1. *EMBO J* 4: 3105-3113.
85. Farzan M., Schnitzler C. E., Vasilieva N., Leung D., Choe H. (2000) BACE2, a beta -secretase homolog, cleaves at the beta site and within the amyloid-beta region of the amyloid-beta precursor protein. *Proc Natl Acad Sci U S A* 97: 9712-9717.
86. Felding-Habermann B., Silletti S., Mei F., Siu C. H., Yip P. M., Brooks P. C., Cheresch D. A., O'Toole T. E., Ginsberg M. H., Montgomery A. M. (1997) A single immunoglobulin-like domain of the human neural cell adhesion molecule L1 supports adhesion by multiple vascular and platelet integrins. *J Cell Biol* 139: 1567-1581.
87. Fields R. D., Itoh K. (1996) Neural cell adhesion molecules in activity-dependent development and synaptic plasticity. *Trends Neurosci* 19: 473-480.
88. Finckh U., Schroder J., Ressler B., Veske A., Gal A. (2000) Spectrum and detection rate of L1CAM mutations in isolated and familial cases with clinically suspected L1-disease. *Am J Med Genet* 92: 40-46.
89. Fischer G., Kunemund V., Schachner M. (1986) Neurite outgrowth patterns in cerebellar microexplant cultures are affected by antibodies to the cell surface glycoprotein L1. *J Neurosci* 6: 605-612.
90. Fliegel L., Burns K., MacLennan D. H., Reithmeier R. A., Michalak M. (1989) Molecular cloning of the high affinity calcium-binding protein (calreticulin) of skeletal muscle sarcoplasmic reticulum. *J Biol Chem* 264: 21522-21528.
91. Fluhner R., Capell A., Westmeyer G., Willem M., Hartung B., Condrón M. M., Teplow D. B., Haass C., Walter J. (2002) A non-amyloidogenic function of BACE-2 in the secretory pathway. *J Neurochem* 81: 1011-1020.
92. Folstein M. F., Folstein S. E., McHugh P. R. (1975) "Mini-mental state". A practical method for grading the cognitive state of patients for the clinician. *J Psychiatr Res* 12: 189-198.
93. Forman M. S., Cook D. G., Leight S., Doms R. W., Lee V. M. (1997) Differential effects of the swedish mutant amyloid precursor protein on beta-amyloid accumulation and secretion in neurons and nonneuronal cells. *J Biol Chem* 272: 32247-32253.

94. Fox G. B., O'Connell A. W., Murphy K. J., Regan C. M. (1995) Memory consolidation induces a transient and time-dependent increase in the frequency of neural cell adhesion molecule polysialylated cells in the adult rat hippocampus. *J Neurochem* 65: 2796-2799.
95. Fransen E., Lemmon V., Van Camp G., Vits L., Coucke P., Willems P. J. (1995a) CRASH syndrome: clinical spectrum of corpus callosum hypoplasia, retardation, adducted thumbs, spastic paraparesis and hydrocephalus due to mutations in one single gene, L1. *Eur J Hum Genet* 3: 273-284.
96. Fransen E., Lemmon V., Van Camp G., Vits L., Coucke P., Willems P. J. (1995b) CRASH syndrome: clinical spectrum of corpus callosum hypoplasia, retardation, adducted thumbs, spastic paraparesis and hydrocephalus due to mutations in one single gene, L1. *Eur J Hum Genet* 3: 273-284.
97. Fraser S. E., Murray B. A., Chuong C. M., Edelman G. M. (1984) Alteration of the retinotectal map in *Xenopus* by antibodies to neural cell adhesion molecules. *Proc Natl Acad Sci U S A* 81: 4222-4226.
98. Frei T., Bohlen und H. F., Wille W., Schachner M. (1992) Different extracellular domains of the neural cell adhesion molecule (N- CAM) are involved in different functions. *J Cell Biol* 118: 177-194.
99. Fruttiger M., Montag D., Schachner M., Martini R. (1995) Crucial role for the myelin-associated glycoprotein in the maintenance of axon-myelin integrity. *Eur J Neurosci* 7: 511-515.
100. Fryer H. J., Hockfield S. (1996) The role of polysialic acid and other carbohydrate polymers in neural structural plasticity. *Curr Opin Neurobiol* 6: 113-118.
101. Galasko D. (1999) Cerebrospinal fluid opens a window on Alzheimer disease. *Arch Neurol* 56: 655-656.
102. Garlind A., Brauner A., Hojeberg B., Basun H., Schultzberg M. (1999) Soluble interleukin-1 receptor type II levels are elevated in cerebrospinal fluid in Alzheimer's disease patients. *Brain Res* 826: 112-116.
103. Gibb W. R., Lees A. J. (1988) The relevance of the Lewy body to the pathogenesis of idiopathic Parkinson's disease. *J Neurol Neurosurg Psychiatry* 51: 745-752.
104. Gilman S., Low P. A., Quinn N., Albanese A., Ben Shlomo Y., Fowler C. J., Kaufmann H., Klockgether T., Lang A. E., Lantos P. L., Litvan I., Mathias C. J., Oliver E., Robertson D., Schatz I., Wenning G. K. (1999) Consensus statement on the diagnosis of multiple system atrophy. *J Neurol Sci* 163: 94-98.
105. Goate A., Chartier-Harlin M. C., Mullan M., Brown J., Crawford F., Fidani L., Giuffra L., Haynes A., Irving N., James L. (1991) Segregation of a missense mutation in the amyloid precursor protein gene with familial Alzheimer's disease. *Nature* 349: 704-706.
106. Growdon J. H. (1999) Biomarkers of Alzheimer disease. *Arch Neurol* 56:281-283

107. Guenette S. Y., Chen J., Jondro P. D., Tanzi R. E. (1996) Association of a novel human FE65-like protein with the cytoplasmic domain of the beta-amyloid precursor protein. *Proc Natl Acad Sci U S A* 93: 10832-10837.
108. Hall H., Williams E. J., Moore S. E., Walsh F. S., Prochiantz A., Doherty P. (1996) Inhibition of FGF-stimulated phosphatidylinositol hydrolysis and neurite outgrowth by a cell-membrane permeable phosphopeptide. *Curr Biol* 6: 580-587.
109. Hampel H., Buerger K., Kohnken R., Teipel S. J., Zinkowski R., Moeller H. J., Rapoport S. I., Davies P. (2001) Tracking of Alzheimer's disease progression with cerebrospinal fluid tau protein phosphorylated at threonine 231. *Ann Neurol* 49: 545-546.
110. Haniu M., Denis P., Young Y., Mendiaz E. A., Fuller J., Hui J. O., Bennett B. D., Kahn S., Ross S., Burgess T., Katta V., Rogers G., Vassar R., Citron M. (2000) Characterization of Alzheimer's beta -secretase protein BACE. A pepsin family member with unusual properties. *J Biol Chem* 275: 21099-21106.
111. Hardy J. A., Higgins G. A. (1992) Alzheimer's disease: the amyloid cascade hypothesis. *Science* 256: 184-185.
112. Hartmann T., Bieger S. C., Bruhl B., Tienari P. J., Ida N., Allsop D., Roberts G. W., Masters C. L., Dotti C. G., Unsicker K., Beyreuther K. (1997) Distinct sites of intracellular production for Alzheimer's disease A beta40/42 amyloid peptides. *Nat Med* 3: 1016-1020.
113. Heber S., Herms J., Gajic V., Hainfellner J., Aguzzi A., Rulicke T., von Kretschmar H., von Koch C., Sisodia S., Tremml P., Lipp H. P., Wolfer D. P., Muller U. (2000) Mice with combined gene knock-outs reveal essential and partially redundant functions of amyloid precursor protein family members. *J Neurosci* 20: 7951-7963.
114. Hebert D. N., Foellmer B., Helenius A. (1996) Calnexin and calreticulin promote folding, delay oligomerization and suppress degradation of influenza hemagglutinin in microsomes. *EMBO J* 15: 2961-2968.
115. Hendriks L., van Duijn C. M., Cras P., Cruts M., Van Hul W., van Harskamp F., Warren A., McInnis M. G., Antonarakis S. E., Martin J. J. (1992) Presenile dementia and cerebral haemorrhage linked to a mutation at codon 692 of the beta-amyloid precursor protein gene. *Nat Genet* 1: 218-221.
116. Hensley K., Hall N., Subramaniam R., Cole P., Harris M., Aksenov M., Aksenova M., Gabbita S. P., Wu J. F., Carney J. M. (1995) Brain regional correspondence between Alzheimer's disease histopathology and biomarkers of protein oxidation. *J Neurochem* 65: 2146-2156.
117. Herreman A., Serneels L., Annaert W., Collen D., Schoonjans L., De Strooper B. (2000) Total inactivation of gamma-secretase activity in presenilin-deficient embryonic stem cells. *Nat Cell Biol* 2: 461-462.
118. Hildebrandt H., Becker C., Gluer S., Rosner H., Gerardy-Schahn R., Rahmann H. (1998a) Polysialic acid on the neural cell adhesion molecule correlates with expression of polysialyltransferases and promotes neuroblastoma cell growth. *Cancer Res* 58: 779-784.

119. Hildebrandt H., Becker C., Murau M., Gerardy-Schahn R., Rahmann H. (1998b) Heterogeneous expression of the polysialyltransferases ST8Sia II and ST8Sia IV during postnatal rat brain development. *J Neurochem* 71: 2339-2348.
120. Hlavin M. L., Lemmon V. (1991) Molecular structure and functional testing of human L1CAM: an interspecies comparison. *Genomics* 11: 416-423.
121. Hock C., Heese K., Muller-Spahn F., Huber P., Riesen W., Nitsch R. M., Otten U. (2000) Increased CSF levels of nerve growth factor in patients with Alzheimer's disease. *Neurology* 54: 2009-2011.
122. Hoffman S., Chuong C. M., Edelman G. M. (1984) Evolutionary conservation of key structures and binding functions of neural cell adhesion molecules. *Proc Natl Acad Sci U S A* 81: 6881-6885.
123. Hoffman S., Sorkin B. C., White P. C., Brackenbury R., Mailhammer R., Rutishauser U., Cunningham B. A., Edelman G. M. (1982) Chemical characterization of a neural cell adhesion molecule purified from embryonic brain membranes. *J Biol Chem* 257: 7720-7729.
124. Horstkorte R., Schachner M., Magyar J. P., Vorherr T., Schmitz B. (1993) The fourth immunoglobulin-like domain of NCAM contains a carbohydrate recognition domain for oligomannosidic glycans implicated in association with L1 and neurite outgrowth. *J Cell Biol* 121: 1409-1421.
125. Hu H., Tomasiewicz H., Magnuson T., Rutishauser U. (1996) The role of polysialic acid in migration of olfactory bulb interneuron precursors in the subventricular zone. *Neuron* 16: 735-743.
126. Hung A. Y., Haass C., Nitsch R. M., Qiu W. Q., Citron M., Wurtman R. J., Growdon J. H., Selkoe D. J. (1993) Activation of protein kinase C inhibits cellular production of the amyloid beta-protein. *J Biol Chem* 268: 22959-22962.
127. Hussain I., Powell D., Howlett D. R., Tew D. G., Meek T. D., Chapman C., Gloger I. S., Murphy K. E., Southan C. D., Ryan D. M., Smith T. S., Simmons D. L., Walsh F. S., Dingwall C., Christie G. (1999) Identification of a novel aspartic protease (Asp 2) as beta-secretase. *Mol Cell Neurosci* 14: 419-427.
128. Ignelzi M. A., Jr., Miller D. R., Soriano P., Maness P. F. (1994) Impaired neurite outgrowth of src-minus cerebellar neurons on the cell adhesion molecule L1. *Neuron* 12: 873-884.
129. Ito K., Shinomura T., Zako M., Ujita M., Kimata K. (1995) Multiple forms of mouse PG-M, a large chondroitin sulfate proteoglycan generated by alternative splicing. *J Biol Chem* 270: 958-965.
130. Jensen O. N., Podtelejnikov A. V., Mann M. (1997) Identification of the components of simple protein mixtures by high- accuracy peptide mass mapping and database searching. *Anal Chem* 69: 4741-4750.
131. Jethmalani S. M., Henle K. J. (1998) Calreticulin associates with stress proteins: implications for chaperone function during heat stress. *J Cell Biochem* 69: 30-43.

132. Johnson R. J., Xiao G., Shanmugaratnam J., Fine R. E. (2001) Calreticulin functions as a molecular chaperone for the beta-amyloid precursor protein. *Neurobiol Aging* 22: 387-395.
133. Jost C. R., Van Der Zee C. E., In 't Zandt H. J., Oerlemans F., Verheij M., Streijger F., Fransen J., Heerschap A., Cools A. R., Wieringa B. (2002) Creatine kinase B-driven energy transfer in the brain is important for habituation and spatial learning behaviour, mossy fibre field size and determination of seizure susceptibility. *Eur J Neurosci* 15: 1692-1706.
134. Jouet M., Rosenthal A., Armstrong G., MacFarlane J., Stevenson R., Paterson J., Metzenberg A., Ionasescu V., Temple K., Kenwrick S. (1994) X-linked spastic paraplegia (SPG1), MASA syndrome and X-linked hydrocephalus result from mutations in the L1 gene. *Nat Genet* 7: 402-407.
135. Kadmon G., Altevogt P. (1997) The cell adhesion molecule L1: species- and cell-type-dependent multiple binding mechanisms. *Differentiation* 61: 143-150.
136. Kadmon G., Bohlen und H. F., Horstkorte R., Eckert M., Altevogt P., Schachner M. (1995) Evidence for cis interaction and cooperative signalling by the heat- stable antigen nectadrin (murine CD24) and the cell adhesion molecule L1 in neurons. *Eur J Neurosci* 7: 993-1004.
137. Kadmon G., Kowitz A., Altevogt P., Schachner M. (1990a) Functional cooperation between the neural adhesion molecules L1 and N- CAM is carbohydrate dependent. *J Cell Biol* 110: 209-218.
138. Kadmon G., Kowitz A., Altevogt P., Schachner M. (1990b) The neural cell adhesion molecule N-CAM enhances L1-dependent cell-cell interactions. *J Cell Biol* 110: 193-208.
139. Kalus I., Schnegelsberg B., Seidah N. G., Kleene R., Schachner M. (2003) The Proprotein Convertase PC5A and a Metalloprotease Are Involved in the Proteolytic Processing of the Neural Adhesion Molecule L1. *J Biol Chem* 278: 10381-10388.
140. Kamiguchi H., Hlavin M. L., Lemmon V. (1998) Role of L1 in neural development: what the knockouts tell us. *Mol Cell Neurosci* 12: 48-55.
141. Kamiguchi H., Lemmon V. (1998) A neuronal form of the cell adhesion molecule L1 contains a tyrosine- based signal required for sorting to the axonal growth cone. *J Neurosci* 18: 3749-3756.
142. Kang D. E., Soriano S., Frosch M. P., Collins T., Naruse S., Sisodia S. S., Leibowitz G., Levine F., Koo E. H. (1999) Presenilin 1 facilitates the constitutive turnover of beta-catenin: differential activity of Alzheimer's disease-linked PS1 mutants in the beta-catenin-signaling pathway. *J Neurosci* 19: 4229-4237.
143. Kayyem J. F., Roman J. M., de la Rosa E. J., Schwarz U., Dreyer W. J. (1992) Bravo/Nr-CAM is closely related to the cell adhesion molecules L1 and Ng-CAM and has a similar heterodimer structure. *J Cell Biol* 118: 1259-1270.
144. Kenwrick S., Watkins A., De Angelis E. (2000) Neural cell recognition molecule L1: relating biological complexity to human disease mutations. *Hum Mol Genet* 9: 879-886.

145. Kinoshita G., Keech C. L., Sontheimer R. D., Purcell A., McCluskey J., Gordon T. P. (1998) Spreading of the immune response from 52 kDaRo and 60 kDaRo to calreticulin in experimental autoimmunity. *Lupus* 7: 7-11.
146. Kiss J. Z., Wang C., Rougon G. (1993) Nerve-dependent expression of high polysialic acid neural cell adhesion molecule in neurohypophyseal astrocytes of adult rats. *Neuroscience* 53: 213-221.
147. Knauer M. F., Orlando R. A., Glabe C. G. (1996) Cell surface APP751 forms complexes with protease nexin 2 ligands and is internalized via the low density lipoprotein receptor-related protein (LRP). *Brain Res* 740: 6-14.
148. Kobayashi S., Miura M., Asou H., Inoue H. K., Ohye C., Uyemura K. (1995) Grafts of genetically modified fibroblasts expressing neural cell adhesion molecule L1 into transected spinal cord of adult rats. *Neurosci Lett* 188: 191-194.
149. Kojima N., Kono M., Yoshida Y., Tachida Y., Nakafuku M., Tsuji S. (1996) Biosynthesis and expression of polysialic acid on the neural cell adhesion molecule is predominantly directed by ST8Sia II/STX during in vitro neuronal differentiation. *J Biol Chem* 271: 22058-22062.
150. Kojima N., Yoshida Y., Tsuji S. (1995) A developmentally regulated member of the sialyltransferase family (ST8Sia II, STX) is a polysialic acid synthase. *FEBS Lett* 373: 119-122.
151. Kolkova K., Novitskaya V., Pedersen N., Berezin V., Bock E. (2000) Neural cell adhesion molecule-stimulated neurite outgrowth depends on activation of protein kinase C and the Ras-mitogen-activated protein kinase pathway. *J Neurosci* 20: 2238-2246.
152. Kosaka T., Imagawa M., Seki K., Arai H., Sasaki H., Tsuji S., Asami-Odaka A., Fukushima T., Imai K., Iwatsubo T. (1997) The beta APP717 Alzheimer mutation increases the percentage of plasma amyloid-beta protein ending at A beta42(43). *Neurology* 48: 741-745.
153. Kounnas M. Z., Moir R. D., Rebeck G. W., Bush A. I., Argraves W. S., Tanzi R. E., Hyman B. T., Strickland D. K. (1995) LDL receptor-related protein, a multifunctional ApoE receptor, binds secreted beta-amyloid precursor protein and mediates its degradation. *Cell* 82: 331-340.
154. Kovacs D. M., Fausett H. J., Page K. J., Kim T. W., Moir R. D., Merriam D. E., Hollister R. D., Hallmark O. G., Mancini R., Felsenstein K. M., Hyman B. T., Tanzi R. E., Wasco W. (1996) Alzheimer-associated presenilins 1 and 2: neuronal expression in brain and localization to intracellular membranes in mammalian cells. *Nat Med* 2: 224-229.
155. Kowitz A., Kadmon G., Eckert M., Schirmmacher V., Schachner M., Altevogt P. (1992) Expression and function of the neural cell adhesion molecule L1 in mouse leukocytes. *Eur J Immunol* 22: 1199-1205.
156. Kuentzel S. L., Ali S. M., Altman R. A., Greenberg B. D., Raub T. J. (1993) The Alzheimer beta-amyloid protein precursor/protease nexin-II is cleaved by secretase in a trans-Golgi secretory compartment in human neuroglioma cells. *Biochem J* 295 (Pt 2): 367-378.

157. Kuhn T. B., Stoeckli E. T., Condrau M. A., Rathjen F. G., Sonderegger P. (1991) Neurite outgrowth on immobilized axonin-1 is mediated by a heterophilic interaction with L1 (G4). *J Cell Biol* 115: 1113-1126.
158. Lah J. J., Heilman C. J., Nash N. R., Rees H. D., Yi H., Counts S. E., Levey A. I. (1997) Light and electron microscopic localization of presenilin-1 in primate brain. *J Neurosci* 17: 1971-1980.
159. Lammich S., Kojro E., Postina R., Gilbert S., Pfeiffer R., Jasionowski M., Haass C., Fahrenholz F. (1999) Constitutive and regulated alpha-secretase cleavage of Alzheimer's amyloid precursor protein by a disintegrin metalloprotease. *Proc Natl Acad Sci U S A* 96: 3922-3927.
160. Landmesser L. (1992) The relationship of intramuscular nerve branching and synaptogenesis to motoneuron survival. *J Neurobiol* 23: 1131-1139.
161. Landmesser L., Dahm L., Schultz K., Rutishauser U. (1988) Distinct roles for adhesion molecules during innervation of embryonic chick muscle. *Dev Biol* 130: 645-670.
162. Landmesser L., Dahm L., Tang J. C., Rutishauser U. (1990) Polysialic acid as a regulator of intramuscular nerve branching during embryonic development. *Neuron* 4: 655-667.
163. Lassmann H., Bartsch U., Montag D., Schachner M. (1997) Dying-back oligodendroglialopathy: a late sequel of myelin-associated glycoprotein deficiency. *Glia* 19: 104-110.
164. Law A., Gauthier S., Quirion R. (2001) Say NO to Alzheimer's disease: the putative links between nitric oxide and dementia of the Alzheimer's type. *Brain Res Brain Res Rev* 35: 73-96.
165. LeBaron R. G., Zimmermann D. R., Ruoslahti E. (1992) Hyaluronate binding properties of versican. *J Biol Chem* 267: 10003-10010.
166. Lee S. F., Shah S., Li H., Yu C., Han W., Yu G. (2002) Mammalian APH-1 interacts with presenilin and nicastrin and is required for intramembrane proteolysis of amyloid-beta precursor protein and Notch. *J Biol Chem* 277: 45013-45019.
167. Lehmann D. J., Johnston C., Smith A. D. (1997) Synergy between the genes for butyrylcholinesterase K variant and apolipoprotein E4 in late-onset confirmed Alzheimer's disease. *Hum Mol Genet* 6: 1933-1936.
168. Leissring M. A., Akbari Y., Fanger C. M., Cahalan M. D., Mattson M. P., LaFerla F. M. (2000) Capacitative calcium entry deficits and elevated luminal calcium content in mutant presenilin-1 knockin mice. *J Cell Biol* 149: 793-798.
169. Leissring M. A., LaFerla F. M., Callamaras N., Parker I. (2001) Subcellular mechanisms of presenilin-mediated enhancement of calcium signaling. *Neurobiol Dis* 8: 469-478.

170. Lemire J. M., Merrilees M. J., Braun K. R., Wight T. N. (2002) Overexpression of the V3 variant of versican alters arterial smooth muscle cell adhesion, migration, and proliferation in vitro. *J Cell Physiol* 190:38-45.
171. Levy E., Carman M. D., Fernandez-Madrid I. J., Power M. D., Lieberburg I., van Duinen S. G., Bots G. T., Luyendijk W., Frangione B. (1990) Mutation of the Alzheimer's disease amyloid gene in hereditary cerebral hemorrhage, Dutch type. *Science* 248: 1124-1126.
172. Li X., Greenwald I. (1998) Additional evidence for an eight-transmembrane-domain topology for *Caenorhabditis elegans* and human presenilins. *Proc Natl Acad Sci U S A* 95: 7109-7114.
173. Li Y. M., Lai M. T., Xu M., Huang Q., DiMuzio-Mower J., Sardana M. K., Shi X. P., Yin K. C., Shafer J. A., Gardell S. J. (2000) Presenilin 1 is linked with gamma-secretase activity in the detergent solubilized state. *Proc Natl Acad Sci U S A* 97: 6138-6143.
174. Lin X., Koelsch G., Wu S., Downs D., Dashti A., Tang J. (2000) Human aspartic protease memapsin 2 cleaves the beta-secretase site of beta-amyloid precursor protein. *Proc Natl Acad Sci U S A* 97: 1456-1460.
175. Lindner J., Rathjen F. G., Schachner M. (1983) L1 mono- and polyclonal antibodies modify cell migration in early postnatal mouse cerebellum. *Nature* 305: 427-430.
176. Little E. B., Edelman G. M., Cunningham B. A. (1998) Palmitoylation of the cytoplasmic domain of the neural cell adhesion molecule N-CAM serves as an anchor to cellular membranes. *Cell Adhes Commun* 6: 415-430.
177. Liu H., Miller E., van de W. B., Stevens J. L. (1998) Endoplasmic reticulum stress proteins block oxidant-induced Ca^{2+} increases and cell death. *J Biol Chem* 273: 12858-12862.
178. Lochter A., Vaughan L., Kaplony A., Prochiantz A., Schachner M., Faissner A. (1991) J1/tenascin in substrate-bound and soluble form displays contrary effects on neurite outgrowth. *J Cell Biol* 113: 1159-1171.
179. Lopez-Perez E., Seidah N. G., Checler F. (1999) Proprotein convertase activity contributes to the processing of the Alzheimer's beta-amyloid precursor protein in human cells: evidence for a role of the prohormone convertase PC7 in the constitutive alpha-secretase pathway. *J Neurochem* 73: 2056-2062.
180. Luthi A., Laurent J. P., Figurov A., Muller D., Schachner M. (1994) Hippocampal long-term potentiation and neural cell adhesion molecules L1 and NCAM. *Nature* 372: 777-779.
181. Mackie K., Sorkin B. C., Nairn A. C., Greengard P., Edelman G. M., Cunningham B. A. (1989) Identification of two protein kinases that phosphorylate the neural cell-adhesion molecule, N-CAM. *J Neurosci* 9: 1883-1896.
182. Malorni W., Rainaldi G., Rivabene R., Santini M. T., Peterson S. W., Testa U., Donelli G. (1994) Cytoskeletal oxidative changes lead to alterations of specific cell surface receptors. *Eur J Histochem* 38 Suppl 1: 91-100.

183. Martini R., Schachner M. (1986) Immunolectron microscopic localization of neural cell adhesion molecules (L1, N-CAM, and MAG) and their shared carbohydrate epitope and myelin basic protein in developing sciatic nerve. *J Cell Biol* 103: 2439-2448.
184. Martins V. R., Graner E., Garcia-Abreu J., de Souza S. J., Mercadante A. F., Veiga S. S., Zanata S. M., Neto V. M., Brentani R. R. (1997) Complementary hydropathy identifies a cellular prion protein receptor. *Nat Med* 3: 1376-1382.
185. Matsuoka K., Seta K., Yamakawa Y., Okuyama T., Shinoda T., Isobe T. (1994) Covalent structure of bovine brain calreticulin. *Biochem J* 298 (Pt 2): 435-442.
186. McCauliffe D. P., Lux F. A., Lieu T. S., Sanz I., Hanke J., Newkirk M. M., Bachinski L. L., Itoh Y., Siciliano M. J., Reichlin M. (1990) Molecular cloning, expression, and chromosome 19 localization of a human Ro/SS-A autoantigen. *J Clin Invest* 85: 1379-1391.
187. McDonald W. I., Compston A., Edan G., Goodkin D., Hartung H. P., Lublin F. D., McFarland H. F., Paty D. W., Polman C. H., Reingold S. C., Sandberg-Wollheim M., Sibley W., Thompson A., van den N. S., Weinshenker B. Y., Wolinsky J. S. (2001) Recommended diagnostic criteria for multiple sclerosis: guidelines from the International Panel on the diagnosis of multiple sclerosis. *Ann Neurol* 50: 121-127.
188. McGuire J. C., Greene L. A., Furano A. V. (1978) NGF stimulates incorporation of fucose or glucosamine into an external glycoprotein in cultured rat PC12 pheochromocytoma cells. *Cell* 15: 357-365.
189. McKeith I. G. (2002) Dementia with Lewy bodies. *Br J Psychiatry* 180: 144-147.
190. McKhann G., Drachman D., Folstein M., Katzman R., Price D., Stadlan E. M. (1984) Clinical diagnosis of Alzheimer's disease: report of the NINCDS-ADRDA Work Group under the auspices of Department of Health and Human Services Task Force on Alzheimer's Disease. *Neurology* 34: 939-944.
191. Michalak M., Milner R. E., Burns K., Opas M. (1992) Calreticulin. *Biochem J* 285 (Pt 3): 681-692.
192. Michalides R., Kwa B., Springall D., van Zandwijk N., Koopman J., Hilkens J., Mooi W. (1994) NCAM and lung cancer. *Int J Cancer Suppl* 8: 34-37.
193. Mikkonen M., Soininen H., Tapiola T., Alafuzoff I., Miettinen R. (1999) Hippocampal plasticity in Alzheimer's disease: changes in highly polysialylated NCAM immunoreactivity in the hippocampal formation. *Eur J Neurosci* 11: 1754-1764.
194. Miller P. D., Chung W. W., Lagenaur C. F., DeKosky S. T. (1993) Regional distribution of neural cell adhesion molecule (N-CAM) and L1 in human and rodent hippocampus. *J Comp Neurol* 327: 341-349.
195. Miragall F., Kadmon G., Husmann M., Schachner M. (1988) Expression of cell adhesion molecules in the olfactory system of the adult mouse: presence of the embryonic form of N-CAM. *Dev Biol* 129: 516-531.

196. Mok S. S., Clippingdale A. B., Beyreuther K., Masters C. L., Barrow C. J., Small D. H. (2000) A beta peptides and calcium influence secretion of the amyloid protein precursor from chick sympathetic neurons in culture. *J Neurosci Res* 61: 449-457.
197. Montag D., Giese K. P., Bartsch U., Martini R., Lang Y., Bluthmann H., Karthigasan J., Kirschner D. A., Wintergerst E. S., Nave K. A. (1994) Mice deficient for the myelin-associated glycoprotein show subtle abnormalities in myelin. *Neuron* 13: 229-246.
198. Montgomery A. M., Becker J. C., Siu C. H., Lemmon V. P., Cheresch D. A., Pancook J. D., Zhao X., Reisfeld R. A. (1996) Human neural cell adhesion molecule L1 and rat homologue NILE are ligands for integrin alpha v beta 3. *J Cell Biol* 132: 475-485.
199. Moore S. E., Walsh F. S. (1986) Nerve dependent regulation of neural cell adhesion molecule expression in skeletal muscle. *Neuroscience* 18: 499-505.
200. Mortz E., Vorm O., Mann M., Roepstorff P. (1994) Identification of proteins in polyacrylamide gels by mass spectrometric peptide mapping combined with database search. *Biol Mass Spectrom* 23: 249-261.
201. Muhlenhoff M., Eckhardt M., Bethe A., Frosch M., Gerardy-Schahn R. (1996) Autocatalytic polysialylation of polysialyltransferase-1. *EMBO J* 15: 6943-6950.
202. Mullan M., Crawford F., Axelman K., Houlden H., Lilius L., Winblad B., Lannfelt L. (1992) A pathogenic mutation for probable Alzheimer's disease in the APP gene at the N-terminus of beta-amyloid. *Nat Genet* 5:345-347.
203. Muller D., Wang C., Skibo G., Toni N., Cremer H., Calaora V., Rougon G., Kiss J. Z. (1996) PSA-NCAM is required for activity-induced synaptic plasticity. *Neuron* 17: 413-422.
204. Murase S., Schuman E. M. (1999) The role of cell adhesion molecules in synaptic plasticity and memory. *Curr Opin Cell Biol* 11: 549-553.
205. Nakayama J., Fukuda M. N., Fredette B., Ranscht B., Fukuda M. (1995) Expression cloning of a human polysialyltransferase that forms the polysialylated neural cell adhesion molecule present in embryonic brain. *Proc Natl Acad Sci U S A* 92: 7031-7035.
206. Naruse S., Thinakaran G., Luo J. J., Kusiak J. W., Tomita T., Iwatsubo T., Qian X., Ginty D. D., Price D. L., Borchelt D. R., Wong P. C., Sisodia S. S. (1998) Effects of PS1 deficiency on membrane protein trafficking in neurons. *Neuron* 21: 1213-1221.
207. Nauseef W. M., McCormick S. J., Clark R. A. (1995) Calreticulin functions as a molecular chaperone in the biosynthesis of myeloperoxidase. *J Biol Chem* 270: 4741-4747.
208. Nayeem N., Silletti S., Yang X., Lemmon V. P., Reisfeld R. A., Stallcup W. B., Montgomery A. M. (1999) A potential role for the plasmin(ogen) system in the posttranslational cleavage of the neural cell adhesion molecule L1. *J Cell Sci* 112 (Pt 24): 4739-4749.
209. Nelson R. W., Bates P. A., Rutishauser U. (1995) Protein determinants for specific polysialylation of the neural cell adhesion molecule. *J Biol Chem* 270: 17171-17179.

210. Neugebauer K. M., Tomaselli K. J., Lilien J., Reichardt L. F. (1988) N-cadherin, NCAM, and integrins promote retinal neurite outgrowth on astrocytes in vitro. *J Cell Biol* 107: 1177-1187.
211. Neve R. L., McPhie D. L., Chen Y. (2000) Alzheimer's disease: a dysfunction of the amyloid precursor protein (1). *Brain Res* 886: 54-66.
212. Niethammer P., Delling M., Sytnyk V., Dityatev A., Fukami K., Schachner M. (2002) Cosignaling of NCAM via lipid rafts and the FGF receptor is required for neuritogenesis. *J Cell Biol* 157: 521-532.
213. Ninomiya H., Roch J. M., Sundsmo M. P., Otero D. A., Saitoh T. (1993) Amino acid sequence RERMS represents the active domain of amyloid beta/A4 protein precursor that promotes fibroblast growth. *J Cell Biol* 121: 879-886.
214. Nishimoto I., Okamoto T., Matsuura Y., Takahashi S., Okamoto T., Murayama Y., Ogata E. (1993) Alzheimer amyloid protein precursor complexes with brain GTP-binding protein G(o). *Nature* 362: 75-79.
215. Nishimura M., Yu G., George-Hyslop P. H. (1999) Biology of presenilins as causative molecules for Alzheimer disease. *Clin Genet* 55: 219-225.
216. Nybroe O., Dalseg A. M., Bock E. (1990) A developmental study of soluble L1. *Int J Dev Neurosci* 8: 273-281.
217. Oliver J. D., Hresko R. C., Mueckler M., High S. (1996) The glut 1 glucose transporter interacts with calnexin and calreticulin. *J Biol Chem* 271: 13691-13696.
218. Olsen M., Krog L., Edvardsen K., Skovgaard L. T., Bock E. (1993) Intact transmembrane isoforms of the neural cell adhesion molecule are released from the plasma membrane. *Biochem J* 295 (Pt 3): 833-840.
219. Ong E., Nakayama J., Angata K., Reyes L., Katsuyama T., Arai Y., Fukuda M. (1998) Developmental regulation of polysialic acid synthesis in mouse directed by two polysialyltransferases, PST and STX. *Glycobiology* 8: 415-424.
220. Opas M., Dziak E., Fliegel L., Michalak M. (1991) Regulation of expression and intracellular distribution of calreticulin, a major calcium binding protein of nonmuscle cells. *J Cell Physiol* 149: 160-171.
221. Owens G. C., Edelman G. M., Cunningham B. A. (1987) Organization of the neural cell adhesion molecule (N-CAM) gene: alternative exon usage as the basis for different membrane-associated domains. *Proc Natl Acad Sci U S A* 84: 294-298.
222. Paulus W., Baur I., Dours-Zimmermann M. T., Zimmermann D. R. (1996) Differential expression of versican isoforms in brain tumors. *J Neuropathol Exp Neurol* 55: 528-533.
223. Perez R. G., Soriano S., Hayes J. D., Ostaszewski B., Xia W., Selkoe D. J., Chen X., Stokin G. B., Koo E. H. (1999) Mutagenesis identifies new signals for beta-amyloid precursor protein endocytosis, turnover, and the generation of secreted fragments, including Abeta42. *J Biol Chem* 274: 18851-18856.

224. Perez R. G., Zheng H., Van der Ploeg L. H., Koo E. H. (1997) The beta-amyloid precursor protein of Alzheimer's disease enhances neuron viability and modulates neuronal polarity. *J Neurosci* 17: 9407-9414.
225. Persohn E., Pollerberg G. E., Schachner M. (1989) Immunoelectron-microscopic localization of the 180 kD component of the neural cell adhesion molecule N-CAM in postsynaptic membranes. *J Comp Neurol* 288: 92-100.
226. Peterson J. R., Ora A., Van P. N., Helenius A. (1995) Transient, lectin-like association of calreticulin with folding intermediates of cellular and viral glycoproteins. *Mol Biol Cell* 6: 1173-1184.
227. Pipe S. W., Morris J. A., Shah J., Kaufman R. J. (1998) Differential interaction of coagulation factor VIII and factor V with protein chaperones calnexin and calreticulin. *J Biol Chem* 273: 8537-8544.
228. Podlisny M. B., Citron M., Amarante P., Sherrington R., Xia W., Zhang J., Diehl T., Levesque G., Fraser P., Haass C., Koo E. H., Seubert P., George-Hyslop P., Teplow D. B., Selkoe D. J. (1997) Presenilin proteins undergo heterogeneous endoproteolysis between Thr291 and Ala299 and occur as stable N- and C-terminal fragments in normal and Alzheimer brain tissue. *Neurobiol Dis* 3: 325-337.
229. Poirier J., Minnich A., Davignon J. (1995) Apolipoprotein E, synaptic plasticity and Alzheimer's disease. *Ann Med* 27: 663-670.
230. Pollerberg E. G., Sadoul R., Goridis C., Schachner M. (1985) Selective expression of the 180-kD component of the neural cell adhesion molecule N-CAM during development. *J Cell Biol* 101: 1921-1929.
231. Pollerberg G. E., Burridge K., Krebs K. E., Goodman S. R., Schachner M. (1987) The 180-kD component of the neural cell adhesion molecule N-CAM is involved in a cell-cell contacts and cytoskeleton-membrane interactions. *Cell Tissue Res* 250: 227-236.
232. Pollerberg G. E., Schachner M., Davoust J. (1986) Differentiation state-dependent surface mobilities of two forms of the neural cell adhesion molecule. *Nature* 324: 462-465.
233. Poltorak M., Frye M. A., Wright R., Hemperly J. J., George M. S., Pazzaglia P. J., Jerrels S. A., Post R. M., Freed W. J. (1996) Increased neural cell adhesion molecule in the CSF of patients with mood disorder. *J Neurochem* 66: 1532-1538.
234. Poltorak M., Khoja I., Hemperly J. J., Williams J. R., el Mallakh R., Freed W. J. (1995) Disturbances in cell recognition molecules (N-CAM and L1 antigen) in the CSF of patients with schizophrenia. *Exp Neurol* 131: 266-272.
235. Probstmeier R., Kuhn K., Schachner M. (1989) Binding properties of the neural cell adhesion molecule to different components of the extracellular matrix. *J Neurochem* 53: 1794-1801.
236. Purcell A. E., Rocco M. M., Lenhart J. A., Hyder K., Zimmerman A. W., Pevsner J. (2001) Assessment of neural cell adhesion molecule (NCAM) in autistic serum and postmortem brain. *J Autism Dev Disord* 31: 183-194.

237. Rathjen F. G., Schachner M. (1984) Immunocytological and biochemical characterization of a new neuronal cell surface component (L1 antigen) which is involved in cell adhesion. *EMBO J* 3: 1-10.
238. Reid R. A., Hemperly J. J. (1992) Variants of human L1 cell adhesion molecule arise through alternate splicing of RNA. *J Mol Neurosci* 3: 127-135.
239. Richter-Landsberg C., Lee V. M., Salton S. R., Shelanski M. L., Greene L. A. (1984) Release of the NILE and other glycoproteins from cultured PC12 rat pheochromocytoma cells and sympathetic neurons. *J Neurochem* 43: 841-848.
240. Rojiani M. V., Finlay B. B., Gray V., Dedhar S. (1991) In vitro interaction of a polypeptide homologous to human Ro/SS-A antigen (calreticulin) with a highly conserved amino acid sequence in the cytoplasmic domain of integrin alpha subunits. *Biochemistry* 30: 9859-9866.
241. Roman G. C., Tatemichi T. K., Erkinjuntti T., Cummings J. L., Masdeu J. C., Garcia J. H., Amaducci L., Orgogozo J. M., Brun A., Hofman A. (1993) Vascular dementia: diagnostic criteria for research studies. Report of the NINDS-AIREN International Workshop. *Neurology* 43: 250-260.
242. Ronn L. C., Bock E., Linnemann D., Jahnsen H. (1995) NCAM-antibodies modulate induction of long-term potentiation in rat hippocampal CA1. *Brain Res* 677: 145-151.
243. Rosenthal A., Jouet M., Kenwrick S. (1992) Aberrant splicing of neural cell adhesion molecule L1 mRNA in a family with X-linked hydrocephalus. *Nat Genet* 2: 107-112.
244. Runker A. E., Bartsch U., Nave K. A., Schachner M. (2003) The C264Y missense mutation in the extracellular domain of L1 impairs protein trafficking in vitro and in vivo. *J Neurosci* 23: 277-286.
245. Ruppert M., Aigner S., Hubbe M., Yagita H., Altevogt P. (1995) The L1 adhesion molecule is a cellular ligand for VLA-5. *J Cell Biol* 131: 1881-1891.
246. Rutishauser U. (1993) Adhesion molecules of the nervous system. *Curr Opin Neurobiol* 3: 709-715.
247. Rutishauser U., Acheson A., Hall A. K., Mann D. M., Sunshine J. (1988) The neural cell adhesion molecule (NCAM) as a regulator of cell-cell interactions. *Science* 240: 53-57.
248. Rutishauser U., Edelman G. M. (1980) Effects of fasciculation on the outgrowth of neurites from spinal ganglia in culture. *J Cell Biol* 87: 370-378.
249. Rutishauser U., Jessell T. M. (1988) Cell adhesion molecules in vertebrate neural development. *Physiol Rev* 68: 819-857.
250. Sadoul K., Sadoul R., Faissner A., Schachner M. (1988) Biochemical characterization of different molecular forms of the neural cell adhesion molecule L1. *J Neurochem* 50: 510-521.

251. Saffell J. L., Williams E. J., Mason I. J., Walsh F. S., Doherty P. (1997) Expression of a dominant negative FGF receptor inhibits axonal growth and FGF receptor phosphorylation stimulated by CAMs. *Neuron* 18: 231-242.
252. Santoni M. J., Barthels D., Barbas J. A., Hirsch M. R., Steinmetz M., Goridis C., Wille W. (1987) Analysis of cDNA clones that code for the transmembrane forms of the mouse neural cell adhesion molecule (NCAM) and are generated by alternative RNA splicing. *Nucleic Acids Res* 15: 8621-8641.
253. Santoni M. J., Barthels D., Vopper G., Boned A., Goridis C., Wille W. (1989) Differential exon usage involving an unusual splicing mechanism generates at least eight types of NCAM cDNA in mouse brain. *EMBO J* 8: 385-392.
254. Schachner M. (1997) Neural recognition molecules and synaptic plasticity. *Curr Opin Cell Biol* 9: 627-634.
255. Schaefer A. W., Kamiguchi H., Wong E. V., Beach C. M., Landreth G., Lemmon V. (1999) Activation of the MAPK signal cascade by the neural cell adhesion molecule L1 requires L1 internalization. *J Biol Chem* 274: 37965-37973.
256. Scheidegger E. P., Sternberg L. R., Roth J., Lowe J. B. (1995) A human STX cDNA confers polysialic acid expression in mammalian cells. *J Biol Chem* 270: 22685-22688.
257. Scheidegger P., Papay J., Zuber C., Lackie P. M., Roth J. (1994) Cellular site of synthesis and dynamics of cell surface re-expression of polysialic acid of the neural cell adhesion molecule. *Eur J Biochem* 225: 1097-1103.
258. Scheuner D., Eckman C., Jensen M., Song X., Citron M., Suzuki N., Bird T. D., Hardy J., Hutton M., Kukull W., Larson E., Levy-Lahad E., Viitanen M., Peskind E., Poorkaj P., Schellenberg G., Tanzi R., Wasco W., Lannfelt L., Selkoe D., Younkin S. (1996) Secreted amyloid beta-protein similar to that in the senile plaques of Alzheimer's disease is increased in vivo by the presenilin 1 and 2 and APP mutations linked to familial Alzheimer's disease. *Nat Med* 2: 864-870.
259. Schmalfeldt M., Dours-Zimmermann M. T., Winterhalter K. H., Zimmermann D. R. (1998) Versican V2 is a major extracellular matrix component of the mature bovine brain. *J Biol Chem* 273: 15758-15764.
260. Schmid R. S., Graff R. D., Schaller M. D., Chen S., Schachner M., Hemperly J. J., Maness P. F. (1999) NCAM stimulates the Ras-MAPK pathway and CREB phosphorylation in neuronal cells. *J Neurobiol* 38: 542-558.
261. Scholey A. B., Rose S. P., Zamani M. R., Bock E., Schachner M. (1993) A role for the neural cell adhesion molecule in a late, consolidating phase of glycoprotein synthesis six hours following passive avoidance training of the young chick. *Neuroscience* 55: 499-509.
262. Schuch U., Lohse M. J., Schachner M. (1989) Neural cell adhesion molecules influence second messenger systems. *Neuron* 3: 13-20.
263. Seilheimer B., Schachner M. (1987) Regulation of neural cell adhesion molecule expression on cultured mouse Schwann cells by nerve growth factor. *EMBO J* 6: 1611-1616.

264. Seilheimer B., Schachner M. (1988) Studies of adhesion molecules mediating interactions between cells of peripheral nervous system indicate a major role for L1 in mediating sensory neuron growth on Schwann cells in culture. *J Cell Biol* 107: 341-351.
265. Selkoe D. J. (1994a) Alzheimer's disease: a central role for amyloid. *J Neuropathol Exp Neurol* 53: 438-447.
266. Selkoe D. J. (1994b) Cell biology of the amyloid beta-protein precursor and the mechanism of Alzheimer's disease. *Annu Rev Cell Biol* 10: 373-403.
267. Selkoe D. J. (1999) Translating cell biology into therapeutic advances in Alzheimer's disease. *Nature* 399: A23-A31.
268. Sinha S., Anderson J. P., Barbour R., Basi G. S., Caccavello R., Davis D., Doan M., Dovey H. F., Frigon N., Hong J., Jacobson-Croak K., Jewett N., Keim P., Knops J., Lieberburg I., Power M., Tan H., Tatsuno G., Tung J., Schenk D., Seubert P., Suomensaaari S. M., Wang S., Walker D., John V. (1999) Purification and cloning of amyloid precursor protein beta-secretase from human brain. *Nature* 402: 537-540.
269. Sinha S., Lieberburg I. (1999) Cellular mechanisms of beta-amyloid production and secretion. *Proc Natl Acad Sci U S A* 96: 11049-11053.
270. Small D. H. (1998) The role of the amyloid protein precursor (APP) in Alzheimer's disease: does the normal function of APP explain the topography of neurodegeneration? *Neurochem Res* 23: 795-806.
271. Small D. H., McLean C. A. (1999) Alzheimer's disease and the amyloid beta protein: What is the role of amyloid? *J Neurochem* 73: 443-449.
272. Small D. H., Nurcombe V., Clarris H., Beyreuther K., Masters C. L. (1993) The role of extracellular matrix in the processing of the amyloid protein precursor of Alzheimer's disease. *Ann N Y Acad Sci* 695: 169-174.
273. Small S. J., Akeson R. (1990) Expression of the unique NCAM VASE exon is independently regulated in distinct tissues during development. *J Cell Biol* 111: 2089-2096.
274. Small S. J., Haines S. L., Akeson R. A. (1988) Polypeptide variation in an N-CAM extracellular immunoglobulin-like fold is developmentally regulated through alternative splicing. *Neuron* 1: 1007-1017.
275. Smith C. D., Carney J. M., Starke-Reed P. E., Oliver C. N., Stadtman E. R., Floyd R. A., Markesbery W. R. (1991) Excess brain protein oxidation and enzyme dysfunction in normal aging and in Alzheimer disease. *Proc Natl Acad Sci U S A* 88: 10540-10543.
276. Smith M. J., Koch G. L. (1989) Multiple zones in the sequence of calreticulin (CRP55, calregulin, HACBP), a major calcium binding ER/SR protein. *EMBO J* 8: 3581-3586.
277. Sontheimer R. D., Nguyen T. Q., Cheng S. T., Lieu T. S., Capra J. D. (1995) The unveiling of calreticulin--a clinically relevant tour of modern cell biology. *J Investig Med* 43: 362-370.

278. Sorkin B. C., Hoffman S., Edelman G. M., Cunningham B. A. (1984) Sulfation and phosphorylation of the neural cell adhesion molecule, N- CAM. *Science* 225: 1476-1478.
279. Spiro R. G., Zhu Q., Bhoyroo V., Soling H. D. (1996) Definition of the lectin-like properties of the molecular chaperone, calreticulin, and demonstration of its copurification with endomannosidase from rat liver Golgi. *J Biol Chem* 271: 11588-11594.
280. Steiner H., Winkler E., Edbauer D., Prokop S., Basset G., Yamasaki A., Kostka M., Haass C. (2002) PEN-2 is an integral component of the gamma-secretase complex required for coordinated expression of presenilin and nicastrin. *J Biol Chem* 277: 39062-39065.
281. Suzuki N., Cheung T. T., Cai X. D., Odaka A., Otvos L., Jr., Eckman C., Golde T. E., Younkin S. G. (1994) An increased percentage of long amyloid beta protein secreted by familial amyloid beta protein precursor (beta APP717) mutants. *Science* 264: 1336-1340.
282. Taguchi J., Fujii A., Fujino Y., Tsujioka Y., Takahashi M., Tsuboi Y., Wada I., Yamada T. (2000) Different expression of calreticulin and immunoglobulin binding protein in Alzheimer's disease brain. *Acta Neuropathol (Berl)* 100: 153-160.
283. Tanaka F., Otake Y., Nakagawa T., Kawano Y., Miyahara R., Li M., Yanagihara K., Nakayama J., Fujimoto I., Ikenaka K., Wada H. (2000) Expression of polysialic acid and STX, a human polysialyltransferase, is correlated with tumor progression in non-small cell lung cancer. *Cancer Res* 60: 3072-3080.
284. Tanzi R. E., Vaula G., Romano D. M., Mortilla M., Huang T. L., Tupler R. G., Wasco W., Hyman B. T., Haines J. L., Jenkins B. J. (1992) Assessment of amyloid beta-protein precursor gene mutations in a large set of familial and sporadic Alzheimer disease cases. *Am J Hum Genet* 51: 273-282.
285. Tatu U., Helenius A. (1997) Interactions between newly synthesized glycoproteins, calnexin and a network of resident chaperones in the endoplasmic reticulum. *J Cell Biol* 136: 555-565.
286. Thanos S., Bonhoeffer F., Rutishauser U. (1984) Fiber-fiber interaction and tectal cues influence the development of the chicken retinotectal projection. *Proc Natl Acad Sci U S A* 81: 1906-1910.
287. Thelin J., Waldenstrom A., Bartsch U., Schachner M., Schouenborg J. (2003) Heat nociception is severely reduced in a mutant mouse deficient for the L1 adhesion molecule. *Brain Res* 965: 75-82.
288. Theodosis D. T., Poulain D. A. (1993) Activity-dependent neuronal-glial and synaptic plasticity in the adult mammalian hypothalamus. *Neuroscience* 57: 501-535.
289. Theodosis D. T., Rougon G., Poulain D. A. (1991) Retention of embryonic features by an adult neuronal system capable of plasticity: polysialylated neural cell adhesion molecule in the hypothalamo-neurohypophyseal system. *Proc Natl Acad Sci U S A* 88: 5494-5498.
290. Thor G., Probstmeier R., Schachner M. (1987) Characterization of the cell adhesion molecules L1, N-CAM and J1 in the mouse intestine. *EMBO J* 6: 2581-2586.

291. Tomita S., Kirino Y., Suzuki T. (1998) A basic amino acid in the cytoplasmic domain of Alzheimer's beta- amyloid precursor protein (APP) is essential for cleavage of APP at the alpha-site. *J Biol Chem* 273: 19304-19310.
292. Trommsdorff M., Borg J. P., Margolis B., Herz J. (1998) Interaction of cytosolic adaptor proteins with neuronal apolipoprotein E receptors and the amyloid precursor protein. *J Biol Chem* 273: 33556-33560.
293. Vassar R., Bennett B. D., Babu-Khan S., Kahn S., Mendiaz E. A., Denis P., Teplow D. B., Ross S., Amarante P., Loeloff R., Luo Y., Fisher S., Fuller J., Edenson S., Lile J., Jarosinski M. A., Biere A. L., Curran E., Burgess T., Louis J. C., Collins F., Treanor J., Rogers G., Citron M. (1999) Beta-secretase cleavage of Alzheimer's amyloid precursor protein by the transmembrane aspartic protease BACE. *Science* 286: 735-741.
294. Vawter M. P., Cannon-Spoor H. E., Hemperly J. J., Hyde T. M., VanderPutten D. M., Kleinman J. E., Freed W. J. (1998) Abnormal expression of cell recognition molecules in schizophrenia. *Exp Neurol* 149: 424-432.
295. Vawter M. P., Frye M. A., Hemperly J. J., VanderPutten D. M., Usen N., Doherty P., Saffell J. L., Issa F., Post R. M., Wyatt R. J., Freed W. J. (2000) Elevated concentration of N-CAM VASE isoforms in schizophrenia. *J Psychiatr Res* 34: 25-34.
296. Wada I., Kai M., Imai S., Sakane F., Kanoh H. (1997) Promotion of transferrin folding by cyclic interactions with calnexin and calreticulin. *EMBO J* 16: 5420-5432.
297. Wallimann T., Wyss M., Brdiczka D., Nicolay K., Eppenberger H. M. (1992) Intracellular compartmentation, structure and function of creatine kinase isoenzymes in tissues with high and fluctuating energy demands: the 'phosphocreatine circuit' for cellular energy homeostasis. *Biochem J* 281 (Pt 1): 21-40.
298. Walsh F. S., Doherty P. (1997) Neural cell adhesion molecules of the immunoglobulin superfamily: role in axon growth and guidance. *Annu Rev Cell Dev Biol* 13: 425-456.
299. Wang C., Rougon G., Kiss J. Z. (1994) Requirement of polysialic acid for the migration of the O-2A glial progenitor cell from neurohypophyseal explants. *J Neurosci* 14: 4446-4457.
300. Watanabe D., Yamada K., Nishina Y., Tajima Y., Koshimizu U., Nagata A., Nishimune Y. (1994) Molecular cloning of a novel Ca (2+)-binding protein (calmegin) specifically expressed during male meiotic germ cell development 269: 7744-7749.
301. Weidemann A., Paliga K., Durrwang U., Czech C., Evin G., Masters C. L., Beyreuther K. (1997) Formation of stable complexes between two Alzheimer's disease gene products: presenilin-2 and beta-amyloid precursor protein. *Nat Med* 3: 328-332.
302. Wheal H. V., Chen Y., Mitchell J., Schachner M., Maerz W., Wieland H., Van Rossum D., Kirsch J. (1998) Molecular mechanisms that underlie structural and functional changes at the postsynaptic membrane during synaptic plasticity. *Prog Neurobiol* 55: 611-640.

303. Williams A. F., Barclay A. N. (1988) The immunoglobulin superfamily--domains for cell surface recognition. *Annu Rev Immunol* 6: 381-405.
304. Williams E. J., Furness J., Walsh F. S., Doherty P. (1994) Activation of the FGF receptor underlies neurite outgrowth stimulated by L1, N-CAM, and N-cadherin. *Neuron* 13: 583-594.
305. Williamson T. G., Mok S. S., Henry A., Cappai R., Lander A. D., Nurcombe V., Beyreuther K., Masters C. L., Small D. H. (1996) Secreted glypican binds to the amyloid precursor protein of Alzheimer's disease (APP) and inhibits APP-induced neurite outgrowth. *J Biol Chem* 271: 31215-31221.
306. Wolfe M. S., Xia W., Moore C. L., Leatherwood D. D., Ostaszewski B., Rahmati T., Donkor I. O., Selkoe D. J. (1999a) Peptidomimetic probes and molecular modeling suggest that Alzheimer's gamma-secretase is an intramembrane-cleaving aspartyl protease. *Biochemistry* 38: 4720-4727.
307. Wolfe M. S., Xia W., Ostaszewski B. L., Diehl T. S., Kimberly W. T., Selkoe D. J. (1999b) Two transmembrane aspartates in presenilin-1 required for presenilin endoproteolysis and gamma-secretase activity. *Nature* 398: 513-517.
308. Wolff J. M., Frank R., Mujoo K., Spiro R. C., Reisfeld R. A., Rathjen F. G. (1988) A human brain glycoprotein related to the mouse cell adhesion molecule L1. *J Biol Chem* 263: 11943-11947.
309. Wolozin B., Iwasaki K., Vito P., Ganjei J. K., Lacana E., Sunderland T., Zhao B., Kusiak J. W., Wasco W., D'Adamio L. (1996) Participation of presenilin 2 in apoptosis: enhanced basal activity conferred by an Alzheimer mutation. *Science* 274: 1710-1713.
310. Wong E. V., Schaefer A. W., Landreth G., Lemmon V. (1996) Casein kinase II phosphorylates the neural cell adhesion molecule L1. *J Neurochem* 66: 779-786.
311. Xia W., Zhang J., Perez R., Koo E. H., Selkoe D. J. (1997) Interaction between amyloid precursor protein and presenilins in mammalian cells: implications for the pathogenesis of Alzheimer disease. *Proc Natl Acad Sci U S A* 94: 8208-8213.
312. Xu X., Yang D., Wyss-Coray T., Yan J., Gan L., Sun Y., Mucke L. (1999) Wild-type but not Alzheimer-mutant amyloid precursor protein confers resistance against p53-mediated apoptosis. *Proc Natl Acad Sci U S A* 96: 7547-7552.
313. Yamatsuji T., Okamoto T., Takeda S., Murayama Y., Tanaka N., Nishimoto I. (1996) Expression of V642 APP mutant causes cellular apoptosis as Alzheimer trait-linked phenotype. *EMBO J* 15: 498-509.
314. Yan R., Bienkowski M. J., Shuck M. E., Miao H., Tory M. C., Pauley A. M., Brashier J. R., Stratman N. C., Mathews W. R., Buhl A. E., Carter D. B., Tomasselli A. G., Parodi L. A., Heinrikson R. L., Gurney M. E. (1999) Membrane-anchored aspartyl protease with Alzheimer's disease beta- secretase activity. *Nature* 402: 533-537.
315. Yokoi T., Nagayama S., Kajiwara R., Kawaguchi Y., Horiuchi R., Kamataki T. (1993) Identification of protein disulfide isomerase and calreticulin as autoimmune antigens in LEC strain of rats. *Biochim Biophys Acta* 1158: 339-344.

316. Yoo A. S., Cheng I., Chung S., Grenfell T. Z., Lee H., Pack-Chung E., Handler M., Shen J., Xia W., Tesco G., Saunders A. J., Ding K., Frosch M. P., Tanzi R. E., Kim T. W. (2000) Presenilin-mediated modulation of capacitative calcium entry. *Neuron* 27: 561-572.
317. Yu G., Chen F., Levesque G., Nishimura M., Zhang D. M., Levesque L., Rogaeva E., Xu D., Liang Y., Duthie M., George-Hyslop P. H., Fraser P. E. (1998) The presenilin 1 protein is a component of a high molecular weight intracellular complex that contains beta-catenin. *J Biol Chem* 273: 16470-16475.
318. Yu G., Nishimura M., Arawaka S., Levitan D., Zhang L., Tandon A., Song Y. Q., Rogaeva E., Chen F., Kawarai T., Supala A., Levesque L., Yu H., Yang D. S., Holmes E., Milman P., Liang Y., Zhang D. M., Xu D. H., Sato C., Rogaev E., Smith M., Janus C., Zhang Y., Aebersold R., Farrer L. S., Sorbi S., Bruni A., Fraser P., George-Hyslop P. (2000) Nicastrin modulates presenilin-mediated notch/glp-1 signal transduction and betaAPP processing. *Nature* 407: 48-54.
319. Zako M., Shinomura T., Ujita M., Ito K., Kimata K. (1995) Expression of PG-M (V3), an alternatively spliced form of PG-M without a chondroitin sulfate attachment in region in mouse and human tissues. *J Biol Chem* 270: 3914-3918.
320. Zhang H., Miller R. H., Rutishauser U. (1992) Polysialic acid is required for optimal growth of axons on a neuronal substrate. *J Neurosci* 12: 3107-3114.
321. Zhang Y., Cao L., Yang B. L., Yang B. B. (1998a) The G3 domain of versican enhances cell proliferation via epidermal growth factor-like motifs. *J Biol Chem* 273: 21342-21351.
322. Zhang Z., Hartmann H., Do V. M., Abramowski D., Sturchler-Pierrat C., Staufenbiel M., Sommer B., van de W. M., Clevers H., Saftig P., De Strooper B., He X., Yankner B. A. (1998b) Destabilization of beta-catenin by mutations in presenilin-1 potentiates neuronal apoptosis. *Nature* 395: 698-702.
323. Zheng P., Eastman J., Vande P. S., Pimplikar S. W. (1998) PAT1, a microtubule-interacting protein, recognizes the basolateral sorting signal of amyloid precursor protein. *Proc Natl Acad Sci U S A* 95: 14745-14750.
324. Zimmermann D. R., Dours-Zimmermann M. T., Schubert M., Bruckner-Tuderman L. (1994) Versican is expressed in the proliferating zone in the epidermis and in association with the elastic network of the dermis. *J Cell Biol* 124: 817-825.
325. Zimmermann D. R., Ruoslahti E. (1989) Multiple domains of the large fibroblast proteoglycan, versican. *EMBO J* 8: 2975-2981.
326. Zisch A. H., Stallcup W. B., Chong L. D., Dahlin-Huppe K., Voshol J., Schachner M., Pasquale E. B. (1997) Tyrosine phosphorylation of L1 family adhesion molecules: implication of the Eph kinase Cek5. *J Neurosci Res* 47: 655-665.

Poster presentations

H. Strekalova, R. Kleene, J. Hemperly, C. Buhmann, T. Müller-Thomsen and M. Schachner. Elevated levels of neural recognition molecules L1 and NCAM in the cerebrospinal fluids of patients with Alzheimer disease and other dementia syndroms. International Conference on Cell and Molecular Biology of Alzheimer disease, Hamburg, 8-11 September, 2002

CURRICULUM VITAE

Name:	Elena Strekalova
Date of birth:	January 2, 1976
Place of birth:	Russia, Shadrinsk, Kurgan region
Nationality:	Russian
Citizenship:	Russia
Education:	
1993-1999	Moscow Academy of Fine Chemical Technology, Dept. of Biotechnology and Fine Organic Synthesis.
1997	Bachelor diploma in the Shemyakin & Ovchinnikov Institute of Bioorganic Chemistry, Russian Academy of Sciences, Laboratory of Carbohydrate Chemistry, Moscow Theme: "Epitope mapping: study of the fine specificity of monoclonal antibodies to carbohydrate determinants (ELISA method)"
1999	Diploma in the Engelhardt Institute of Molecular Biology, Russian Academy of Sciences, Laboratory of sequencing and mapping of the human genome, Moscow. Theme: "Representational difference analysis (RDA) method in the study of tumour suppressor genes of the human chromosome 3"
1999 - present	Ph.D. Student, Zentrum für Molekulare Neurobiologie UKE, Universität Hamburg
Honors:	1996 – "in recognition and appreciation of outstanding achievements in the study of science at the student level" is selected and named as a SOROS STUDENT 1998 – Certificate of Academic Record for participation in Finnish-Russian Winter School "Growth and Development from Molecules to the Organisms"

Acknowledgments

This study has been performed in the Institute for Biosynthesis of Neuronal Structures of the Centre for Molecular Neurobiology (ZMNH) at the University of Hamburg. I would like to thank sincerely Prof. Melitta Schachner for providing facilities for this research, for constant support during these years and interesting discussions.

I am especially grateful to Dr. Ralf Kleene for nice supervision, for providing me with a big source of ideas and for fruitful discussions.

I would like to thank Dr. Carsten Schmidt for helpful discussions and participation in APP project.

I want to say many thanks to Galina Dityateva for preparation of hippocampal cultures and Dr. Alexander Dityatev for help in the confocal microscope, statistical analysis and corrections of this manuscript.

I would like to thank our collaborators Dr. Carsten Buhmann, Dr. Christian Eggers and Dr. Tomas Müller-Thomsen for CSF collection and diagnostics of patients.

I also wish to thank the present and former colleagues in the lab for their help and support during all these years. I thank to Dr. Frank Plöger, who supervised me in the beginning of my project. My thanks to Dr. Melanie Richter and Tanja Odenthal who helped me a lot with the first steps in this project. I am grateful to Dr. Markus Delling for help with translation and corrections of this manuscript.

Many thanks to Dr. Olena Bukalo, Dr. Gaby Loers, Jens Franke, Oleg Senkov, Dr. Tatjana Kharkovets, Igor Abdurakhmanov and all colleagues for their friendship and understanding, which helped me a lot during everyday work.

I am also grateful to my relatives and friends in Russia who supported me all this time.

I want to express my special thanks to my sister Tatyana for constant support during all my life and my friend Dmitriy Malin for trusting in me.



Universität Hamburg

Hamburg, den,22.05.2003

Dr. Heather P. Ostendorff
ZMNH
Martinistr.52
D-20246 Hamburg

Bestätigung der Korrektheit der englischen Sprache in der Dissertation von Helen Strekalova mit dem Thema „Alzheimer disease: Identification and characterization of putative binding partners of amyloid precursor protein (APP) and cell adhesion molecules as biochemical markers“.

Hiermit bestätige ich, Dr. Heather P. Ostendorff, die Korrektheit der englischen Sprache in Wort und Schrift.

Dr. Heather P. Ostendorff